NASA SP-90

PROGRESS OF THE X-15 RESEARCH AIRPLANE PROGRAM

Flight Research Center
Edwards Air Force Base, California
October 7, 1965

Sponsored by
United States Air Force
United States Navy
National Aeronautics and Space Administration

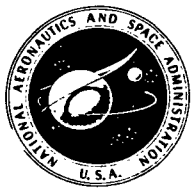

Scientific and Technical Information Division 1965
NATIONAL AERONAUTICS AND SPACE ADMINISTRATION
Washington, D.C.

NOTICE

THIS DOCUMENT HAS BEEN REPRODUCED FROM THE BEST COPY FURNISHED US BY THE SPONSORING AGENCY. ALTHOUGH IT IS RECOGNIZED THAT CERTAIN PORTIONS ARE ILLEGIBLE, IT IS BEING RELEASED IN THE INTEREST OF MAKING AVAILABLE AS MUCH INFORMATION AS POSSIBLE.

PREFACE

This compilation consists of papers presented at the fourth conference on progress of the X-15 Research Airplane Program held at the NASA Flight Research Center, Edwards Air Force Base, California, October 7, 1965. This conference was sponsored by the Research Airplane Committee of the U.S. Air Force, the U.S. Navy, and the National Aeronautics and Space Administration. Papers were presented by representatives from the NASA Flight Research Center, the NASA Langley Research Center, the U.S. Air Force Flight Test Center, and the U.S. Air Force Aeronautical Systems Division.

CONTENTS

1. STATUS OF X-15 PROGRAM

By James E. Love and Jack Fischel
NASA Flight Research Center

SUMMARY

The overall status of the X-15 program is reviewed and program plans for future flights are considered. Since the initiation of the flight program, approximately 150 flights have been performed over a broad altitude and Mach number range. This paper presents background information on the basic research studies and test-bed experiments to be presented at this Conference and reviews the operational problems encountered since the 1961 Conference on the X-15. A comprehensive bibliography of reports resulting from the X-15 program, arranged according to subject matter, is included.

INTRODUCTION

An X-15 airplane, this nation's only manned aircraft capable of operation at hypersonic speeds in excess of Mach 4, completed the 151st flight of the program on September 30, 1965.

Data from these flights have already been used in the design and operational phases of many of our aircraft and space programs, and a wealth of data, which are available for advanced designs, is still being generated by this program. Information from these flights has vastly broadened our knowledge of the aerodynamics, structure, systems, and general behavior of winged vehicles in all phases of supersonic and hypersonic flight as well as in reentry research. Also, technological advances have been made in the operation of recoverable vehicles over a vast speed and altitude range.

In its most recent role as a carrier of test-bed experiments to specific altitude or speed conditions, the X-15 has made possible investigations of many natural phenomena from a point in the ionosphere. This capability was not hitherto available to scientists.

As a background for the present conference, it would be well to review briefly a few pertinent events in the overall X-15 program as shown in figure 1. Two industry conferences, indicated by arrows, were held prior to the first X-15 flight. The purpose of these conferences was to describe the hardware, the configuration, and the predicted performance. A third conference held in 1961 reported the flight results of the 45 flights up to that date.

Many development problems had been resolved during the first 30 flights in which the two LR11 engines with a total of 16 000 pounds of thrust were used. Velocities in excess of 6000 feet per second had been achieved using the YLR99 engine with the 60 000 pounds of thrust at the time of that third conference.

The X-15-3 was being prepared for its first flight with the adaptive flight control system. Since that time, the three X-15's have made an additional 106 flights and have provided much significant information to the scientific and engineering community. Some of the more significant information obtained is discussed in the papers presented herein. A comprehensive bibliography of information related to the X-15 program is included at the end of this paper.

The present paper briefly reviews the significant activities and present status of the project in order to aid you in properly relating the information presented during this conference to the total X-15 program.

DISCUSSION

Flight Performance

The comparative performance envelopes of the X-15 prior to and subsequent to November, 1961, are shown in figure 2. The design velocity of 6000 feet per second, which is still the maximum velocity attained, was reached prior to the 1961 conference, as shown in the shaded area. However, since that date the altitude envelope has been expanded by about 50 percent to its current value of over 354 000 feet.

As an indication of the capability of the airplane in obtaining research data for use by vehicle investigators as well as by test-bed experimenters, figure 3 shows the total time experienced above various velocities and altitudes since the beginning of the program. For instance, the X-15's have flown at altitudes above 200 000 feet for almost 1 hour and at speeds in excess of Mach 4 for a total of nearly 4 hours.

Ten pilots have participated in the flight program and the eleventh is to have his first flight this month.

Flight Objectives

A chronological summary of the X-15 flight program is presented in figure 4. Shown are the total number of flights performed each year and the approximate number of flights performed in each of the listed categories. Most of the envelope-expansion and primary research flights occurred in 1960 and 1961. The detailed research programs have been vigorously pursued since then and should continue for some time ahead. In 1963 various flights in which the airplane served as a test bed for experiments were initiated and have since been performed on the three X-15's--either alone or in conjunction with tests for the basic research program. At present, it appears that the basic research program and the test-bed experiments are receiving approximately equal attention, as regards flight allocation. Most flights now obtain aircraft research data as well as data from test-bed experiments; hence, the overlap in the time allotted to these two categories during 1964-65.

The original primary research studies can be categorized in the following areas:

*Flight control

*Aerodynamics

Structures and loads

Performance

Environmental factors

Bioastronautics

*Operational and research systems

They pertain to all phases of flight, particularly to hypersonic flight and reentry to the atmosphere. The scope of these studies has been extended in a few cases, but the program has remained essentially unchanged from the beginning. Many facets of these studies are in the final stages of analysis or have been reported previously and, therefore, will not be discussed today. However, a brief discussion of some of the research progress on the more significant items marked with an asterisk appears quite pertinent.

Flight control studies.- At the last conference complete information on the capability of the X-15 for providing supersonic-hypersonic controllability information and baseline reentry control criteria was not available.

Some of the flight control studies performed since that time are worthy of discussion, as follows:

Stability augmentation system (SAS)

Reaction augmentation system (RAS)

Adaptive control system

Ventral-off controllability

High-altitude reentry

To improve vehicle controllability, a stability augmentation system (SAS) is now installed in two of the X-15 airplanes. An independent augmentation system having only pitch and roll modes has since been installed to give increased reliability through redundancy to the stability augmentation system. A reaction augmentation system (RAS), which automatically operates the peroxide-fueled reaction controls, was added to provide better vehicle damping at the higher altitudes. These damper systems have enabled the pilots to evaluate X-15 controllability over a large range of speed and dynamic pressures and during the more critical and transient conditions encountered in boost and reentry maneuvers.

The adaptive control system, which was installed in the X-15-3 but had not been tested at the time of the last conference, has now been evaluated. The potential advantages of its peripheral systems—such as attitude hold modes, g-limiting, and reaction and aerodynamic control blending—have been investigated in a number of missions. In fact, the reliability and redundancy built into this system, as well as its other desirable characteristics, have enabled the altitude envelope to be expanded to 354 000 feet.

The original X-15 configuration shown in figure 5, top diagram, included a lower movable rudder or "ventral." The envelope expansion to Mach 6 and an altitude of almost 315 000 feet was acheived with this configuration. Because of improved controllability available with ventral off--particularly in the dampers-off condition--all flights since 1962 have been made in the ventral-removed configuration (lower diagram).

The results of these flight control and reentry studies are discussed in two subsequent papers (papers number 6 by Holleman and 5 by Taylor, Robinson, and Iliff).

Detailed aerodynamic studies.— Aerodynamic data of a preliminary nature had been obtained prior to the 1961 conference and were presented at that time. These studies have since been expanded in the areas given in the following list:

Flow field

Boundary-layer measurements

Skin friction

Boundary-layer noise

Heat transfer

Thermal protection

The more recent detailed measurements made ascertained the local flow field and boundary-layer edge conditions at specific locations on the fuselage, wing, or empennage. They provided information on the local environment affecting skin friction, boundary-layer noise, and heat-transfer measurements. As illustrated in figure 6, some of the heat-transfer studies performed included measurements on various parts of the X-15 structure and measurements on panels behind sharp and blunt leading edges.

The sampling of boundary-layer noise at various locations and the evaluation of several thermal-protection coatings on the X-15 structure have been two of the most recent areas of interest and are still in progress.

Details and results of these studies are discussed subsequently in paper 2 by Banner and Kuhl, paper 3 by Lewis and McLeod, and paper 11 by Watts, Cary, and Dow.

Test-bed investigations.— The following list shows the areas of test-bed investigations performed and planned for the X-15:

Ultraviolet stellar photography

Infrared scanner

Horizon definition

Ultraviolet background

Micrometeorite collection

Atmospheric-density measurement

High-altitude sky brightness measurements

High-altitude infrared background measurements

High-altitude photography

Heat transfer at zero g

Air-breathing propulsion

The use of the airplane as an experimental test bed is one of the most significant extensions in the research capability of the X-15 airplanes. They have been utilized to carry various experimental packages to required environments, obtaining measurements with these packages, and then returning the experiment and results to the experimenters. Many of these experiments required specific missions to altitudes above 150 000 feet, whereas others obtained information at various flight conditions in piggyback fashion. Several experiments were installed on each aircraft for better flight utilization. For this reason, on the X-15-1 airplane, specially constructed tip pods and tail-cone box have been installed, as shown in figure 7(a), to accommodate the experiments listed in figure 7(b). The circled numbers correspond on both parts of figure 7. Three experiments have been completed, five are in progress, and three more are planned for early next year.

These studies are performed for the benefit of the Air Force, NASA, other governmental agencies, or scientific groups. The data are analyzed by the experimenter. Results of two of these studies, the horizon spectrum definition and photography from high-speed aircraft, are presented in paper 9 by Jalink and paper 8 by Groening, respectively.

The scope of the test-bed experiments demonstrates the versatility of the X-15 in adding to the nation's reservoir of scientific information.

Operational Experience

In a program as diversified as the one outlined in this paper, a great many aircraft configuration changes have had to be made. Unfortunately, many of the changes resulted in a more complicated mechanism.

The three X-15 airplanes that NASA is now maintaining and flying are not three identical aircraft, but are three different and more complex vehicles than ever before. Some of the differences are the inertial systems and control systems. The modified X-15-2 is essentially a different airplane, particularly with tanks installed. The X-15 program has never settled down to a routine operation because of the continued increase in complexity and the nature of experiments and research performed by each aircraft. This attribute is probably characteristic of research programs. Because of the similarity of X-15 hardware to that of other chemically fueled vehicles now in use or planned, one would be led to believe that the problems which have arisen during the execution of the program and their solutions are of general interest.

Problem areas.– In a research program utilizing a small number of vehicles, there is usually no formal product improvement phase. Therefore, operational problems are solved when they begin to affect the accomplishment of the mission. We have been no worse than others, and probably somewhat more fortunate in identifying and resolving the problems before they seriously affected the progress of the program. Some of the basic subsystems which had been expected to cause delays in the early flights did not become trouble spots until the 1961-1964 period, as are now discussed.

Inertial flight data system.– Considering the problem areas chronologically, one would first discuss the inertial flight data system (IFDS), because it has required an excessive amount of manpower to maintain and has exhibited low reliability from the first flights.

The serious operational problems led to a two-pronged approach to their solutions. One approach resulted in the redesign of 60 percent of the subassemblies of the original IFDS. The other approach led to the installation of a completely different inertial system in one X-15.

The subject is more thoroughly explored in paper 7 by Burke and Basso.

Windshield cracks.– It was reported at the last conference that windshield cracking had occurred. The original Inconel X windshield frames were replaced with thicker titanium frames in order to take advantage of the lower coefficient of expansion of the latter material. But as the flight envelope expanded and the environment became more severe, the glass deteriorated along the rear edge just forward of the aft windshield frame.

Figure 8 shows the windshield frame after having cut away the aft retainer. This modification eliminated the lip which was causing the hot spot on the glass.

YLR99 engine, second-stage detonation.– In the fall of 1962 during post-flight inspection of an engine, it was found that the injector face of the second-stage igniter and the liquid oxygen line to that igniter had been ruptured. These are shown in figure 9. An intensive investigation was conducted by the propulsion specialists of the Air Force Flight Test Center, the NASA Flight Research Center, and the engine contractor. This investigation revealed that during a shutdown due to liquid oxygen exhaustion, the second-stage liquid-oxygen manifold pressure fell below that of the chamber pressure. This condition allowed fuel and hot gases to enter the manifold and caused detonation.

The problem was solved by replacing the single-pressure purge system with a dual pressure system which maintains a suitable second-stage liquid-oxygen manifold pressure until the main stage is completely shut down.

Auxiliary power unit pinion gear.– The first flights of the X-15 in 1959 were delayed because of problems with pressure vessel regulators, valves, and relief devices in the hydrogen-peroxide supply systems of the auxiliary power unit (APU). Those who were associated with the program at that time were pleasantly surprised by the excellent performance of the basic APU because the specifications and requirements were exceedingly stringent for a device of such high rotative speeds.

The surprise was even greater when in late 1962 excessive wear was found on the high speed (52 000 rpm) turbine shaft pinion. On October 4, the first in-flight APU failure occurred. On January 17, 1963, the second in-flight failure took place, and flight operations were therefore deferred for almost three months while a team of specialists from the Air Force, NASA, and the airplane and engine contractors identified the problem and produced a solution. This delay has been the only significant cessation of flight operations in the program.

The solution became obvious when simulated altitude tests revealed that when seal leakage was eliminated from the drive-turbine case into the gear reduction box, the gear box was no longer pressurized. This is shown diagrammatically in figure 10. The lower ambient pressure at altitude reduced the efficiency of the lubricant as a coolant and as a film between the gear teeth. This deficiency caused pinion failure at altitudes in as short a period as 90 seconds.

Pressurizing the gear box has reinstated high confidence in the APU.

X-15-2 emergency landing.– On November 9, 1962, the X-15-2 was landed soon after launch because the rocket engine could not be advanced beyond the 30-percent thrust level. Although the pilot demonstrated excellent judgment and piloting technique, the aircraft suffered extensive damage because of the inability of the landing gear to absorb the high landing loads sustained under emergency conditions.

The aircraft was subsequently rebuilt and modified to increase the design Mach number. The higher velocities obtainable with the X-15-2 are required so

that this airplane may be used as a test bed for testing an air-breathing supersonic combustion engine. The proposed engine research is presented in paper 12 by Rubert.

CONCLUDING REMARKS

As of today, the status of the X-15 program consists of active use of three airplanes equipped to carry out various and diverse research projects. The X-15-1 airplane is presently being used to perform the altitude experiments.

The X-15-2 airplane has been redesigned for higher Mach numbers and is being prepared for the first flight with external fuel tanks.

The X-15-3 airplane is presently employed in pilot checkout flights prior to modification for boost-guidance investigation.

Only a small number of the operational lessons that have been learned and a portion of the research areas in the X-15 program have been introduced.

The more important and interesting subjects have been selected for comprehensive discussion in the papers which follow.

BIBLIOGRAPHY OF NASA REPORTS FROM THE X-15 PROGRAM

ARRANGED BY SUBJECT MATTER

Aerodynamic Characteristics

Aerodynamic heating

Reed, Robert D.; and Watts, Joe D.: Skin and Structural Temperatures Measured on the X-15 Airplane During a Flight to a Mach Number of 3.3. NASA TM X-468, 1961.

Banner, Richard D.; Kuhl, Albert E.; and Quinn, Robert D.: Preliminary Results of Aerodynamic Heating Studies on the X-15 Airplane. NASA TM X-638, 1962.

Watts, Joe D.; and Banas, Ronald P.: X-15 Structural Temperature Measurements and Calculations for Flights to Maximum Mach Numbers of Approximately 4, 5, and 6. NASA TM X-883, 1963.

Quinn, Robert D.; and Kuhl, Albert E.: Comparison of Flight-Measured and Calculated Turbulent Heat Transfer on the X-15 Airplane at Mach Numbers From 2.5 to 6.0 at Low Angles of Attack. NASA TM X-939, 1964.

Banas, Ronald P.: Comparison of Measured and Calculated Turbulent Heat Transfer in a Uniform and Nonuniform Flow Field on the X-15 Upper Vertical Fin at Mach Numbers of 4.2 and 5.3. NASA TM X-1136, 1965.

Drag characteristics

Saltzman, Edwin J.: Preliminary Full-Scale Power-Off Drag of the X-15 Airplane for Mach Numbers From 0.7 to 3.1. NASA TM X-430, 1960.

Saltzman, Edwin J.: Preliminary Base Pressures Obtained From the X-15 Airplane at Mach Numbers From 1.1 to 3.2. NASA TN D-1056, 1961.

Hopkins, Edward J.; Fetterman, David E., Jr.; and Saltzman, Edwin J.: Comparison of Full-Scale Lift and Drag Characteristics of the X-15 Airplane With Wind-Tunnel Results and Theory. NASA TM X-713, 1962.

Saltzman, Edwin J.: Base Pressure Coefficients Obtained From the X-15 Airplane for Mach Numbers Up to 6. NASA TN D-2420, 1964.

Aerodynamic derivatives

Walker, Harold J.; and Wolowicz, Chester H.: Theoretical Stability Derivatives for the X-15 Research Airplane at Supersonic and Hypersonic Speeds Including a Comparison With Wind-Tunnel Results. NASA TM X-287, 1960.

Yancey, Roxanah B.; Rediess, Herman A.; and Robinson, Glenn H.: Aerodynamic-Derivative Characteristics of the X-15 Research Airplane as Determined From Flight Tests for Mach Numbers From 0.6 to 3.4. NASA TN D-1060, 1962.

Walker, Harold J.; and Wolowicz, Chester H.: Stability and Control Derivative Characteristics of the X-15 Airplane. NASA TM X-714, 1962.

Yancey, Roxanah B.: Flight Measurements of Stability and Control Derivatives of the X-15 Research Airplane to a Mach Number of 6.02 and an Angle of Attack of 25°. NASA TN D-2532, 1964.

Pressure loads

Keener, Earl R.; and Pembo, Chris: Aerodynamic Forces on Components of the X-15 Airplane. NASA TM X-712, 1962.

Pyle, Jon S.: Comparison of Flight Pressure Measurements With Wind-Tunnel Data and Theory for the Forward Fuselage of the X-15 Airplane at Mach Numbers From 0.8 to 6.0. NASA TN D-2241, 1964.

Pyle, Jon S.: Flight-Measured Wing Surface Pressures and Loads for the X-15 Airplane at Mach Numbers From 1.2 to 6.0. NASA TN D-2602, 1965.

Pyle, Jon S.: Flight Pressure Distributions on the Vertical Stabilizers and Speed Brakes of the X-15 Airplane at Mach Numbers From 1 to 6. NASA TN D-3048, 1965.

Flight Dynamics

General

Finch, Thomas W.; and Matranga, Gene J.: Launch, Low-Speed, and Landing Characteristics Determined From the First Flight of the North American X-15 Research Airplane. NASA TM X-195, 1959.

Flight Research Center: Aerodynamic and Landing Measurements Obtained During the First Powered Flight of the North American X-15 Research Airplane. NASA TM X-269, 1960.

Controllability

Holleman, Euclid C.; and Reisert, Donald: Controllability of the X-15 Research Airplane With Interim Engines During High-Altitude Flights. NASA TM X-514, 1961.

Matranga, Gene J.: Launch Characteristics of the X-15 Research Airplane as Determined in Flight. NASA TN D-723, 1961.

Matranga, Gene J.: Analysis of X-15 Landing Approach and Flare Characteristics Determined From the First 30 Flights. NASA TN D-1057, 1961.

Taylor, Lawrence, W., Jr.: Analysis of a Pilot-Airplane Lateral Instability Experienced With the X-15 Airplane. NASA TN D-1059, 1961.

White, Robert M.; Robinson, Glenn H.; and Matranga, Gene J.: Résumé of Handling Qualities of the X-15 Airplane. NASA TM X-715, 1962.

Petersen, Forrest S.; Rediess, Herman A.; and Weil, Joseph: Lateral-Directional Control Characteristics of the X-15 Airplane. NASA TM X-726, 1962.

Holleman, Euclid C.: Piloting Performance During the Boost of the X-15 Airplane to High Altitude. NASA TN D-2289, 1964.

Control system and control system augmentation

Taylor, Lawrence W., Jr.; and Merrick, George B.: X-15 Airplane Stability Augmentation System. NASA TN D-1157, 1962.

Tremant, Robert A.: Operational Experiences and Characteristics of the X-15 Flight Control System. NASA TN D-1402, 1962.

Jarvis, Calvin R.; and Lock, Wilton P.: Operational Experience With the X-15 Reaction Control and Reaction Augmentation Systems. NASA TN D-2864, 1965.

Flight Operational Research

Flight planning

Hoey, Robert G.; and Day, Richard E.: Mission Planning and Operational Procedures for the X-15 Airplane. NASA TN D-1159, 1962.

Research and pilot instrumentation

Stillwell, Wendell H.; and Larson, Terry J.: Measurement of the Maximum Speed Attained by the X-15 Airplane Powered With Interim Rocket Engines. NASA TN D-615, 1960.

Stillwell, Wendell H.; and Larson, Terry J.: Measurement of the Maximum Altitude Attained by the X-15 Airplane Powered With Interim Rocket Engines. NASA TN D-623, 1960.

Larson, Terry J.; and Webb, Lannie D.: Calibrations and Comparisons of Pressure-Type Airspeed-Altitude Systems of the X-15 Airplane From Subsonic to High Supersonic Speeds. NASA TN D-1724, 1963.

Fischel, Jack; and Webb, Lannie D.: Flight-Informational Sensors, Display, and Space Control of the X-15 Airplane for Atmospheric and Near-Space Flight Missions. NASA TN D-2407, 1964.

Cary, John P.; and Keener, Earl R.: Flight Evaluation of the X-15 Ball-Nose Flow-Direction Sensor as an Air-Data System. NASA TN D-2923, 1965.

Systems operation experience

Maher, James F., Jr.; Ottinger, C. Wayne; and Capasso, Vincent N., Jr.: YLR99-RM-1 Rocket Engine Operating Experience in the X-15 Aircraft. NASA TN D-2391, 1964.

Structures

Aerothermoelastic effects

Kordes, Eldon E.; Reed, Robert D.; and Dawdy, Alpha L.: Structural Heating Experiences on the X-15 Airplane. NASA TM X-711, 1962.

Dynamic loads, including flutter

Kordes, Eldon E.; and Noll, Richard B.: Flight Flutter Results for Flat Rectangular Panels. NASA TN D-1058, 1962.

Jordan, Gareth H.; McLeod, Norman J.; and Guy, Lawrence D.: Structural Dynamic Experiences of the X-15 Airplane. NASA TN D-1158, 1962.

Landing

McKay, James M.: Measurements Obtained During the First Landing of the North American X-15 Research Airplane. NASA TM X-207, 1959.

McKay, James M.; and Scott, Betty J.: Landing-Gear Behavior During Touchdown and Runout for 17 Landings of the X-15 Research Airplane. NASA TM X-518, 1961.

McKay, James M.; and Kordes, Eldon E.: Landing Loads and Dynamics of the X-15 Airplane. NASA TM X-639, 1962.

Noll, Richard B.; and Halasey, Robert L.: Theoretical Investigation of the Slideout Dynamics of a Vehicle Equipped With a Tricycle Skid-Type Landing-Gear System. NASA TN D-1828, 1963.

Noll, Richard B.; Jarvis, Calvin R.; Pembo, Chris; Lock, Wilton P.; and Scott, Betty J.: Aerodynamic and Control-System Contributions to the X-15 Airplane Landing-Gear Loads. NASA TN D-2090, 1963.

Summary Papers

Weil, Joseph: Review of the X-15 Program. NASA TN D-1278, 1962.

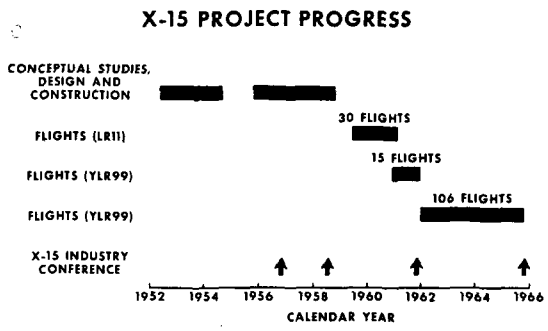

Figure 1

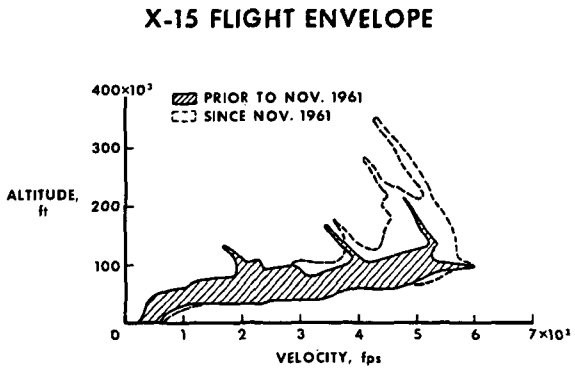

Figure 2

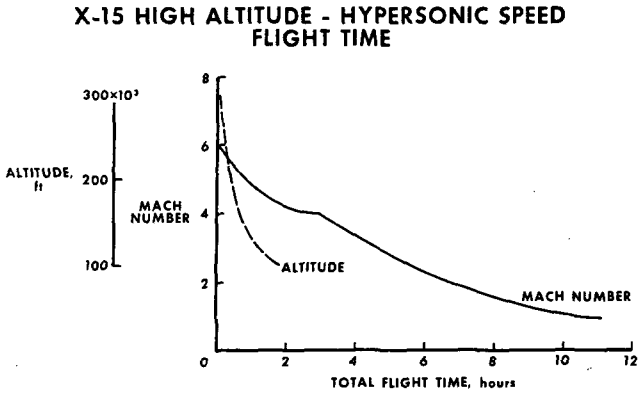

Figure 3

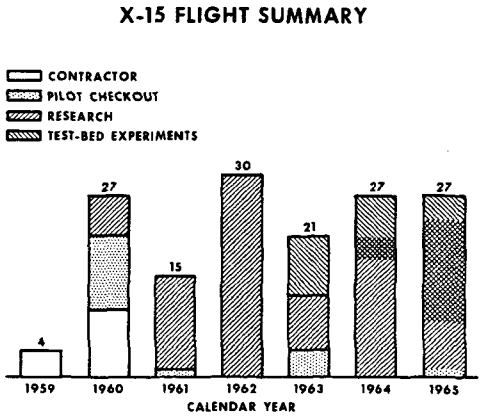

Figure 4

X-15 VENTRAL CONFIGURATIONS

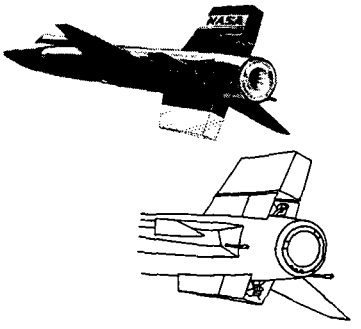

Figure 5

X-15 AERODYNAMIC-HEATING STUDIES

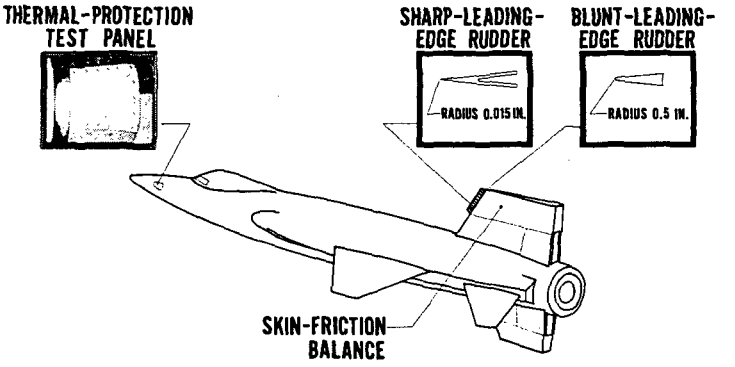

Figure 6

LOCATIONS OF TEST-BED EXPERIMENTS

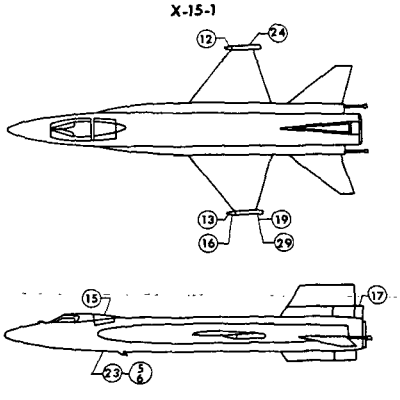

Figure 7(a)

TEST-BED EXPERIMENTS ON X-15-1

EXPERIMENT NUMBER		
5 – 6	OPTICAL-DEGRADATION MEASUREMENTS	COMPLETED
23	IR SCANNING RADIOMETER	
12	ATMOSPHERIC-DENSITY MEASUREMENTS	CURRENTLY INSTALLED
13	MICROMETEORITE COLLECTION	
16	RAREFIED GAS (ATMOSPHERIC-DENSITY PACE TRANSDUCER)	
17	MIT (APOLLO) HORIZON SCANNER	
19	HIGH-ALTITUDE SKY BRIGHTNESS	
15	VAPOR-CYCLE COOLING	PLANNED
24	HIGH-ALTITUDE IR BACKGROUND MEASUREMENTS	
29	JPL SOLAR-SPECTRUM MEASUREMENTS	

Figure 7(b)

X-15 WINDSHIELD RETAINER

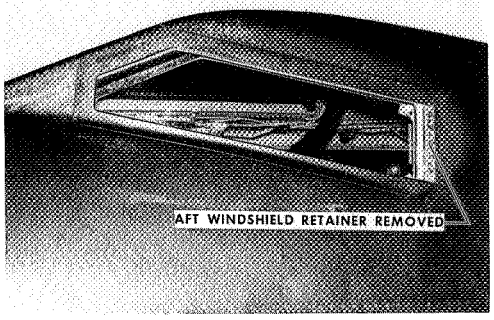

Figure 8

YLR99 ENGINE IGNITER

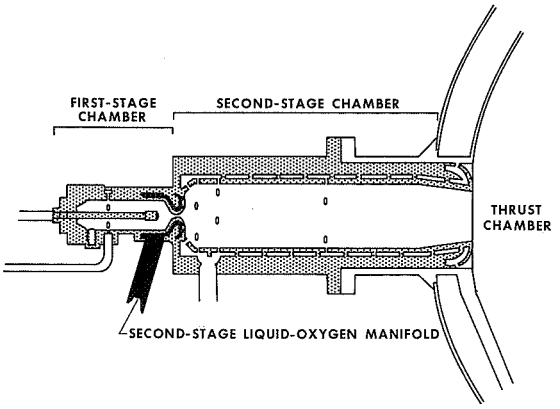

Figure 9

BLOCK DIAGRAM OF AUXILIARY POWER UNIT

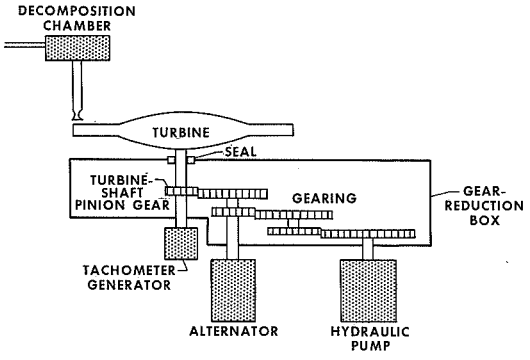

Figure 10

2. A SUMMARY OF X-15 HEAT-TRANSFER AND SKIN-FRICTION MEASUREMENTS

By Richard D. Banner and Albert E. Kuhl
NASA Flight Research Center

SUMMARY

Measured local Mach numbers and heat transfer obtained on the lower surface of the wing and bottom center line of the fuselage at angles of attack up to 18°, and on the vertical fin with both a sharp and a blunt leading edge, are summarized and compared with calculations using Eckert's reference-temperature method. Direct measurements of skin friction on the surface of the sharp-leading-edge vertical fin are also presented. It is shown that both the heat-transfer and skin-friction data can be predicted by neglecting the effect of wall temperature in the calculation of the reference temperature by Eckert's method.

Uncertainties in level and trend of Reynolds analogy factor with Mach number are discussed and a planned flight investigation is described.

INTRODUCTION

The preliminary data (ref. 1) reported at the 1961 X-15 conference indicated the turbulent heat transfer measured on the X-15 to be lower than accepted methods would predict. Eckert's reference-temperature method (ref. 2), or Sommer and Short's T-prime method (ref. 3), and Van Driest's theory (ref. 4) are interpreted as having been acceptable, in that each conservatively predicts an increase in heat transfer with increased heat rate (lower wall-to-adiabatic-wall temperature ratios). The early X-15 results (ref. 1) were of considerable interest, since the X-15 data were obtained at conditions where the little data that existed showed contradicting trends (that is, at low wall-to-adiabatic-wall temperature ratios). From the preliminary analysis (ref. 1), it appeared that the effect of wall temperature on turbulent heat transfer was less than the accepted methods would predict and could possibly be neglected.

At that time, only flight data acquired during the X-15 performance-expansion program were available. Since then, a series of flights has been made specifically to obtain heat-transfer and local-flow data. Attention has been directed to three principal areas on the X-15: the wing midsemispan, the fuselage bottom center line, and the vertical tail. (See fig. 1.) In these areas the geometry of the flow is known best and is the least difficult to measure. Impact-pressure rakes were installed at the locations shown, and local-flow conditions were measured.

SYMBOLS

C_f	local skin-friction coefficient, $\frac{\tau}{q_l}$
C_{f_i}	incompressible value of the local skin-friction coefficient
c_p	specific heat of air at constant pressure, $\frac{\text{Btu}}{\text{lb-}^\circ\text{F}}$
h	heat-transfer coefficient, $\frac{\text{Btu}}{\text{ft}^2\text{-}^\circ\text{F-sec}}$
M	Mach number
q	dynamic pressure, pounds per square foot
R_x	Reynolds number, $\frac{\rho_l V_l x}{\mu_l}$
St	Stanton number, $\frac{h}{\rho_l V_l c_{p_l}}$
St_i	incompressible value of the Stanton number
T_W	wall (or surface) temperature, °R
T_R	boundary-layer recovery (or adiabatic wall) temperature, °R
$\frac{u_L}{u_\infty}$	ratio of the laminar sublayer to boundary-layer-edge velocities for a flat plate
V	velocity, feet per second
x	length, feet
α	angle of attack, degrees
μ	coefficient of viscosity, pounds per foot-second
ρ	density, pounds per cubic foot
τ	surface shear, pounds per square foot

Subscripts:

l	local
∞	free stream

DISCUSSION

Flow Conditions

In order to correlate the heat-transfer data, the boundary-layer-edge flow conditions must be known. In the preliminary analysis, the local-flow conditions were approximated by use of attached-shock methods. In a subsequent analysis of heat-transfer data obtained during the first flight to Mach 6, the local properties were based on calculated detached-shock flow conditions (ref. 5). The rake measurements permitted a check of the analytical methods.

In a study made at the NASA Flight Research Center by Murray Palitz, calculated and measured local Mach numbers on the wing, fuselage, and vertical fin have been compared. Examples of these comparisons are shown in figure 2. The characteristic shear layers produced by the detached shocks from the blunt leading edges are to be noted. An example of the differences in flow conditions behind a blunt and a sharp leading edge is shown in the vertical-fin data. The fin was modified from the normally blunt 0.5-inch-radius leading edge to a sharp 0.015-inch-radius leading edge. Data are included for both configurations. The reduction in local Mach number due to increased bluntness can be seen. In general, good agreement between measured and calculated local Mach numbers has been obtained over a wide range of conditions. Note that the data near the surface of the wing, the fuselage (at zero angle of attack), and the blunt vertical tail fall below the calculated values. This is to be expected, since the inviscid shear-layer calculations do not account for the viscous boundary layer. The Moeckel-Love calculation procedure is described in reference 5. The boundary-layer heights, shown by the arrows, have been estimated by the methods given in references 6 and 7. Note that the measured local Mach numbers drop below the calculated inviscid values at about the estimated boundary-layer heights.

For the fuselage nose location at an angle of attack of 10°, the boundary-layer thickness is estimated to be less than the height of the innermost probe. In cases of this type, the calculated surface Mach numbers have been used to approximate the boundary-layer-edge Mach numbers. For the sharp-leading-edge fin, the calculations show that the shear layer is confined to a narrow region near the surface. In this instance, the boundary-layer edge is in essentially uniform flow. By using the methods just described, the Mach numbers at the boundary-layer edge have been obtained with reasonably good accuracy at all locations.

Heat Transfer

Other boundary-layer-edge conditions (density, velocity, and static temperature) were derived from isentropic-flow relationships. These, in turn, were used with the measured heat-transfer coefficients to obtain dimensionless Stanton numbers for correlation of the data at all locations. At some locations it was necessary to include internal conduction effects when

reducing the measured skin-temperature data to heat-transfer coefficients. The largest effect of conduction losses occurred in the data from the wing and the vertical fin, where corrections up to 18 percent were required.

The wing and fuselage data at low angles of attack from the first flight to Mach 6 (ref. 5), and the blunt- and the sharp-leading-edge fin data (ref. 8), shown in terms of the ratio of the compressible Stanton number to the incompressible value, are plotted against local Mach number in figure 3. For comparison purposes, the variation in the Stanton number ratio given by Eckert's reference-temperature method (ref. 2) is shown for two wall-temperature values that bracket the range of the test data. Although it might be expected that the data would fall throughout this bounded region if the effect of wall temperature were as predicted by Eckert's method, most of the data fall near and slightly below the lower boundary given by assuming the wall temperature to be equal to the boundary-layer recovery temperature. Some data are as much as 35 percent less than values predicted by Eckert's reference-temperature method.

A similar trend has also been noted in data recently obtained at the Flight Research Center by Robert D. Quinn on the X-15 wing and fuselage at angles of attack up to 18° (fig. 4). The wall-to-recovery temperature ratio for these data varied from 0.35 to 0.70. For comparison, the Stanton number ratio that would be calculated by Eckert's method at a wall temperature equal to one-half the recovery temperature is shown. Again, the data are scattered near the level predicted by assuming the wall temperature to be equal to the recovery temperature.

Eckert's method has been used for comparison with the X-15 data because of its general acceptance and use. Also, this method best illustrates the large effect that wall temperature was previously thought to have on heat transfer. Eckert's method agrees closely with the T-prime method (ref. 3), which has been shown to agree particularly well with measured skin friction (ref. 9) at adiabatic-wall conditions ($T_W = T_R$). It is believed that the X-15 results have contributed to a renewed interest in more accurately defining the trend in turbulent heat transfer and skin friction at low wall-to-recovery temperatures.

The effect of low wall temperature has been reexamined by Spalding and Chi (ref. 10), Danberg (ref. 11), Bartz (ref. 12), and more recently by Bertram and Neal (ref. 13). These studies have also indicated that the effect of wall temperature is less than previously thought, but sufficient data to define the exact trend and level are not available.

Most of the methods for calculating turbulent heat transfer have been based on analyses of turbulent skin friction and the use of Reynolds analogy factor. Several methods for predicting turbulent skin friction are compared in figure 5. The incompressible skin-friction values given by the methods noted have been normalized with respect to the values given by Blasius--the method used to compute the incompressible Stanton numbers for the X-15 data--and are plotted against Reynolds number.

These methods are described in reference 14. It is noted in the figure that over the X-15 Reynolds number range there would be only about a 10-percent difference in the calculated skin-friction coefficient regardless of the method used. The simpler Blasius equation, which has been used for X-15 correlation, gives a good average skin-friction level over the X-15 range.

After the skin-friction equation to be used is selected, a Reynolds analogy factor is needed in order to compute the Stanton number. The available data are compared in figure 6 with values given by Dorrance (ref. 15) and Rubesin (ref. 16). Most of the data at low wall-to-recovery temperature ratios have been obtained indirectly from boundary-layer temperature and velocity surveys (refs. 17, 18, and 19). Recent data obtained by Peterson at the NASA Langley Research Center are also shown. These data show a wide variation, about 40 percent. Direct measurements (refs. 13 and 20) have given values between 1.15 and 1.35, which are nearer the predictions and fall about the level found by Colburn (ref. 21) in low-speed pipe-flow experiments. Bertram and Neal (ref. 13) applied the incompressible Von Kármán equation to compressible flow and found good agreement with Neal's direct measurements. For the X-15 data correlation, Colburn's modified Reynolds analogy factor was used. Clearly, additional data are needed.

Skin Friction

An experiment is planned in which skin friction and heat transfer will be measured simultaneously on the sharp-leading-edge fin of the X-15 airplane in order to obtain Reynolds analogy factor data. Some preliminary skin-friction measurements have been made at the Flight Research Center by Darwin J. Garringer at speeds up to Mach 5 by using a direct-reading skin-friction balance installed in the fin surface. Data from two flights are shown in figure 7 as the ratio of the measured skin-friction coefficient to the incompressible skin-friction coefficient plotted against local Mach number. As for the heat-transfer data, the local conditions were derived from measured surface static and impact pressures and isentropic relationships.

The balance was mounted in a manner that produced a longitudinal surface-temperature gradient ahead of the sensing element. The exact effect of this gradient on the measurement is not known. Considering only the surface-temperature levels, values of the wall-to-recovery temperature ratio near the element varied with local Mach number, as shown in the plot at the upper right of the figure. Values between 0.3 and 1.3 were experienced during the flight. The data, however, do not show the effect of this parameter that would be predicted by Eckert's reference-temperature method; the values obtained during both increasing and decreasing speeds are more nearly approximated by assuming the wall temperature to be equal to the recovery temperature.

CONCLUDING REMARKS

From this preliminary analysis, it appears that both the turbulent heat transfer and skin friction measured on the X-15 may be correlated in the same manner, that is, by neglecting the effect of wall temperature in the calculation of the reference temperature. This result suggests that the Reynolds analogy factor is essentially constant for the X-15 heating conditions.

More conclusive results are anticipated from future tests on the X-15 during which skin-friction, heat-transfer, and boundary-layer-noise measurements will be made simultaneously. In addition to obtaining data under the normal X-15 surface heating conditions, it appears that data could be obtained at "very cold wall" conditions. The means of obtaining a "very cold wall" would be similar to the technique used in Project Fire--the instrumented surface would be suddenly exposed to high heating by releasing an insulating cover. Initial wall-to-recovery temperature ratios would be near $T_W/T_R = 0.2$. The high heating rates would improve the accuracy in deriving heat-transfer coefficients from the measured skin temperatures and, with simultaneous measurement of the surface shear, Reynolds analogy factor would be obtained.

REFERENCES

1. Banner, Richard D.; Kuhl, Albert E.; and Quinn, Robert D.: Preliminary Results of Aerodynamic Heating Studies on the X-15 Airplane. NASA TM X-638, 1962.

2. Eckert, Ernst R. G.: Survey on Heat Transfer at High Speeds. WADC Tech. Rep. 54-70 (Contract No. AF 33(616)-2214, RDO No. 474-143), Wright Air Dev. Center, U.S. Air Force, Apr. 1954.

3. Sommer, Simon C.; and Short, Barbara J.: Free-Flight Measurements of Turbulent-Boundary-Layer Skin Friction in the Presence of Severe Aerodynamic Heating at Mach Numbers From 2.8 to 7.0. NACA TN 3391, 1955.

4. Van Driest, E. R.: The Problem of Aerodynamic Heating. Aero. Eng. Rev., vol. 15, no. 10, Oct. 1956, pp. 26-41.

5. Quinn, Robert D.; and Kuhl, Albert E.: Comparison of Flight-Measured and Calculated Turbulent Heat Transfer on the X-15 Airplane at Mach Numbers From 2.5 to 6.0 at Low Angles of Attack. NASA TM X-939, 1964.

6. Reshotko, Eli; and Tucker, Maurice: Approximate Calculation of the Compressible Turbulent Boundary Layer With Heat Transfer and Arbitrary Pressure Gradient. NACA TN 4154, 1957.

7. Persh, Jerome; and Lee, Roland: Tabulation of Compressible Turbulent Boundary Layer Parameters. NAVORD Rep. 4282, U.S. Naval Ordnance Lab. (White Oak, Md.), May 1, 1956.

8. Banas, Ronald P.: Comparison of Measured and Calculated Turbulent Heat Transfer in a Uniform and Nonuniform Flow Field on the X-15 Upper Vertical Fin at Mach Numbers of 4.2 and 5.3. NASA TM X-1136, 1965.

9. Matting, Fred W.; Chapman, Dean R.; Nyholm, Jack R.; and Thomas, Andrew G.: Turbulent Skin Friction at High Mach Numbers and Reynolds Numbers in Air and Helium. NASA TR R-82, 1961.

10. Spalding, D. B.; and Chi, S. W.: The Drag of a Compressible Turbulent Boundary Layer on a Smooth Flat Plate With and Without Heat Transfer. J. Fluid Mech., vol. 18, part I, Jan. 1964, pp. 117-143.

11. Danberg, James E.: Characteristics of the Turbulent Boundary Layer With Heat and Mass Transfer at M=6.7. NOLTR 64-99, U.S. Naval Ordnance Lab. (White Oak, Md.), Oct. 19, 1964.

12. Bartz, D. R.: Turbulent Boundary-Layer Heat Transfer From Rapidly Accelerating Flow of Rocket Combustion Gases and of Heated Air. Vol. 2 of Advances in Heat Transfer, James P. Hartnett and Thomas F. Irvine, Jr., eds., Academic Press, 1965.

13. Bertram, Mitchell H.; and Neal, Luther, Jr.: Recent Erperiments in Hypersonic Turbulent Boundary Layers. Presented at the AGARD Specialists Meeting on Recent Developments in Boundary-Layer Research (Naples, Italy), May 10-14, 1965.

14. Schlichting, Hermann: Boundary Layer Theory. Fourth ed., McGraw-Hill Book Co., Inc., 1960.

15. Dorrance, William H.: Viscous Hypersonic Flow. Theory of Reacting and Hypersonic Boundary Layers. McGraw-Hill Book Co., Inc., 1962, p. 189.

16. Rubesin, Morris W.: A Modified Reynolds Analogy for the Compressible Turbulent Boundary Layer on a Flat Plate. NACA TN 2917, 1953.

17. Winkler, Eva M.; and Cha, Moon H.: Investigation of Flat Plate Hypersonic Turbulent Boundary Layers With Heat Transfer at a Mach Number of 5.3. NAVORD Rep. 6631, U.S. Naval Ordnance Lab. (White Oak, Md.), Sept. 15, 1959.

18. Hill, F. K.: Turbulent Boundary Layer Measurements at Mach Numbers From 8 to 10. The Physics of Fluids, vol. 2, no. 6, Nov.-Dec., 1959.

19. Lobb, R. K.; Winkler, Eva M.; and Persh, Jerome: NOL Hypersonic Tunnel No. 4 Results VII: Experimental Investigation of Turbulent Boundary Layers in Hypersonic Flow. NAVORD Rep. 3880, U.S. Naval Ordnance Lab. (White Oak, Md.), Mar. 1, 1955.

20. Rochelle, William C.: Prandtl Number Distribution in a Turbulent Boundary Layer With Heat Transfer at Supersonic Speeds. DRL-508, Defense Research Lab., Univ. of Texas. Oct. 1963.

21. Colburn, A. P.: A Method of Correlating Forced Convection Heat-Transfer Data and a Comparison With Fluid Friction. Trans. Amer. Inst. Chem. Eng., vol. 29, 1933, pp. 174-210.

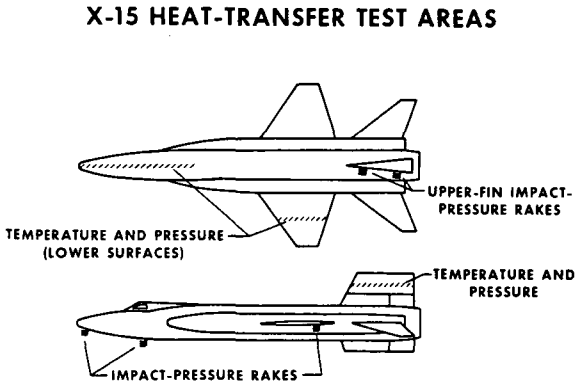

Figure 1

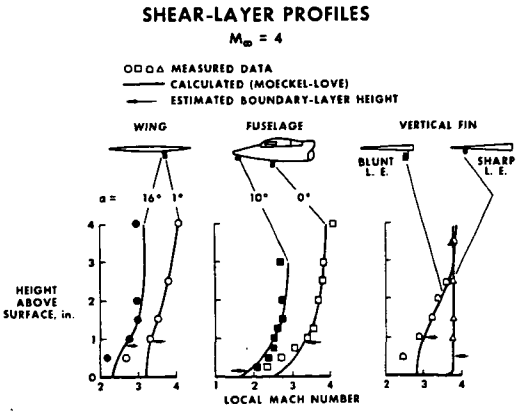

Figure 2

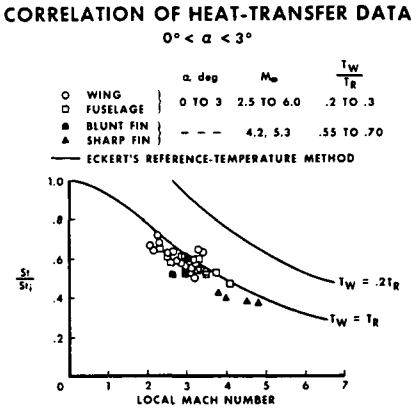

Figure 3

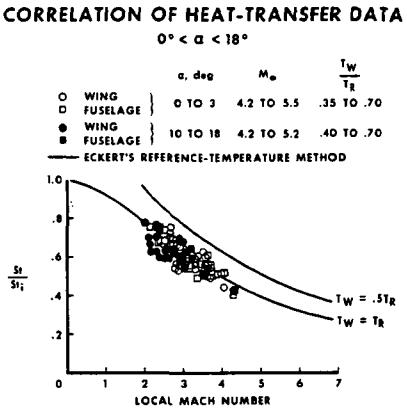

Figure 4

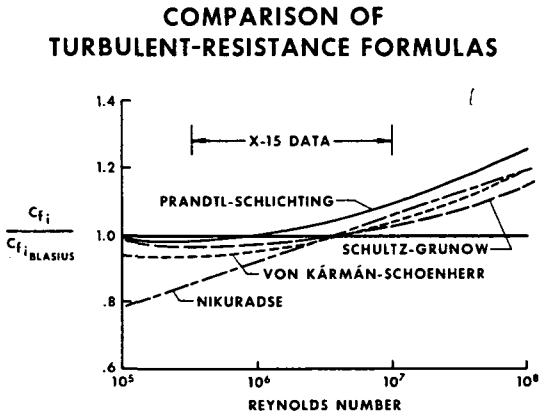

Figure 5

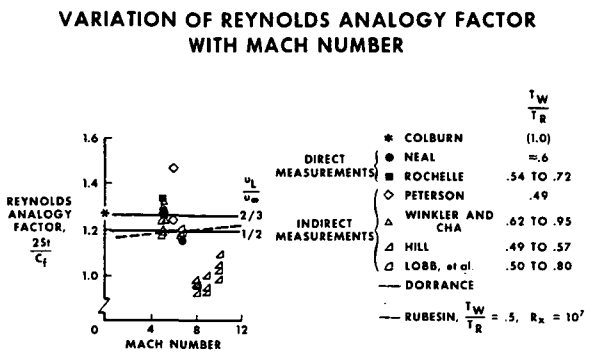

Figure 6

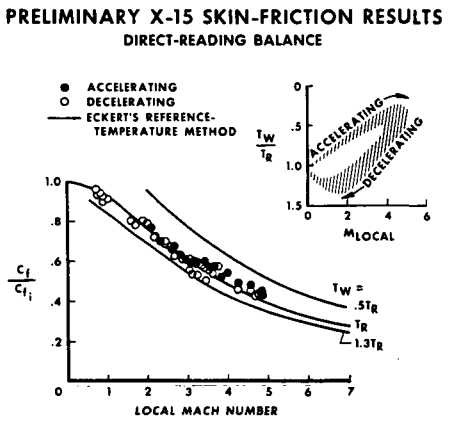

Figure 7

3. FLIGHT MEASUREMENTS OF BOUNDARY-LAYER NOISE ON THE X-15

By Thomas L. Lewis and Norman J. McLeod
NASA Flight Research Center

SUMMARY

Boundary-layer-noise data measured in flight over a Mach number range from 1.0 to 5.4 and at altitudes from 45 000 feet to 105 000 feet are presented. The data were obtained at four locations on the X-15 (selected to provide varied boundary-layer conditions). The highest recorded noise level was 150 decibels. Boundary-layer parameters were measured at one location and are used to present the noise data in a nondimensional form for comparison with data from flat-plate wind-tunnel studies by other experimenters.

INTRODUCTION

The research on heat transfer and skin friction discussed in the previous paper by Banner and Kuhl (paper 2) is only part of the problem associated with boundary-layer flow. Another important aspect is the noise generated in the boundary layer by fluctuating pressures.

One of the factors affected by the fluctuating pressures is structural weight. This effect is demonstrated by use of a simplified structure, as illustrated in figure 1, which is taken from reference 1. In this example, the skin thickness required for adequate fatigue life in an acoustic environment is shown. The schematic diagram at the lower right illustrates the structure. The results presented show that an increase of sound level from 115 dB to 125 dB would require an increase in skin thickness from 0.03 inch to about 0.06 inch. An increase in rib thickness is also required to withstand the more severe environment. This 10-dB increase in sound level would result in a structural weight increase of at least 75 percent.

Noise levels shown in this example are lower than may be encountered in flight, but the curve clearly indicates that for higher noise levels, the increase in weight will be greater. Also, acoustic insulation necessary for passenger comfort will increase the weight.

Graphs of this type established on the basis of ground tests might be used in the design of aircraft structures if the noise levels could be predicted for new flight regimes. Unfortunately, the state of the art leaves much to be desired in this respect, and the designer must rely on measured noise data. In the past only a few in-flight measurements of boundary-layer noise over a significant range of flight conditions have been taken.

The X-15 offers the capability of obtaining noise data over a wide range of dynamic pressure and Mach number that exceeds those available from the flight envelopes of present and proposed aircraft up to Mach 6.

SYMBOLS

C_{f_i} incompressible skin-friction coefficient

dB decibels ($dB = 20 \log_{10} \frac{\sqrt{\bar{p}^2}}{\sqrt{\bar{p}_o^2}}$, where $\sqrt{\bar{p}_o^2}$ 4.177×10^{-7} pounds per square foot)

h_p altitude, feet

l rib spacing, inches

M Mach number

$\sqrt{\bar{p}^2}$ root-mean-square value of pressure fluctuations (sound level), pounds per square foot

$\overline{p^2(\omega)}$ mean-square pressure fluctuation per unit bandwidth (defined by $\overline{p^2} = \int_0^\infty \overline{p^2(\omega)} d\omega$), $lb^2\text{-sec/ft}^4$

q dynamic pressure, pounds per square foot

R_θ Reynolds number based on momentum thickness

t_s skin thickness, inches

U local velocity outside boundary layer, feet per second

β constant of proportionality

δ^* boundary-layer displacement thickness, feet

ω frequency, radians per second

Subscript:

$( )_\infty$ refers to free-stream conditions

INSTRUMENTATION

For the boundary-layer noise experiments on the X-15, five locations have been selected to obtain data. These locations are shown in figure 2 (ref. 2). Location 5 has been recently chosen for investigation because at this location a large amount of boundary-layer information on heat transfer and skin friction has been obtained, as reported by Banner and Kuhl

in paper 2. As yet, however, no noise data have been obtained at this location.

At present, flow measurements have been taken only at location 1. The test panel used for the study is shown in figure 3. On the forward end of the panel is a mounting block which holds the microphone and temperature-sensing elements. These temperatures are used for microphone calibration. An accelerometer that was attached to the back of the mounting block was used to verify that no corrections were necessary to the acoustic data because of vibrations. Behind the microphone is a boundary-layer rake and a static-pressure orifice to determine local flow conditions.

All noise, acceleration, and pressure data were recorded on an onboard tape recorder, and temperature was recorded on an oscillograph.

The microphones were calibrated for linearity, frequency response, the effect of altitude, steady-state temperatures, and transient temperatures. These calibrations resulted in an estimated accuracy of ±3 dB over a frequency range from 50 to 10 000 cycles per second for all flight conditions.

RESULTS AND DISCUSSION

Test conditions for a typical X-15 flight that was made primarily to obtain boundary-layer noise data are shown in figure 4. The vehicle was launched at an altitude of 45 000 feet, was accelerated to a Mach number of 5.4, and attained a maximum altitude of 105 000 feet. The maximum free-stream dynamic pressure is shown to be approximately 1000 pounds per square foot. It should also be mentioned that during the portion of the flight where Mach number and dynamic pressure are changing slowly, the angle of attack was relatively constant. The purpose of this flight profile was to keep the environment from changing too rapidly.

Data illustrating how the noise varied at different points on the airplane during this flight are presented in figure 5. Time histories of the sound level in decibels are shown only for locations 1 to 4 (which are indicated in fig. 2). The times for launch, engine burnout, and Mach 1 during deceleration are marked on the abscissa scale in figure 5.

Noise levels for the two midfuselage stations (locations 1 and 2) are illustrated by the solid and dashed lines, for the aft fuselage station (location 3) by the upper line, and for the base region (location 4) by the lower line. For the most part, there is only a 20-dB spread in the levels--but this 20-dB spread means that the highest sound levels recorded are ten times the lowest, which illustrates the range of the designers' problems. Note also the sudden jump in the traces for locations 3 and 4 at the time when the speed brakes were extended. This result shows that protuberances on the surface of the vehicle can cause large increases in the noise level.

Although the overall sound levels are important, the distribution of the sound in frequency bands is also important, as is shown in figure 6. For these data, the free-stream Mach number was 5.2 and the dynamic pressure was 380 pounds per square foot. The sound level is shown in decibels for the overall noise and for each octave band (center frequencies from 63 to 8000 cps). Locations 1 and 3, which are on the lower surface of the side fairings, have the highest sound levels, particularly at the higher frequencies. Location 2 on the upper side fairing has its highest noise level predominantly in the lower frequencies. The spectrum for location 4 on the left blowout panel is lower in each octave band and is approximately flat.

In order to examine the effect of compressibility on boundary-layer noise, figure 7 shows a comparison of X-15 data with subsonic data obtained by other experimenters (refs. 3, 4, and 5). For this comparison the data from location 1 are examined. For the X-15 data, an equivalent flat plate incompressible skin-friction coefficient was calculated by using Blasius' formula with the measured-momentum-thickness Reynolds number.

According to reference 3, Kraichnan's analysis of the boundary layer on a flat plate indicated the proportionality constant β to be in the range from 2 to 12. Wind-tunnel investigations at low speed have given values from 2.5 to 4.8. The X-15 data indicate values from 2 to 4.6 and show a tendency to decrease slightly with increasing Mach number. (Because this is an equivalent-flat-plate comparison, only X-15 data which closely approximate these conditions are shown here.) The results indicate that the general levels of this dimensionless coefficient, at this location, are changed very little by effects of compressibility.

Since the comparison between data from wind tunnel at subsonic speeds and from flights at high supersonic speeds shown in this figure deals only with the overall sound pressure, it is of interest to compare the frequency content. Willmarth, Serafini, and others (refs. 3 to 6) have shown that the noise power in the frequency bands can be normalized in terms of the boundary-layer displacement thickness and local free-stream velocity. This procedure has been applied to some of the X-15 data, and the results are shown in figure 8. The results on this chart show that the frequency content of the noise measured in flight is significantly different from the wind-tunnel noise. This difference lies in how the energy is distributed over the frequency range. The flight data have more energy at the low frequencies and less energy at the high frequencies than the wind-tunnel data. Even though the data are for two widely different Mach numbers, it cannot be concluded at this time that the difference can be attributed entirely to Mach number, since it is known that the X-15 surface has considerable roughness. In boundary-layer flow, the effects of surface roughness, typical of flight vehicles, perturbs the boundary-layer pressure fluctuations in the lower frequencies even at subsonic speeds.

The results on these two charts, although somewhat preliminary, show that the theory of Kraichnan (as given in ref. 3), supported by wind-tunnel measurements at subsonic speeds, can be used to estimate the total noise expected on a hypersonic flight vehicle but it does not give a true picture of the energy distribution that is important for design.

CONCLUDING REMARKS

Flight results from boundary-layer noise measurements at specific locations on the X-15 have been presented and a limited comparison with analytical equivalent flat-plate results is made. These results indicate that more extensive flight measurements are required to establish a guide for the theoretical studies and laboratory tests that are necessary to define the characteristics of boundary-layer noise.

Continued effort in the X-15 boundary-layer-noise program is necessary to provide for the extension of the range of the present data, as well as to permit a comprehensive analysis of the noise at other locations, particularly on the vertical tail where data can be obtained that can be favorably compared with flat-plate experiments of other investigations.

REFERENCES

1. Hubbard, Harvey H.; Edge, Philip M., Jr.; and Modlin, Clarence T., Jr.: Design Considerations for Minimizing Acoustical Fatigue in Aircraft Structures. WADC-University of Minnesota Conference on Acoustical Fatigue, W. J. Trapp and D. M. Forney, Jr., eds., WADC Tech Rep. 59-676, U.S. Air Force, March 1961, pp. 321-338.

2. Kordes, Eldon E.; and Tanner, Carole S.: Preliminary Results of Boundary Layer Noise Measured on the X-15 Airplane. Acoustical Fatigue in Aerospace Structures. Walter J. Trapp and Donald M. Forney, Jr., eds., Syracuse University Press, May 1964, pp. 85-96.

3. Serafini, John S.: Wall-Pressure Fluctuations and Pressure-Velocity Correlations in a Turbulent Boundary Layer. NASA TR R-165, 1963.

4. Willmarth, William W.: Wall Pressure Fluctuations in a Turbulent Boundary Layer. NACA TN 4139, 1958.

5. Willmarth, W. W.: Space-Time Correlations and Spectra of Wall Pressure in a Turbulent Boundary Layer. NASA MEMO 3-17-59W, 1959.

6. Lilley, G. M.; and Hodgson, T. H.: On Surface Pressure Fluctuations in Turbulent Boundary Layers. AGARD Rep. 276, April 1960.

EFFECT OF NOISE ON SKIN THICKNESS

EXAMPLE FOR TYPICAL SKIN-STRINGER CONSTRUCTION

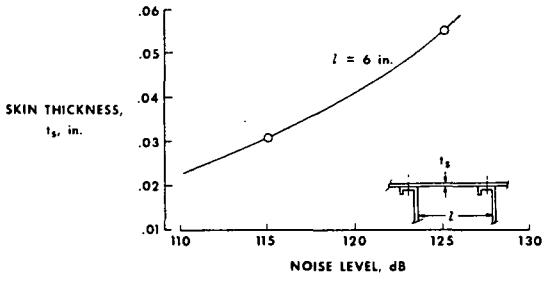

Figure 1

MICROPHONE LOCATIONS ON THE X-15

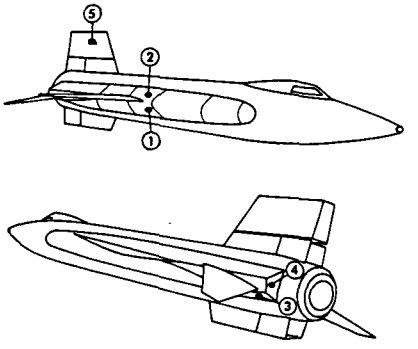

Figure 2

BOUNDARY-LAYER-NOISE TEST PANELS

LOCATION 1 (RIGHT SIDE FAIRING)

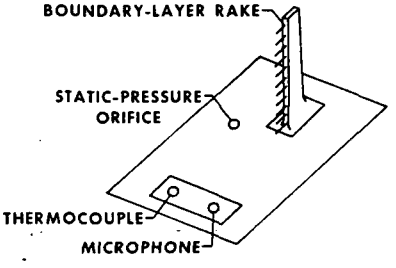

Figure 3

TYPICAL FLIGHT CONDITIONS FOR MEASUREMENT OF X-15 BOUNDARY-LAYER NOISE

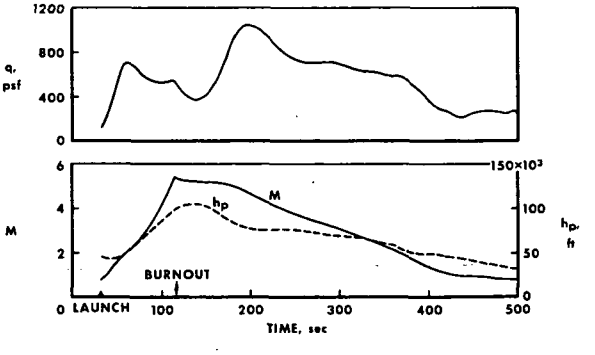

Figure 4

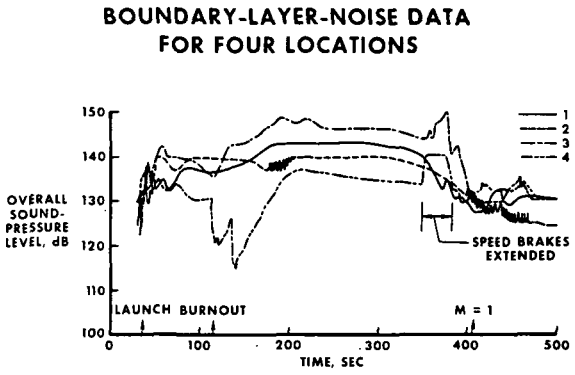

Figure 5

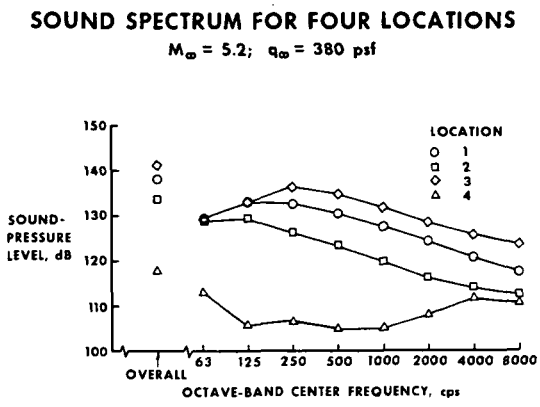

Figure 6

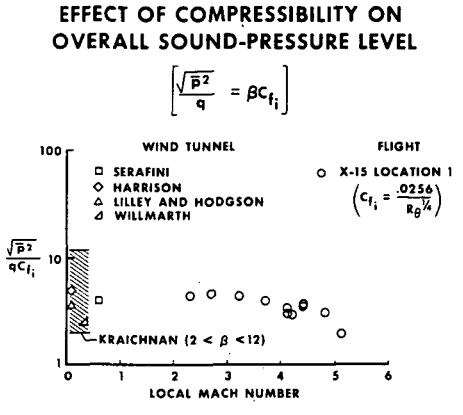

Figure 7

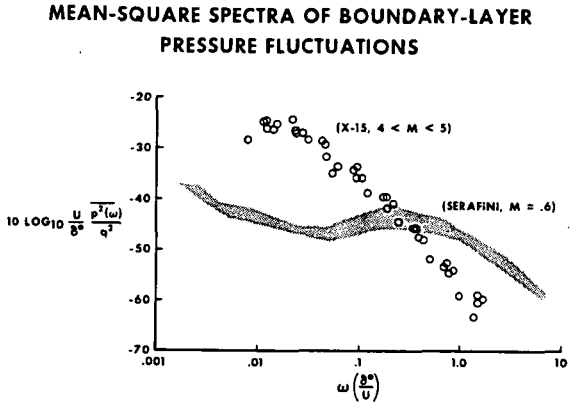

Figure 8

4. A SUMMARY OF THE X-15 LANDING LOADS

By James M. McKay and Richard B. Noll
NASA Flight Research Center

SUMMARY

The dynamic response of the X-15 airplane at touchdown is reviewed briefly to show the unusual landing characteristics resulting from the airplane configuration. The effect of sinking speed is discussed, as well as the influence of the horizontal-stabilizer load, wing lift, and increased landing weight on the landing characteristics. Consideration is given to some factors providing solutions to these problems, such as stability augmentation damper cutout at gear contact, pilot manipulation of the stabilizer, the use of a stick pusher at touchdown, and a proposed third skid installed in the unjettisoned portion of the lower ventral fin. Studies have been made to determine the effect on the main-landing-gear loads of relocating the X-15 nose gear.

INTRODUCTION

A short summary of the X-15 landing-gear-loads results was presented in reference 1, in which the landing gear was indicated to be a source of concern. Because of the marked departure of the X-15 landing-gear system from conventional aircraft landing gear, the unexpectedly high loads that occurred did not correlate with the normally used design parameters of angle of attack, sinking speed, and weight. These high loads and the parameters affecting them can be explained only by means of an overall dynamic analysis. With the dynamic analysis and the experience gained in 151 landings, a better understanding was obtained of the landing-gear loads and the dynamics which affect them. Throughout the program typical modifications were made to increase the energy-absorption capacity of the gear. However, these changes were restricted by practical hardware considerations with the result that some problems were unresolved. These problems have been overcome to date by modifying the landing procedure. The purpose of this paper is to review the present status of the X-15 landing-gear loads, to discuss the parameters which affect these loads, and to show additional modifications that might be made to improve the landing-gear system.

SYMBOLS

F_T	horizontal-stabilizer aerodynamic load, pounds
L	lifting force, pounds
W	airplane landing weight, pounds

α angle of attack, degrees

δ_h horizontal-stabilizer deflection, degrees

GENERAL DESCRIPTION

The locations of the landing gear are shown in figure 1, which also includes a diagram to indicate the nature of the main-gear operation. The main landing gear, located well aft on the fuselage and directly beneath the horizontal tail, consists of steel skids and Inconel X struts attached through bellcrank arms to shock struts inside the fuselage. Drag braces are attached to the fuselage ahead of the trunnion and to the skid at the strut-attachment pin. During flight, the skids and landing-gear legs are folded forward against the outside of the fuselage. The nose gear, located very far forward on the fuselage, is of conventional design, nonsteerable, with dual co-rotating wheels for the prevention of shimmy.

DISCUSSION

Main-Gear Response

Many of the features of an X-15 landing are very unusual, and these characteristics are illustrated in figure 2. The main-gear shock-strut force, measured with respect to time from main-gear touchdown, is shown, and sketches are included to identify the landing sequence. The airplane weight, wing lift, and tail loads are indicated by the arrows on each sketch. The sketch at the left shows that a nose-high attitude is established just prior to touchdown. The first peak on the force curve occurs as the vertical velocity at the main gear is arrested, as indicated by the second sketch. Up to this time, the reactions are similar to those for a conventional airplane because the force in the gear depends upon the weight and the vertical velocity of the airplane. Here the similarity ends. Since the center of gravity of the airplane is well ahead of the main gear, a rapid nose-down rotation occurs, and the airplane impacts hard on the nose gear, as illustrated in the third sketch. The high pitch rate cannot be controlled by the pilot because the stabilizer is directly above the main gear. The nose-gear touchdown for the landing illustrated occurred about 0.8 second after the initial main-gear touchdown and usually occurs within 1.0 second for all X-15 landings. As the airplane rotates downward, the wing lift is rapidly decreased and a pronounced down load occurs on the stabilizer. The result is an increased force on the main gear shown as the second peak in the last sketch. Notice that the force at the second peak is much greater than at the first peak.

The design of the X-15 landing gear, based on weight and sinking speed, as for conventional systems, does not consider all factors that contribute to the gear loads. This is emphasized in figure 3, which shows shock-strut force plotted against sinking speed at touchdown for many landings. The first peak, indicated by the circular symbols, has a definite relationship to the sinking

speed, but the second peak, which is the critical one, identified in the plot by the square symbols, is essentially independent of sinking speed. Note that the values for the second peak closely approach the design limit and some exceed this limit.

Effect of Horizontal-Stabilizer Angle

An analytical study of the landing dynamics showed that several important parameters affecting the second reaction involved aerodynamic factors. At this point in the X-15 program the problem was no longer one of understanding the nature of the loads but rather one of how best to reduce them. It was realized that the stabilizer down loads were caused by efforts of both the pilot and the stabilizer augmentation system to prevent the rapid rotation onto the nose gear (ref. 2). The effect of stabilizer angle on the gear loads is shown in figure 4, where the maximum shock-strut load is plotted as a function of the stabilizer setting that occurred at nose-gear touchdown. Immediately prior to touchdown, the stabilizer trim position is between 4° and 5° leading edge down. If the pilot pulls back on the stick and puts the leading edge farther down, the loads increase. If he pushes the stick forward and gets the leading edge up, the loads decrease, as shown at the right of this figure. It is evident that the gear loads can be significantly reduced if the stabilizer angle is prevented from moving in the leading-edge-down direction during the landing itself. It is important to note that this parameter was the first one with which the landing data appeared to be correlated.

Effect of Wing Lift

The second factor affecting the landing-gear loads is the wing lift. Again, the inability to prevent rapid rotation onto the nose gear results in higher gear loads because of the sudden decrease in wing lift (ref. 2). Figure 5 shows the effect of wing lift on the main-gear loads as a function of touchdown velocity. Notice that increasing wing lift on the ordinate scale designates a decreasing gear load. Data at nose-gear touchdown fall between the calculated curves for angles of attack of 0° and -4°. The overall trend, as expected, is an alleviation of the main-gear load with increasing angle of attack. These results also indicate that, as long as a positive wing lift can be maintained during the nose-gear touchdown, any increase in landing velocity is also an alleviating factor.

In the data obtained for the only flaps-up landing made to date, shown by the solid symbol, the wing lift decreased to a down load, which added to the load on the main gear. The rapid loss of wing lift is minimized in conventional aircraft by locating the main gear so that the stabilizer is effective in controlling the rotation. This location for the landing gear, however, is impractical for the X-15 configuration.

Effect of Landing Weight

The third factor of major concern is weight. The X-15 landing weight has increased steadily from the initial landing weight of 13 230 pounds and presently ranges between 15 000 pounds and 15 500 pounds. Although weight alone is not the most significant factor in determining the maximum gear load, it is still true that, other things being equal, the greater the weight, the higher the load. The effect of weight is shown in figure 6, where data are presented for which all parameters except weight are constant, or at least tightly bounded. Two sets of points are shown representing maximum shock-strut load as a function of landing weight. The circular points are from landings with stabilizer settings at nose-gear touchdown of -16° to -24°. The square points are from landings at lower stabilizer settings of -4° to 4°. A line has been faired through each set of points. For the landings made with the higher stabilizer settings, the limit load would be reached at a landing weight of 15 700 pounds. In the event of an emergency, the landing weight with residual fuel aboard may run as high as 17 000 pounds. Only by a pilot push maneuver to obtain low stabilizer settings can this type of landing be accomplished successfully. Although the design limit would be exceeded, the loads could be held below the yield limit as indicated.

The extreme values of the stabilizer setting, wing lift, and increased landing weight occurred simultaneously during an emergency landing of the X-15-2 airplane in Nevada. The pilot routinely pulled back on the control stick, driving the stabilizer leading edge down to its maximum value. In addition, the flap mechanism failed at the same time and resulted in a down load on the wing and, therefore, on the gear. And finally, residual fuel increased the landing weight by about 1000 pounds. The combined result was an overstressed gear, which, of course, failed.

Of all the factors affecting the gear loads, the most difficult to control, without restricting the research role of the aircraft, is weight. The contribution of the stabilizer setting is more easily controlled by the pilot push maneuver. In addition, a switch has been installed to disengage the stability-augmentation system at main-gear touchdown to prevent the control system from forcing the stabilizer leading edge down. Experience has shown that the pilot can be depended upon to push the stick during normal landings even though the push maneuver must occur within 0.4 second after main-gear touchdown to be effective in reducing the gear loads. However, this maneuver is unnatural for the pilot and, in an emergency, he is apt to revert to habits formed through prior experience and pull back on the stick. For these reasons, an automatic stick pusher has been developed, which, like the disengage switch, will be activated at touchdown. This device is being installed on the aircraft and will undergo flight evaluation.

Another approach under consideration is to alleviate the main-gear loads by use of a third skid. This concept is shown in figure 7, in which a photograph has been retouched to show a third skid located in the unjettisoned portion of the lower vertical stabilizer between the present two skids. The skid would be effective in redistributing the load and in relieving the critically stressed gear components, particularly if either the stick pusher or the

landing flaps failed to operate. The third skid concept is presently undergoing design evaluation.

Following the accident of the X-15-2 airplane, consideration was given to a design for a new landing gear which would apply the experience gained with the basic X-15 gear system. However, constraints on the program, which dictated minimum modifications, resulted in a gear system that was changed very little from the original. The present gear locations were used and a dynamic analysis was utilized to aid the designers in rebuilding the gear system on the basis of the second reaction. Figure 8 shows the basic changes that were made. The gear was lengthened, the shock-strut stroke was increased, and the strut hydraulic and air-spring characteristics were altered for additional energy dissipation. However, the landing dynamics of the new gear were not appreciably changed and most of the deficiencies of the basic system were inherited. It was necessary, therefore, to incorporate the disengage switch for the stability augmentation system and the use of the pilot push maneuver in the gear design to permit operation of the X-15-2 airplane in all of its planned configurations.

Some changes also were made in the nose gear. The shock-strut stroke was increased to accommodate the increased weight of the vehicle. The trunnion was lowered 9 inches to allow an attitude at nose-gear touchdown similar to that of the basic X-15.

Further modifications of the X-15-2 main gear will be required for use with the proposed ramjet package. The landing-gear legs must be lengthened to provide ground clearance for the ramjet. This increase in length will reduce the attitude at nose-gear touchdown, but the length of the new nose gear is sufficient to maintain an attitude similar to the basic X-15. An emergency landing with the ramjet on board could be at a weight of almost 20 000 pounds, which is far beyond the capability of the present gear. However, dynamic analysis of a lengthened gear with modified shock-strut characteristics shows that by use of the disengage switch and an automatic stick pusher, the emergency condition can be tolerated. The third skid concept is also being considered to provide an additional margin of safety for the ramjet project.

Effect of Nose-Gear Location

If future modifications are to be made to the X-15 landing-gear system because of increased airplane weight or length, structural modifications will be required. Relocation of the main gear will still be impractical, but relocation of the nose gear is possible. The results of analytical studies on relocation of the nose gear on the basic X-15 are presented in figure 9, where maximum main-gear shock-strut load is shown as a function of nose-gear distance ahead of the center of gravity. Present location of the nose gear on the basic X-15 is approximately 23 feet ahead of the center of gravity as indicated in the figure. The main-gear loads can be significantly reduced by moving the gear farther back. The X-15 nose gear can be relocated behind the cockpit between 12 and 14 feet ahead of the center of gravity. Liquid-oxygen tank structure prevents a farther rearward location. Fortunately, the optimum

position is at 12 feet ahead of the center of gravity as a result of its close proximity to the center of percussion.

CONCLUSIONS

The X-15 landing-gear system is representative of a compromise between a gear of conventional design and location and a gear which possessed qualities of simplicity, ease of stowage, clearance for the lower vertical stabilizer, and slideout stability. Subsequent experience with the airplane has proved that the gear location caused much higher landing loads than were expected. These experiences, coupled with the increasing weight of the X-15 airplane, have required periodic modifications to the landing-gear system to provide an acceptable factor of safety. Most important, however, has been the success of the X-15 landing loads program in providing an understanding of the nature of the loads which established the requirement for the use of a dynamic analysis for predicting the loads.

REFERENCES

1. McKay, James M.; and Kordes, Eldon E.: Landing Loads and Dynamics of the X-15 Airplane. NASA TM X-639, 1962.

2. Noll, Richard B.; Jarvis, Calvin R.; Pembo, Chris; Lock, Wilton P.; and Scott, Betty J.: Aerodynamic and Control-System Contributions to the X-15 Airplane Landing-Gear Loads. NASA TN D-2090, 1963.

X-15 LANDING-GEAR SYSTEM

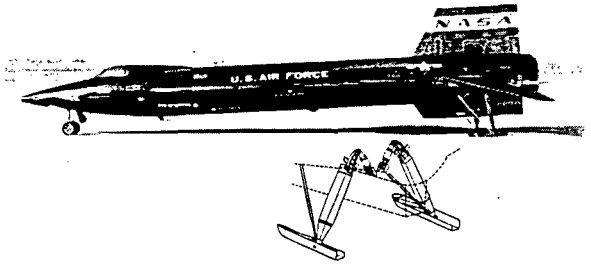

Figure 1

MAIN-GEAR SHOCK-STRUT FORCE

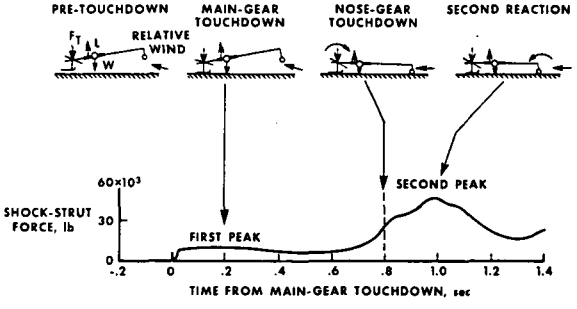

Figure 2

INFLUENCE OF AIRPLANE SINK SPEED ON MAIN-GEAR LOAD

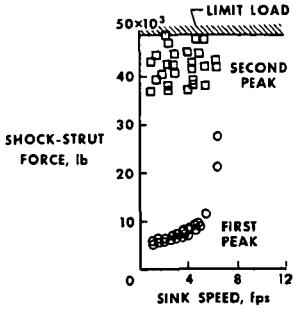

Figure 3

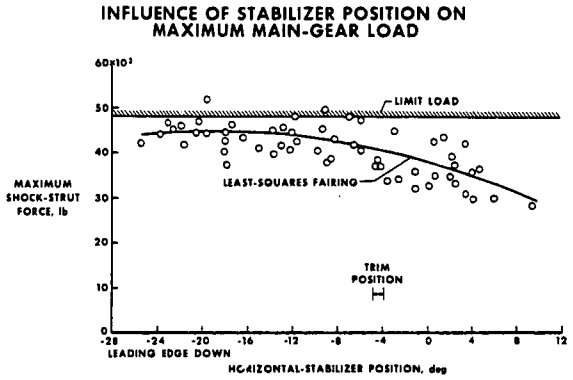

Figure 4

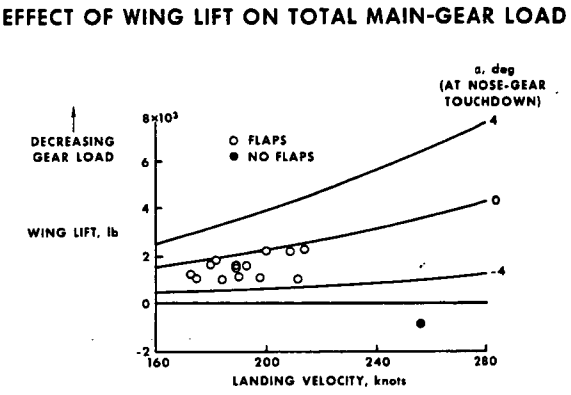

Figure 5

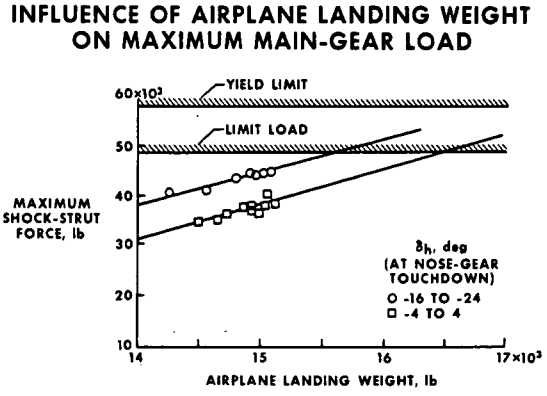

Figure 6

PROPOSED X-15 THIRD MAIN-SKID CONFIGURATION

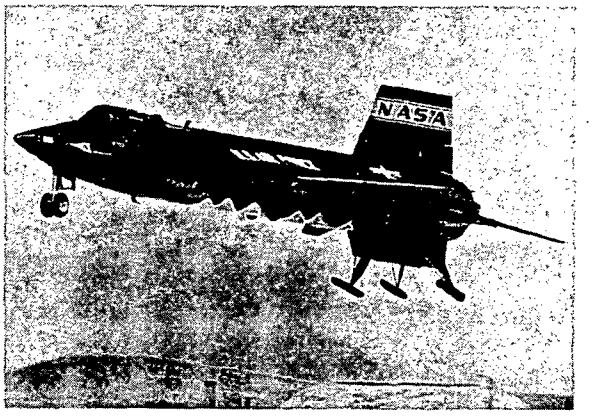

Figure 7

X-15 MAIN-LANDING-GEAR CHARACTERISTICS

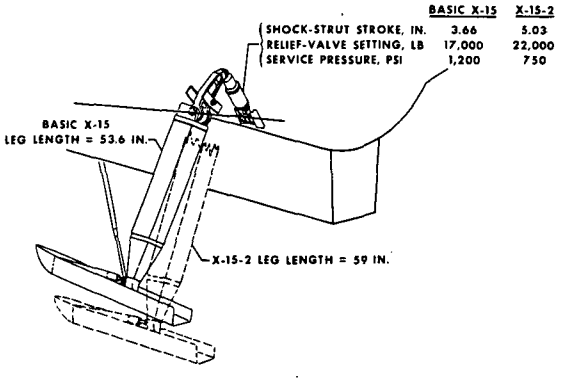

	BASIC X-15	X-15-2
SHOCK-STRUT STROKE, IN.	3.66	5.03
RELIEF-VALVE SETTING, LB	17,000	22,000
SERVICE PRESSURE, PSI	1,200	750

Figure 8

INFLUENCE OF NOSE-GEAR LOCATION ON MAIN-GEAR LOAD

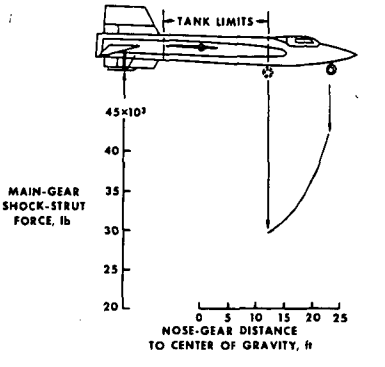

Figure 9

5. A REVIEW OF LATERAL-DIRECTIONAL HANDLING-QUALITIES CRITERIA AS APPLIED TO THE X-15

By Lawrence W. Taylor, Jr., Glenn H. Robinson, and Kenneth W. Iliff
NASA Flight Research Center

SUMMARY

The lateral-directional handling qualities of the X-15 have been extensively surveyed in terms of pilot ratings and vehicle response characteristics throughout the operational envelope of the airplane. Results are reviewed for two vertical-tail configurations as well as for dampers on and off, and significant problem areas are discussed in relation to the basic stability and control parameters and the influence of the pilot's control. These results are used to assess the validity and limitations of some of the lateral-directional handling-qualities design criteria currently in use. Finally, a new and more generally applicable criterion recently proposed by the NASA Flight Research Center is described and similarly assessed against a broad range of test conditions available with the X-15 vehicles.

5

INTRODUCTION

The flight experience with several X-15 airplane and damper configurations has provided the unique opportunity to obtain handling-qualities evaluations over a wide range of Mach number, angle of attack, and dynamic pressure. Inasmuch as the longitudinal handling qualities of the X-15 airplane were discussed at the last X-15 conference and subsequently published in reference 1, only the lateral-directional handling is discussed in this paper. Pilot ratings from flight and simulator are used to survey the handling qualities of the X-15 with and without the lower portion of the ventral fin and with and without the dampers operative. These results are then used to evaluate some of the more widely used handling-qualities criteria by comparing the X-15 ratings with those predicted by the criteria. A similar comparison is made with predicted pilot ratings obtained by using a recent method proposed by the NASA Flight Research Center. This method is described and charts are presented for use in predicting pilot ratings of the lateral-directional handling of many airplane configurations.

SYMBOLS

$C_{1/2}$ cycles to damp to one-half amplitude

K correction for roll coupling effect, $\left(\frac{\omega_\phi}{\omega_D}\right)^2$

L_{δ_a} roll acceleration due to aileron deflection, $1/second^2$

L_β roll acceleration due to sideslip, $1/second^2$

M Mach number

N_{δ_a} yaw acceleration due to aileron deflection, $1/second^2$

N_β yaw acceleration due to sideslip, $1/second^2$

V flight velocity, feet per second

v_e equivalent side velocity, $\beta V\sqrt{\sigma}$

α angle of attack, radians or degrees

α_o angle of attack of the principal X-axis, radians

β angle of sideslip, radians

δ_a aileron deflection, radians

ζ_D damping ratio of the Dutch roll mode

φ bank angle, radians

σ ratio of air density at altitude to that at sea level

τ_R time constant of the roll mode, seconds

ω_D undamped natural frequency of the Dutch roll mode, radians per second

ω_φ undamped natural frequency of the numerator of the roll to aileron transfer function, radians per second

Subscript:

max maximum

SUMMARY OF X-15 CHARACTERISTICS

The scope of the X-15 handling-qualities survey is indicated in figure 1 in terms of Mach number and angle of attack for all X-15 configurations investigated. Mach number and angle of attack are chosen because of the

influence of these parameters on the stability derivatives and, consequently, on the handling of the airplane. Significant changes in handling qualities also result from changes in configuration and from the use of dampers. Four configurations are considered consisting of dampers on and off and lower ventral on and off. Although flight evaluations were restricted to a range of dynamic pressures of 200 to 1000 pounds per square foot, with a rocket-powered airplane such as the X-15, evaluation time at each condition is limited because of the highly transient nature of the flight. Therefore, the pilot was required to assess the handling qualities in a much briefer period of time than is available with other airplanes. In general, the ratings reflect the airplane response to control pulses, roll commands, sideslips, turns, or similar maneuvers.

Since all flight conditions of interest could not be adequately covered for the specific configurations considered, the X-15 flight simulator was used to supplement the data obtained in flight. The simulator was particularly useful in assessing marginally controllable conditions where undue risk would be incurred in attempting to obtain flight ratings.

The overall assessment of the lateral-directional handling qualities used is based on the pilot-rating scale shown in table I. The pilot ratings are defined by a 10-point scale similar to the Cooper scale with ratings from 1 to 3.5 being satisfactory; 3.5 to 6.5, unsatisfactory; and 6.5 to 10, unacceptable. These ratings will be designated by symbols with increased shading to represent less favorable ratings and with squares and circles to differentiate flight from simulator data, respectively.

The lateral-directional pilot ratings for the X-15 configuration with the lower ventral on are presented in figures 2 and 3. In figure 2 the dampers are disengaged, whereas in figure 3, the dampers are on. Pilot ratings are shown as a function of angle of attack and Mach number with simulator results represented by the contours and the flight data by the squares. With the dampers off (fig. 2) two areas of extremely poor handling qualities are evident in the contours for a pilot rating of 10. One is in the neighborhood of an angle of attack of 11° and Mach 3.5 and the other is in the region of combined high angle of attack and high Mach number. In both areas, coupling of the lateral and directional motions is severe and results in uncontrollable pilot-induced lateral oscillations. The coupling is caused principally by excessive "favorable yaw" (yaw in the direction of the roll) in conjunction with very low Dutch roll damping. The strong coupling actually decreases the damping. Note that the pilot ratings from flight show the same trend as those from the simulator, but the simulator data are generally optimistic for this condition.

Figure 3 shows the effect of engaging the damper systems and, as expected, the handling qualities are substantially improved. The configuration is now controllable throughout the entire envelope, although some unacceptable simulator ratings remain in the formerly uncontrollable region at high Mach numbers and angles of attack. Even with the dampers engaged (fig. 3), the effect of the coupling is objectionable at the high angles of attack. The dampers do not materially alter the coupling, but do remove or

reduce the tendency for the pilot to feed an oscillation of the Dutch roll mode. The few flight ratings that have been obtained at the high angles of attack do not indicate this trend, however.

The comparison of figures 2 and 4 shows the effect of removing the lower portion of the ventral with the dampers off. This change in configuration is seen generally to improve the lateral-directional handling, particularly in the area which was formerly uncontrollable. The principal reason for this improvement, as discussed at some length in reference 2, is the elimination of the negative dihedral effect. Removing the ventral, however, also reduces the static stability and, as a result, the handling qualities are slightly degraded at the lower speeds. The reduced stability also gives rise to roll sluggishness (and even roll reversal) at high angles of attack in the subsonic range. The roll reversal is of little consequence, however, since it lies outside the operating envelope. A trace of the pilot-induced lateral-oscillation problem still exists with the ventral and dampers off, at high Mach numbers at an angle of attack near zero degrees. However, with the coarse simulator contours used, the problem is not evident in figure 4, although it is predicted by the simulator. The flight and simulator ratings generally show the same trend with angle of attack, but the simulator ratings are more pessimistic than those from flight.

A comparison of figures 4 and 5 shows the effect of engaging the dampers with the ventral-off configuration. With the dampers on, satisfactory ratings are obtained from flight and the simulator for the lower angles of attack. No worse than unsatisfactory ratings were given for the higher angles of attack. For this reason, almost all of the flights since the last X-15 conference (1961) have been flown with the lower ventral off.

EVALUATION OF CRITERIA

This summary of the handling qualities in flight regimes not generally operational with other aircraft affords the opportunity to investigate the applicability to the X-15 of some of the more widely used handling-qualities criteria. The criteria considered were derived with varied, though well defined, control objectives and flight missions using various airplanes and simulators. These missions may or may not have been appropriate for current airplanes, such as the X-15. However, it should be of interest to compare the predicted handling with the pilot ratings of the overall lateral-directional dynamic stability and control of the X-15.

Consider first the lateral control criterion proposed in reference 3 (fig. 6). This criterion was developed originally for fighter-type airplanes and was later revised for reentry vehicles (ref. 4). In this study, pilot-rating contours were established in terms of lateral control power and roll damping. The abscissa is the roll time constant, which is inversely proportional to the roll damping. Damping, therefore, increases to the left. The ordinate is the maximum roll control power available to the pilot and has been adjusted to account for coupling of the roll and Dutch roll modes and the

nonlinear gearing of the X-15. Because the maximum control stick deflections are about the same for all airplanes, the parameter also reflects control sensitivity.

This criterion, it should be noted, was based on single-degree-of-freedom uncoupled roll studies performed on fixed and moving base simulators. Good correlation with results from flight, especially where the lateral-directional motions are highly coupled, would, therefore, not be expected. The limitations of the criterion are pointed out in reference 4. A comparison with X-15 flight ratings in this paper is intended only to examine the adequacy of the criterion for evaluation of the overall handling qualities.

If there were perfect correlation between the X-15 pilot ratings (given by the symbols) and the contours of the criterion, only unshaded symbols (satisfactory) would appear in the innermost area, half-shaded symbols (unsatisfactory) between the contours for pilot ratings of 3.5 and 6.5, and shaded symbols (unacceptable) outside the 6.5 contour. The data, unfortunately, do not correlate in this manner. There is, however, a reasonable division between the satisfactory and unacceptable pilot ratings. The unacceptable ratings which fall in the satisfactory area are attributed to unsatisfactory characteristics due to coupling effects, such as a pilot-induced oscillation tendency not predicted by this criterion.

The histogram shown in figure 7 indicates the degree of correlation and bias between the actual X-15 pilot ratings and those predicted by using this criterion (ref. 4). This diagram shows the distribution of error in the predicted ratings for intervals of three pilot rating units. A single bar at the center reaching 100 percent would correspond to perfect correlation within one and one-half units. The ordinate shows that, for the criterion under discussion, only about 50 percent of the predicted ratings come within ±1.5 rating units of the actual ratings. In addition, further evidence of bias indicates the predicted ratings to be very optimistic.

In addition to control considered in the last criteria, the response characteristics of the airplane must be considered also. The criteria proposed in reference 5 predicts handling qualities based on the Dutch roll characteristics, cycles to damp, and roll-to-sideslip coupling. A fighter-type variable stability airplane was used for the program and simulated gunnery tracking was included as an evaluation maneuver. Figures 8 and 9 compare this criterion with the X-15 pilot ratings. In figure 8, the abscissa is φ/v_e, a measure of the roll-to-yaw ratio during the Dutch roll oscillation. The ordinate is $1/C_{1/2}$, in which damping increases toward the top. The open symbols should lie above the upper contour, the half-shaded symbols between the two contours, and the shaded symbols should fall under the lower contour. It is obvious from figures 8 and 9 that there is considerable scatter, which indicates generally poor correlation between the X-15 pilot ratings and those predicted using this criterion. Again, only about 50 percent of the predicted ratings have an error less than 1.5 pilot ratings (fig. 9). A study of the work on which this criterion (ref. 5) is based reveals that although φ/v_e worked fairly well in separating the tolerable and the intolerable conditions of that study, the effect of strong control coupling was not taken into account in the chosen parameters.

The effects of control coupling for fighter operations using a variable stability airplane and a simulator are considered in reference 6. Although the X-15 is not a fighter airplane, a comparison is made in figure 10 of the X-15 ratings with those of this work. The criterion has the damping ratio of the Dutch roll as the abscissa and the control-coupling derivative N_{δ_a} (which is the yaw acceleration due to aileron deflection) as the ordinate. Although all of the unsatisfactory pilot ratings (except one) do not fall in the satisfactory area in this case, a fairly large number of satisfactory pilot ratings are found in areas predicted to be unsatisfactory. The result is a very pessimistic prediction evidenced by the marked asymmetry in the distribution of the error shown in the histogram in figure 11. As a result, less than 30 percent of the points fall within the band of perfect correlation. Although there are some satisfactory ratings in regions predicted to be unacceptable (fig. 10), there is fair correlation in the satisfactory and unsatisfactory regions.

PROPOSED CRITERIA

From the foregoing correlations with previously used criteria, it is apparent that two improvements are needed, namely, (1) a better measure of the effect of control coupling, and (2) a means for taking into account more than two parameters at a time. Ashkenas and McRuer have suggested in reference 7 use of an improved control-coupling parameter in the form of the ratio ω_φ/ω_D. Pilot-rating contours are plotted as functions of ω_φ and ω_D in figure 12. The term ω_D is simply the Dutch roll frequency in radians per second and is related to the directional stability and dihedral parameters, N_β and L_β, as follows:

$$\omega_D \approx \sqrt{N_\beta - \alpha_o L_\beta}$$

All stability derivatives, as well as angle of attack, are with respect to principal axes. The term ω_φ along the ordinate is a control-coupling parameter which includes the roll-control derivatives L_{δ_a} and N_{δ_a}, as follows:

$$\omega_\varphi \approx \sqrt{N_\beta - \frac{N_{\delta_a}}{L_{\delta_a}} L_\beta}$$

When $\omega_\varphi = 0$, the coupling effect is so severe that the airplane only yaws and does not roll. When $\omega_\varphi = \omega_D$ (along the diagonal), essentially no sideslip is induced. This condition is usually the most desirable. Values of ω_φ exceeding ω_D cause sideslip to be induced in such a way that the pilot tends to excite the Dutch roll oscillation while attempting to stabilize bank angle. Extreme ratios of ω_φ to ω_D make control impossible.

The second improvement to the existing criteria, that is, the need to consider several of the pertinent parameters at once, has been achieved to some

degree by Harper (ref. 8), but the coverage is not sufficient to be generally useful. In light of this problem, the Flight Research Center has undertaken a general study of the lateral-control problem with the intent of developing criteria that are more generally applicable than those available. An example of the results of this study is shown in figure 13(a). This plot of pilot rating as a function of ω_φ and ω_D is part of a generalized pilot-rating survey in which five independent parameters, the Dutch roll stability (ω_D), control-coupling parameter (ω_φ), control power, Dutch roll and roll damping (which are tied together as one parameter), and dihedral effect are taken into account. Pilot ratings were obtained on a fixed-base simulator in conjunction with a color contact analog display, as the five selected parameters were systematically varied over ranges that covered most airplane configurations. Of the many parameters involved in describing the lateral-directional behavior of an aircraft, these five are found to have the strongest influence. All of the parameters except L_β may be recognized as being directly related to the coefficients of the transfer function for roll response to aileron deflection. The parameter L_β was introduced because of its relationship to the amount of sideslip that is induced in a roll maneuver. The elimination of other but less important factors is predicated on two overall assumptions: (1) the spiral mode is neutrally stable and (2) the ratio of the roll to Dutch roll damping is constant.

Because the effect on only two variables can be shown in a single plot, the values of the variables which were held constant are listed in each figure. Notice that for the case of moderate damping (fig. 13(a)) the pilot ratings are not particularly sensitive to small changes in the ratio ω_φ to ω_D. Figure 13(b) shows an identical set of characteristics but with much less damping. In this case, a ratio ω_φ/ω_D of only 1.1 is seen to be uncontrollable. A comparison of figure 13(a) and 13(b) shows the marked effect of damping on a pilot's acceptance of control coupling of the type which causes pilot-induced lateral-oscillation tendencies. The result of the complete survey is a compilation of over 1500 pilot ratings in 45 plots of the type shown in figure 13(a) and (b).

Although it would be possible to use these plots to predict lateral-directional pilot ratings by interpolating between charts by hand computing for a particular application, the procedure would be tedious and time consuming. In order to provide a more rapid means for hand computing the pilot ratings, much of the information contained in the full set of charts has been reduced to three summary charts given in figure 14 $\left(\tan^{-1} \omega_\varphi/\omega_D \text{ against } \log L_{\delta_a}\delta_{a_{MAX}}\right)$. Predicted pilot ratings are obtained by interpolating between the appropriate charts. It should be noted that if the pilot rating from one of the charts is 10, an extrapolated value must first be obtained to get a proper interpolation between charts. The charts are applicable to many airplane configurations, although the parameter coverage is necessarily more restricted than that of the complete survey.

The full set of charts is best utilized by mechanizing the data in a digital computer program. Such a program now in use at the NASA Flight Research

Center is illustrated in figure 15. The block in the upper left corner represents the information contained in the 45 plots of the pilot-rating survey being fed into a digital computer. The block on the right represents several sets of airplane characteristics, stability derivatives, moments of inertia, and such, also being fed into the computer. The digital computer then computes the dimensional stability derivatives, numerous parameters of interest, and the predicted pilot ratings. One of the greatest values of these predictions is that a great number of airplane configurations and flight conditions can be assessed very quickly and at very little cost. This capability is particularly important to the preliminary designer and the flight test engineer.

APPLICATION OF PROPOSED CRITERION

Application of this criterion to the X-15 is shown in figure 16(a), which presents the predicted pilot ratings in the form of contour lines as a function of Mach number and angle of attack. The configuration in this case is that with the ventral off and dampers off and, as before, the squares and circles denote flight and simulator pilot ratings, respectively. In general, the predicted pilot ratings are seen to compare well with the actual ratings, going from unsatisfactory to satisfactory, then to unsatisfactory, and finally to unacceptable with increasing angle of attack. Figure 16(b) shows similar comparisons for four other configurations of the X-15. The comparison between the predicted and actual pilot ratings is equally as good for these cases as for the one discussed in detail which demonstrates the wide range of configurations and flight conditions for which it can be used. Figure 17 is a histogram showing the distribution of the difference between predicted and actual pilot ratings for the five plots just shown for the different X-15 configurations. Good correlation is borne out by the fact that over 70 percent of the predicted ratings lie within 1.5 pilot ratings, as compared with 28 to 50 percent for the other criteria discussed. The degree of scatter of the predicted ratings closely approaches that expected of the actual pilot ratings obtained in flight and on the simulator.

The prediction technique has also been applied to a limited degree but with comparable success to a current fighter airplane, to the B-70, and to a lifting-body vehicle. Many more correlations are planned as part of a program to test and refine this technique. The proposed method of predicting pilot ratings gives promise of becoming a valuable tool to the preliminary designer, the flight test engineer, and the writer of handling-qualities specifications.

CONCLUDING REMARKS

In summary, the pilot's ratings of lateral-directional characteristics of the X-15 aircraft have been reviewed for a wide variety of flight conditions both with and without damping augmentation. Because of the limitations of the handling-qualities criteria considered, particularly where the roll control and Dutch roll modes are strongly coupled, a newly developed criterion, involving five controlling parameters and having the potential for a much

broader range of application, was described and partly demonstrated in the light of pilots' assessments of the X-15 lateral-directional handling qualities.

REFERENCES

1. White, Robert M.; Robinson, Glenn H.; and Matranga, Gene J.: Résumé of Handling Qualities of the X-15 Airplane. NASA TM X-715, 1962.

2. Petersen, Forrest S.; Rediess, Herman A.; and Weil, Joseph: Lateral-Directional Control Characteristics of the X-15 Airplane. NASA TM X-726, 1962.

3. Creer, Brent Y.; Stewart, John D.; Merrick, Robert B.; and Drinkwater, Fred J., III: A Pilot Opinion Study of Lateral Control Requirements for Fighter-Type Aircraft. NASA MEMO 1-29-59A, 1959.

4. Creer, Brent Y.; Heinle, Donovan R.; and Wingrove, Rodney C.: Study of Stability and Control Characteristics of Atmosphere-Entry Type Aircraft Through Use of Piloted Flight Simulators. Seventh Anglo-American Aeronautical Conference (New York), Vehig S. Tavitian, ed., Inst. Aeron. Sci., Inc., c.1960, pp. 66-102.

5. Liddell, Charles J., Jr.; Creer, Brent Y.; and Van Dyke, Rudolph D., Jr.: A Flight Study of Requirements for Satisfactory Lateral Oscillatory Characteristics of Fighter Aircraft. NACA RM A51E16, 1951.

6. Vomaske, Richard F.; Sadoff, Melvin; and Drinkwater, Fred J., III: The Effect of Lateral-Directional Control Coupling on Pilot Control of an Airplane as Determined In Flight and In a Fixed-Base Flight Simulator. NASA TN D-1141, 1961.

7. Ashkenas, Irving L.; and McRuer, Duane T.: The Determination of Lateral Handling Quality Requirements From Airframe Human Pilot System Studies. WADC Tech. Rep. 59-135 (Contract No. AF 33(616)-5661), Wright Air Dev. Center, U.S. Air Force, June 1959. (Available from ASTIA as AD 212 152.)

8. Harper, Robert P., Jr.: In-Flight Simulation of Re-Entry Vehicle Handling Qualities. IAS Paper No. 60-93, June 1960.

TABLE I

PILOT-RATING SCALE

NUMERICAL RATING	SYMBOL		GENERAL CLASSIFICATION
	FLIGHT	SIMULATOR	
1 2 3	□	○	SATISFACTORY
4 5 6	◨	◑	UNSATISFACTORY
7 8 9	■	●	UNACCEPTABLE
10	■	●	UNCONTROLLABLE

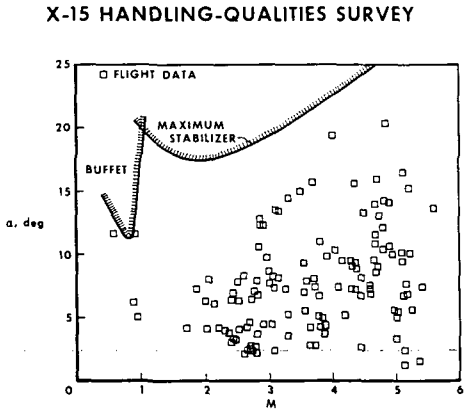

Figure 1

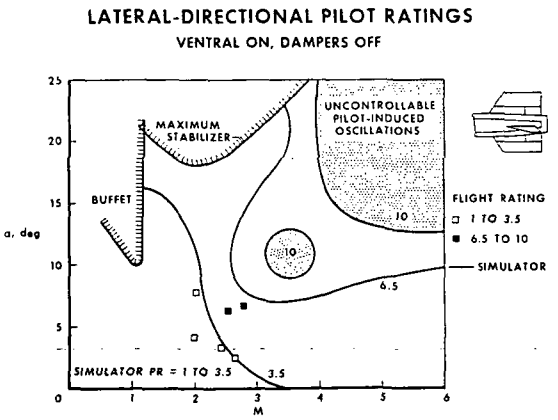

Figure 2

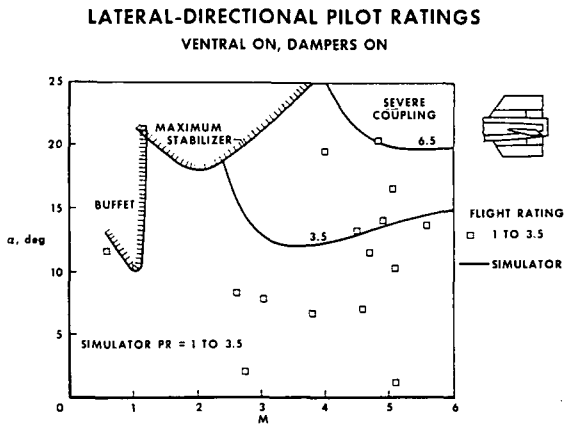

Figure 3

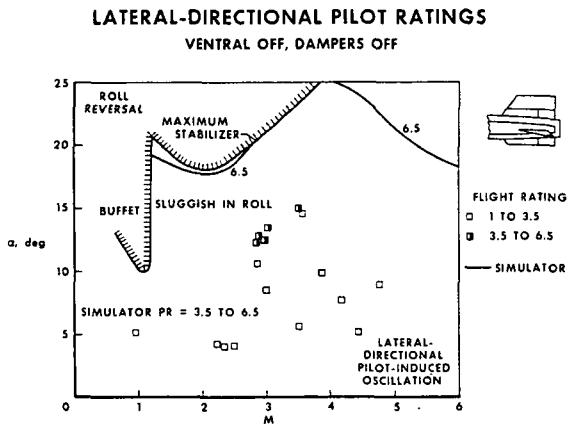

Figure 4

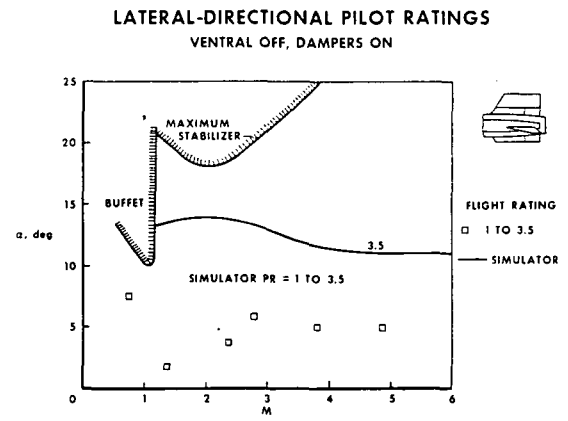

Figure 5

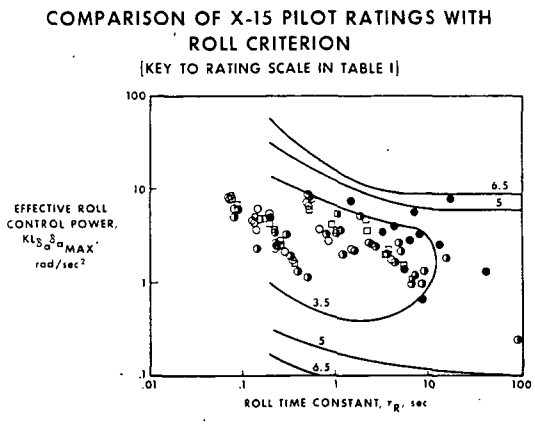

Figure 6

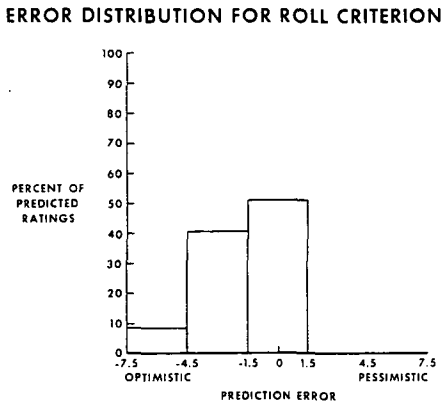

Figure 7

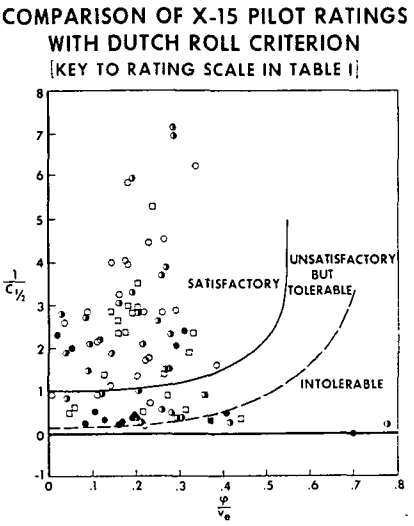

Figure 8

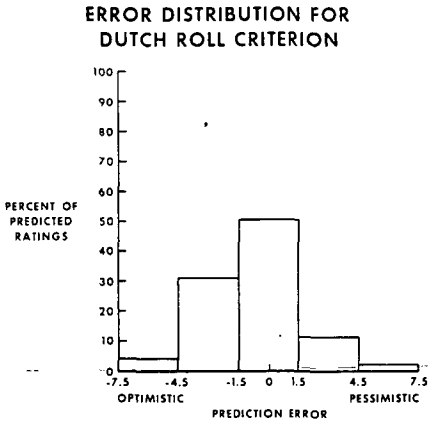

Figure 9

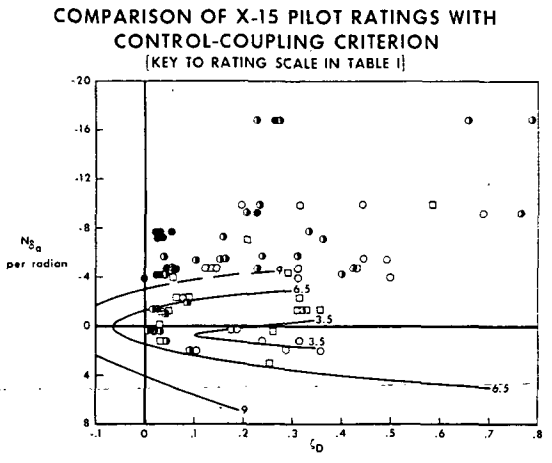

Figure 10

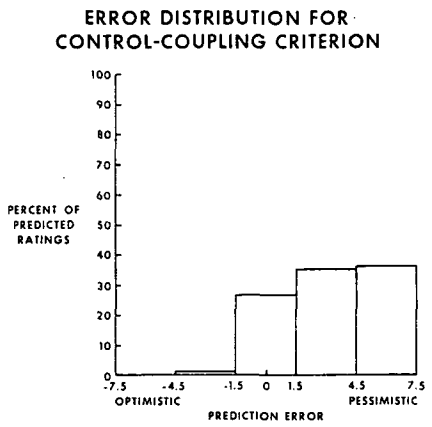

Figure 11

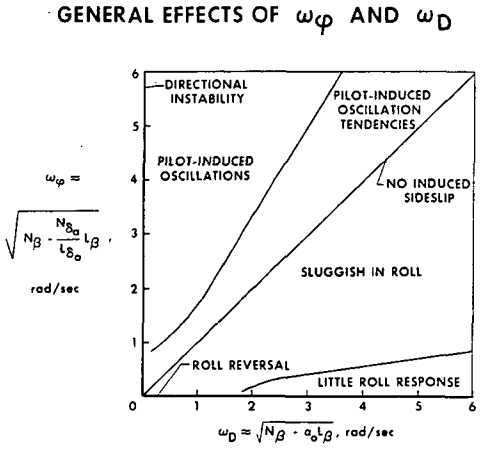

Figure 12

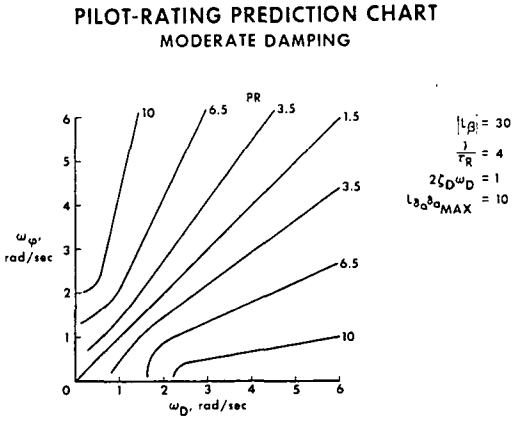

Figure 13(a)

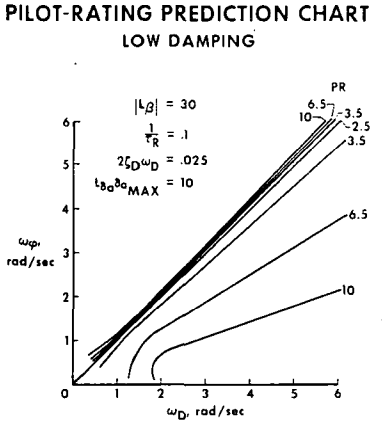

Figure 13(b)

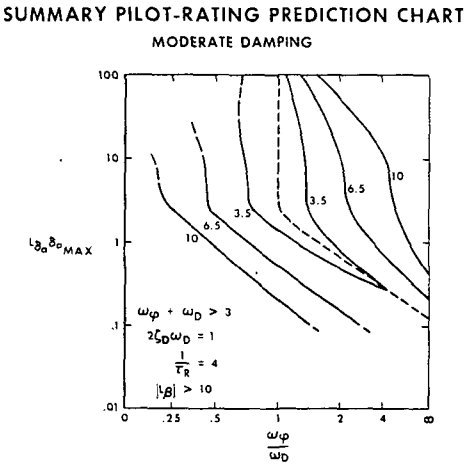

Figure 14(a)

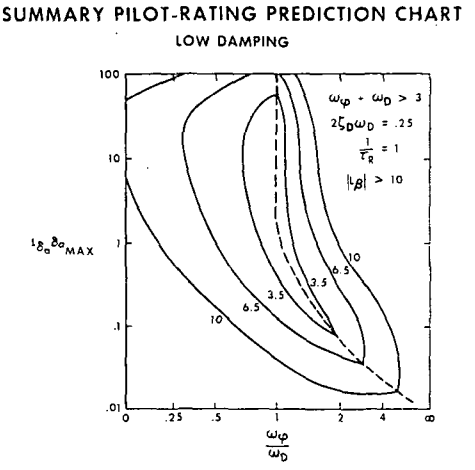

Figure 14(b)

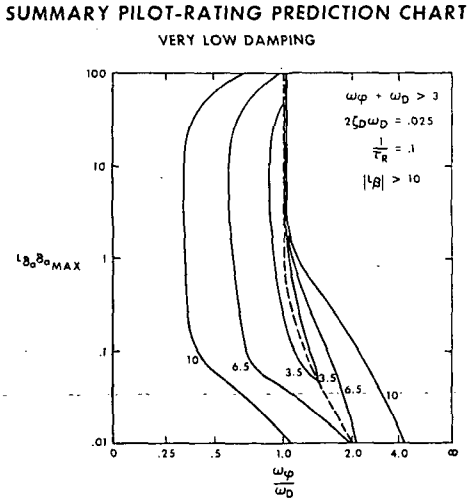

Figure 14(c)

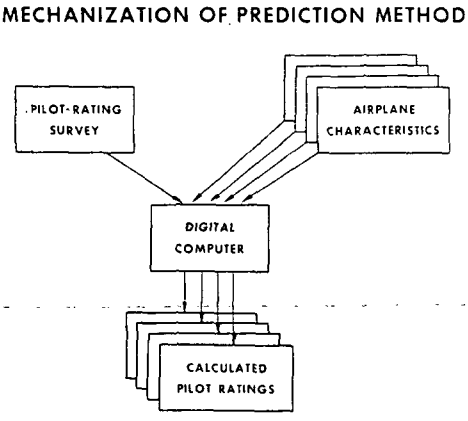

Figure 15

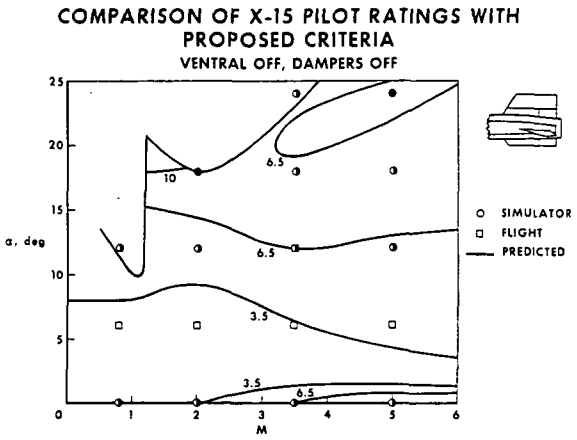

Figure 16(a)

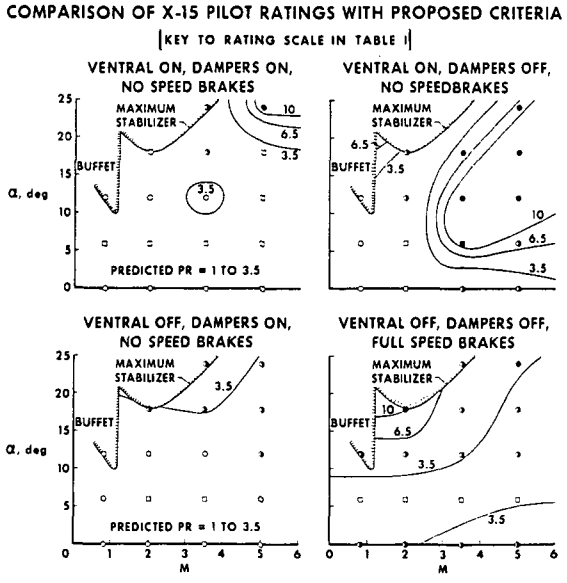

Figure 16(b)

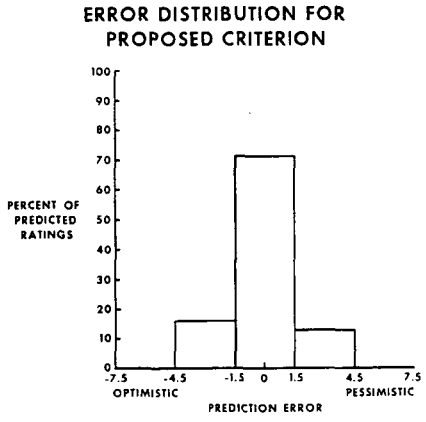
ERROR DISTRIBUTION FOR
PROPOSED CRITERION
PERCENT OF
PREDICTED
RATINGS
100
90
80
70
60
50
40
30
20
10
0
-7.5
-4.5
-1.5
0
1.5
4.5
7.5
OPTIMISTIC
PESSIMISTIC
PREDICTION ERROR

Figure 17

6. CONTROL EXPERIENCES OF THE X-15 PERTINENT TO LIFTING ENTRY

By Euclid C. Holleman
NASA Flight Research Center

SUMMARY

During the program to expand the flight envelope of the X-15 airplane, flights to and entries from altitudes up to 350 000 feet have been accomplished. During these entries, flight-control experience was obtained with four different control-system configurations having varying degrees of complexity. This experience is discussed in terms of systems requirements for piloted reentries.

INTRODUCTION

At the time of the last X-15 conference, the immediate goal of the X-15 program was the expansion of the flight envelope of the airplane. An altitude of 217 000 feet had been reached in preparation for flights to the design altitude of 250 000 feet. During this early part of the program, several problems were encountered that threatened to curtail the program. Some of these problems were the general controllability (ref. 1) of the basic airplane and the reliability of the inertial and stability augmentation systems (ref. 2). However, these difficulties were solved and the original program objectives have been accomplished. The purpose of this paper is to discuss the flight experiences obtained in recovering the X-15 airplanes from high altitude with conventional and adaptive controls, and to place these experiences in proper perspective relative to future lifting entry programs.

SYMBOLS

a_x	longitudinal acceleration, g units
a_y	lateral acceleration, g units
a_z	normal acceleration, g units
g	acceleration due to gravity, feet per second^2
h	altitude, feet
L_{δ_a}	roll acceleration due to aileron deflection, 1/second^2
M	Mach number

M_{δ_h}	pitch acceleration due to horizontal-tail deflection, $1/second^2$
N_{δ_r}	yaw acceleration due to vertical-tail deflection, $1/second^2$
p	rolling velocity, degrees per second
q	dynamic pressure, pounds per square foot
t	time, seconds
V	velocity, feet per second
α	angle of attack, degrees
β	angle of sideslip, degrees
φ	angle of bank, degrees
δ_a	aileron deflection, radians
δ_h	horizontal-tail deflection, radians
δ_r	vertical-tail deflection, radians

Subscripts:

av	average
max	maximum

HIGH ALTITUDE AND ENTRY EXPERIENCE

A time history of a flight to an altitude of 354 200 feet (fig. 1) illustrates the type of mission of which the X-15 is capable. Following launch at about 45 000 feet, the pilot advances the throttle and climbs to high altitudes into the region of extremely low dynamic pressure. After maximum altitude is reached, during descent, the pilot stabilizes the airplane at the desired angle of attack for reentry. Reentry flight path angle is high, approximately 38° for this flight. The buildup in dynamic pressure, acceleration, and temperature is rapid, but is of short duration.

Entries have been made with each of two variations of two basic control systems. Two X-15 airplanes are equipped with conventional aerodynamic controls with stability augmentation and acceleration command reaction controls. Backup aerodynamic damping augmentation has been added for redundancy and reaction augmentation has been added for increased controllability at low dynamic pressure. Another X-15 airplane is equipped with an adaptive control system, the MH-96 flight control system, which was developed under Air Force contract for evaluation in advanced vehicles. The X-15 program provided the

opportunity for the evaluation of its design capabilities in actual entry flight. The system has adaptive gain changing rate-command aerodynamic and rate-command reaction controls in all three control axes, blended aerodynamic and reaction controls, attitude command or hold modes, and normal acceleration limiting.

Flight experience with the X-15 during high altitude flights and entries with these controls is summarized in table I. Since 1961, the design altitude has been demonstrated by using the airplanes with conventional and adaptive control systems, and flights to much higher altitudes have been made with the airplanes equipped with the adaptive control system. Since 1962 all flights have been made with the lower ventral removed, because it was found that the airplane configuration without the lower ventral was more controllable (ref. 3).

The X-15 entry control task requires the pilot to establish and hold the desired angle of attack until normal acceleration builds to the desired value, and then to hold normal acceleration until a constant glide angle of attack or constant rate of descent was achieved.

By means of this control technique, entries from high altitudes have been made to cover a wide range of entry parameters, average values of entry angle of attack α_{av}, maximum values of normal acceleration $(a_z)_{max}$, and maximum dynamic pressure q_{max} (fig. 2). These values are not unique functions of the maximum altitude, since the values may be altered by piloting technique; however, they represent the entry experience obtained. The design altitude of 250 000 feet is shown for reference. Entry angle of attack has varied from about 12° to 20° during entries from the lower altitudes. During entries from higher altitudes, angles of attack up to about 25° were used. The use of entry angles of attack higher than these values is not planned, inasmuch as trim capability is limited because of the increased static longitudinal stability at high angle of attack. Also, some control must be reserved for the stability augmentation system.

A range of normal acceleration of only about 3g to 5g has been covered, since higher accelerations were not required for recovery and there was no need to test to the design limit of the airplane. A wide range of entry dynamic pressure was covered, inasmuch as this quantity is more critically dependent on piloting technique. Maximum entry dynamic pressure was about 1900 pounds per square foot.

ENTRY CONTROL EXPERIENCE

During flights to high altitudes, the control problems of lifting entry at relatively low velocities have been met and solved by utilizing the attributes of the pilot and automatic systems. Entries have been accomplished in a variety of entry environments and with several degrees of control-system sophistication.

A comparison of entry controllability with the most and the least sophisticated control systems is shown in figure 3. The entries were made with the ventral-on airplane configuration.

On the left in figure 3 is presented an entry with the pilot flying manually using the conventional control system which has acceleration reaction controls and aerodynamic damping augmentation. On the right in figure 3, the pilot is using the adaptive control system with attitude hold modes operative. This system also has command reaction controls that are automatically blended with the aerodynamic controls.

The most significant difference between the two entries is the magnitude of the angle-of-sideslip oscillation as normal acceleration and dynamic pressure build up. The excursions are smaller and the controllability was superior with the higher gain system. The entries were made by different pilots; however, their evaluations of the entry control tasks were similar--namely satisfactory, with a slight deterioration in the lateral directional mode. At angles of attack higher than achieved during these entries, however, the controllability of the airplane with the adaptive control system is predicted on the X-15 simulator to be clearly superior.

Entry controllability with the other controls evaluated, conventional controls with stability augmentation (SAS) and reaction damping (RAS) and the adaptive rate command controls, has been rated satisfactory also by the pilots. The pilots' average rating of entry pitch, roll, and yaw controllability with the various control systems is summarized in table II. Although entry controllability with all the controls was rated satisfactory, the adaptive rate command controls were rated superior to the other controls. The conventional controls with reaction augmentation were rated least satisfactory; however, the pilots did appreciate the addition of the reaction damping. All flights to high altitude, since the addition of reaction augmentation, have been made with this system. Recent flights have been made with better-defined control objectives for the follow-on program. The pilot ratings probably reflect these control requirements. Only a limited number of entries have been made with the adaptive system hold modes; however, these control modes have been used more extensively in other phases of flight. Pilot opinion on the use of hold modes is mixed. These modes greatly reduce the pilot's concentration and workload, but some pilots prefer to be active in the control loop at all times. An acceptable compromise preferred by some is active control of the primary control mode, pitch, and the use of attitude command in roll and yaw.

The amount of controls used during X-15 entries is summarized and compared to the control available in figure 4. The aerodynamic control angular acceleration used in pitch, roll, and yaw includes the critical setup period prior to dynamic pressure buildup through pullout to a constant glide angle of attack or rate of descent. The controls used include both the pilot and the augmentation system.

A much higher percentage of available aerodynamic control was used in pitch, primarily for trim to establish and hold angle of attack, than was

used in the other control modes. During the initial part of the entry, nearly 100 percent of the control available was used to initiate pullout, but as dynamic pressure increased and the pullout developed, a lower percentage of control was required. The control used in roll and yaw was low and was for stabilization. Similar requirements for stabilization in pitch were indicated. Reaction controls were used during the first part of the entry. Reaction controls with an authority of only about 1 percent of the maximum available aerodynamic controls were found to be completely satisfactory.

Since the pilot is dependent on systems for stabilization during the entry, some discussion of systems experience is in order. Many of the problems with the various control systems were solved during the design and early flight tests. Some of these, such as limit cycles, structural coupling, and overall reliability (ref. 2), have been analyzed and solutions for the problems found. Other problems were recognized, but, because they were never expected to be encountered in flight, no hardware changes were made to the X-15 airplane. However, some were encountered in flight. Typical of these problems was saturation, which led to nonlinear system instability with the high-gain adaptive system.

Early in the design of the adaptive controls it was recognized that high rate commands from the pilot could not be followed by the control surface actuators. Servo motion would be reflected back to the pilot's stick as stick kicks, and system instability would be experienced because of the inability of the system to follow the commanded rate. For nearly 40 flights, rate-limit problems were not encountered, even during entries from the highest altitudes. However, the problem was experienced during a relatively routine flight and the airplane became uncontrollable in roll for a short time. A flight record of that experience is presented in figure 5. Roll and pitch rate exceeded the recorded limits during the maneuver, as indicated by the dashed lines. The straight segments of the time history indicate that the servo rate limit was exceeded.

The incident was initiated by a rather modest pitch control command with some roll command by the pilot. The resulting rate limiting of the servo produced sufficient system lag to reduce the pitch damper effectiveness and actually to cause the roll command system to go unstable. Reduced commands and adaptive gains restored the system to operational status, and the airplane motions were again damped.

Analysis of the problem showed that the system nonlinear instability was caused by rate-limit induced lag at low frequencies. The inclusion of a simple lag-lead circuit in the servo loop to reduce the lag at the critical low frequencies appeared promising, and simulation tests indicate that this change will result in improved controllability with little degradation in overall system performance. Incidentally, many of the control system problems have been studied on the fixed-base simulator; however, this phenomenon was nonreproducible on the simulator until the capacity and hydraulic pressure of the hydraulic system were increased to be similar to that of the airplane.

During the design and flight testing of the X-15 airplane, simulation has been relied on more heavily than in any other airplane program. Both general and specific control problems have been investigated by use of various ground-based and airborne simulators, as illustrated in figure 6. A complete six-degree-of-freedom simulation using the cockpit and actual control hardware, shown in the center of figure 6, was mechanized early in the design of the airplane. The simulator is still used for flight planning and pilot familiarization (ref. 4). Routinely, pilots have evaluated the fidelity of the simulator in comparison with actual flight. The consensus of the pilots is that the fixed-base simulation satisfactorily duplicates the X-15 instrument flight-control task. However, it is only as good as its mechanization and, therefore, for realism, must be as complete as possible and must be updated on the basis of actual flight experience.

Before the flights to high altitude, the first pilots practiced entry flight on a moving-base simulator under the actual acceleration environment to determine the detrimental effects of acceleration on controllability. However, they, and pilots added to the program later, have since concluded that practice under high acceleration was unnecessary. Entry acceleration of 5g (normal) and 1 to 2g (longitudinal) had little, if any, effect on their control performance during entry.

One possible exception was the pilot-induced oscillation with the dampers-off, ventral-on configuration (ref. 5). The fixed-base simulator for this configuration, with the pilot using a special control technique, gave an optimistic indication of the controllability compared with that experienced in actual flight, since it provided no kinesthetic or outside visual cues. In this case, the acceleration environment was detrimental to control.

POSSIBLE APPLICATIONS

A comparison of X-15 entry with a simulated orbital lifting body entry (fig. 7) shows little similarity. The X-15 entries are of much shorter duration and present a more severe control problem with the rapid buildup in dynamic pressure and acceleration than the orbital entry.

However, the X-15 entry experience does provide results that may be applicable to certain launch abort situations and to terminal ranging to a landing for future lifting entry vehicles. Figure 8 shows an X-15 entry from 285 000 feet and an M2-F2 simulated lifting body entry following abort during the first stage launch. Similar levels of acceleration are required for each vehicle pullout. Although the "wing" loading of the lifting body is somewhat greater than that of the X-15, the effect of the lower lift-drag ratio of the lifting body is larger and results in lower peak dynamic pressure during entry. Like the X-15 airplane, the controllability of the lifting body was indicated to be satisfactory with moderate gain dampers.

RECOVERY GLIDE

In addition to the entry experience with the X-15 airplane, many flights have been made to hypersonic speeds for research purposes. Several recovery techniques have been investigated. Some of these were to maintain constant angle of attack for maximum range, constant dynamic pressure for obtaining heating and other aerodynamic data, and constant rate of change of altitude for controlling range by flight-path control. These flights have been planned as straight approaches to the landing area from about 100 000 feet and a Mach number of 5. Only terminal maneuvering to the landing was required and, with the X-15 airplane, the pilots have preferred a 360° approach to landing. This approach allows the pilot to deplete excess range by bank-angle modulation.

This recovery technique will be representative of a lifting-entry vehicle approach to the landing site from the initial conditions of 100 000 feet and a Mach number of 5. Although reaction controls may be used during the initial phase of entry at higher Mach numbers, aerodynamic controls are expected to be used for the control of airplane attitude while controlling range and approach to landing.

The aerodynamic controls used and the maneuvering required during the X-15 recovery from Mach 5 to landing is summarized in figure 9. Note that the Mach number is highest at the right, decreasing to landing speed to the left. Only small bank angles and low roll rates were used by the pilots during the stabilized high Mach number portion of the recovery. Less than 10 percent of the roll control available was used. Although about 40 percent of the longitudinal control available was used, it was used for trimming to the desired angle of attack for control of range.

At the lower Mach number, significantly more bank angle and roll rate were used for terminal maneuvering; however, a much lower percentage of control available was used in both roll and pitch, inasmuch as effectiveness is higher and much less control is required for longitudinal trim. From these results it can be inferred that this part of the recovery of entry vehicles will require substantially less control than conventional fighter aircraft maneuvering, inasmuch as maneuvering is minimal except during landing approach.

CONCLUDING REMARKS

Successful piloted entries from high altitudes, the most extreme from 354 200 feet, have been accomplished with the X-15 airplane. The high steady acceleration and rapidly changing aerodynamic environment did not affect the pilot's capability to control the entry. All the control systems evaluated were judged by the pilots to be satisfactory for the control of the X-15 entry from the design altitude. The overall X-15 flight experience should be useful in assessing control requirements for future lifting-entry vehicles. Entries have been made that presented more severe control problems than predicted for entries of advanced vehicles at higher velocities.

REFERENCES

1. Petersen, Forrest S.; Rediess, Herman A.; and Weil, Joseph: Lateral-Directional Control Characteristics of the X-15 Airplane. NASA TM X-726, 1962.

2. Taylor, Lawrence W., Jr.; and Merrick, George B.: X-15 Airplane Stability Augmentation System. NASA TN D-1157, 1962.

3. Weil, Joseph: Review of the X-15 Program. NASA TN D-1278, 1962.

4. Hoey, Robert G.; and Day, Richard E.: Mission Planning and Operational Procedures for the X-15 Airplane. NASA TN D-1159, 1962.

5. Holleman, Euclid C.; and Wilson, Warren S.: Flight-Simulator Requirements for High-Performance Aircraft Based on X-15 Experience. Paper No. 63-AHGT-81, ASME, 1963.

TABLE I.- SUMMARY OF HIGH-ALTITUDE EXPERIENCE

Year	Maximum altitude, ft	Control system	Configuration
1961	217 000	Conventional - SAS	Ventral on
1962	246 700	Adaptive (hold)	Ventral on
1962	247 000	Conventional - SAS	Ventral on
1962	193 600	Adaptive (rate command)	Ventral on
1962	314 750	Adaptive (hold)	Ventral on
1963	271 700	Adaptive (rate command)	Ventral off
1963	209 400	Adaptive (rate command)	Ventral off
1963	223 700	Adaptive (rate command)	Ventral off
1963	285 000	Adaptive (rate command)	Ventral off
1963	226 400	Conventional - SAS, RAS	Ventral off
1963	347 800	Adaptive (rate command)	Ventral off
1963	354 200	Adaptive (rate command)	Ventral off
1964	195 800	Conventional - SAS	Ventral off
1965	209 600	Adaptive (rate command)	Ventral off
1965	244 700	Adaptive (rate command)	Ventral off
1965	280 600	Adaptive (rate command)	Ventral off
1965	212 600	Conventional - SAS, RAS	Ventral off
1965	208 700	Conventional - SAS, RAS	Ventral off
1965	271 000	Adaptive (rate command)	Ventral off

TABLE II.- PILOT RATING OF ENTRY CONTROLS

	Conventional SAS		Conventional SAS-RAS		Adaptive		Adaptive (hold)	
	Average rating	No. of flights	Average rating	No. of flights	Average rating	No. of flights	Average rating	No. of flights
Pilot A	2.1	1	1.3	1	1.3	5	---	-
Pilot B	2	1	---	-	---	-	1.8	2
Pilot C	---	-	2.3	1	1.8	3	---	-
Pilot D	1.8	1	---	-	1.8	4	---	-
Pilot E	---	-	2.5	3	---	-	---	-
Pilot F	---	-	3.3	1	---	-	---	-
	2	3	2.4	6	1.6	12	1.8	2

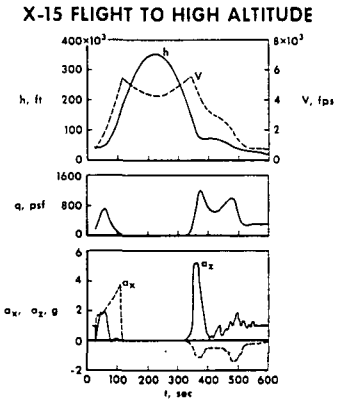

Figure 1

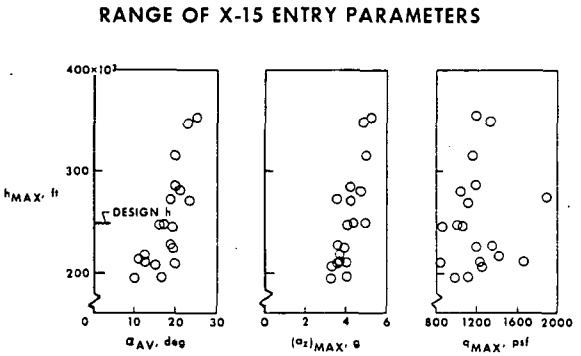

Figure 2

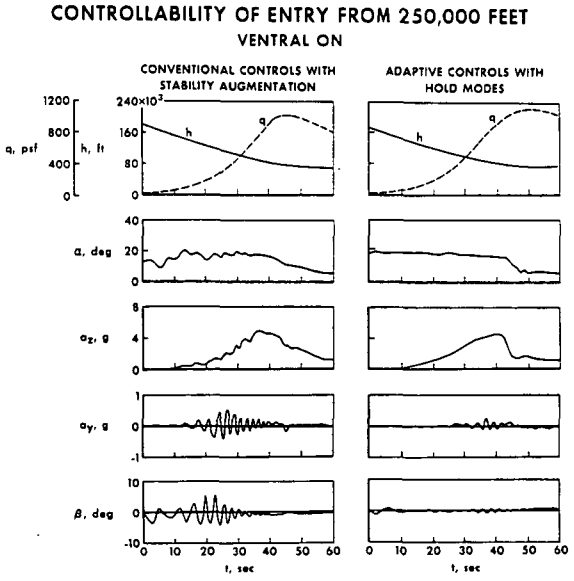

Figure 3

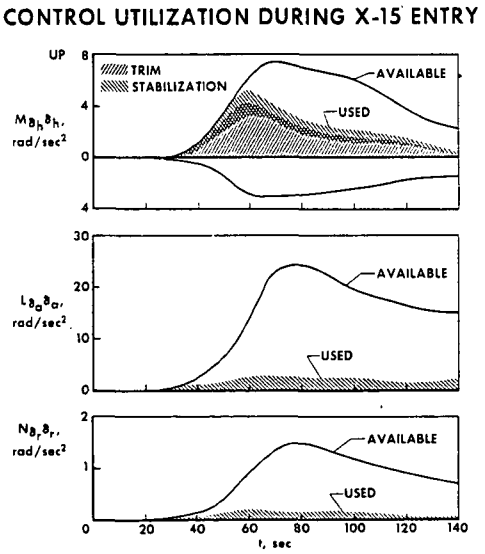

Figure 4

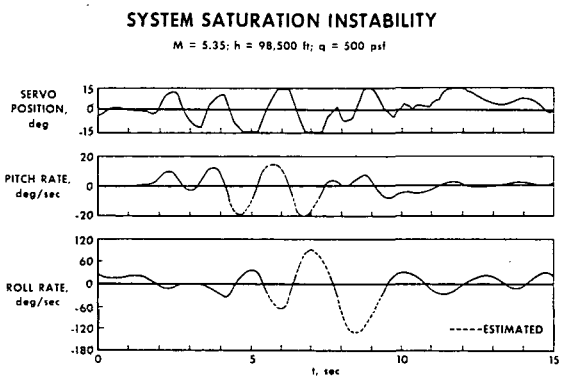

Figure 5

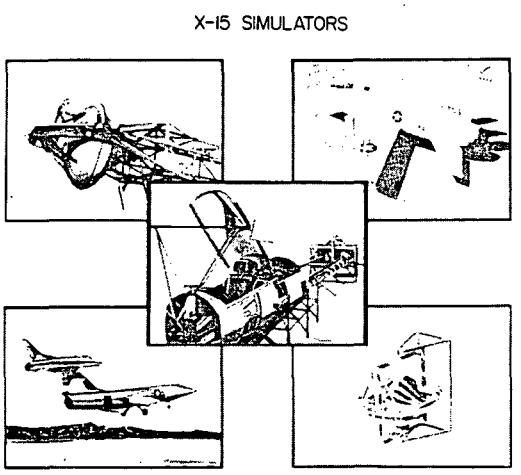

Figure 6

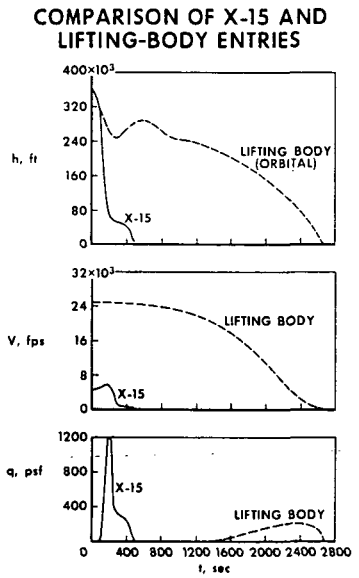

Figure 7

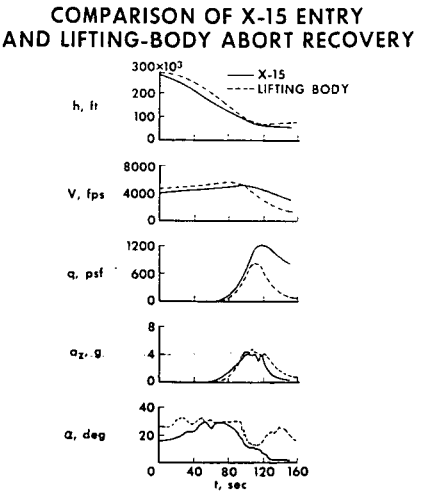

Figure 8

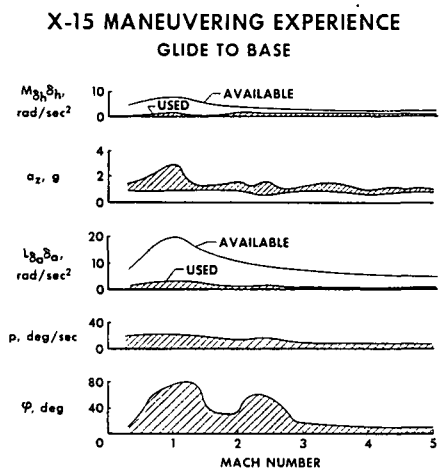
X-15 MANEUVERING EXPERIENCE
GLIDE TO BASE
$M_{\delta_h}\delta_h$, rad/sec²
10
0
USED
AVAILABLE
a_z, g
4
2
0
$L_{\delta_a}\delta_a$, rad/sec²
20
10
0
AVAILABLE
USED
p, deg/sec
40
0
φ, deg
80
40
0
1
2
3
4
5
MACH NUMBER

Figure 9

7. RÉSUMÉ OF X-15 EXPERIENCE RELATED TO FLIGHT GUIDANCE RESEARCH

By Melvin E. Burke and Robert J. Basso
NASA Flight Research Center

SUMMARY

This paper reviews the X-15 flight experience with inertial flight data systems since the previous X-15 conference and describes the guidance research utilizing inertial systems that is now in progress or planned for the near future. Various reliability and performance problems with the original analog system and the mechanization and performance of a redesigned version of the system are discussed. Flight experience with a digital system is similarly reviewed in the light of the basic difference between analog and digital systems. Finally, plans are reviewed for the boost-reentry guidance research program that is presently planned for the X-15.

INTRODUCTION

During the initial planning for the X-15 program, because of the extreme performance ranges anticipated, it was decided that the attitudes, altitude, velocity, and rate of climb could best be measured and/or computed by an inertial flight data system. Such a system was designed and used, essentially in the original form, from early in the flight program until mid-1964. At that time, because of more recent advancements in the state of the art, as well as degradation in the original system, a redesigned version of the original analog system was installed in two of the airplanes, and a digital system was installed in the third airplane.

The purpose of this paper is twofold. The first is to present a résumé of the experience gained to date in using these two systems, and the second is to discuss a planned guidance research program that will be implemented in the near future on the X-15.

DISCUSSION

Analog System

The analog system is illustrated in figures 1 and 2. A block-diagram representation of the system is shown in figure 1, and photographs of the actual hardware are shown in figure 2. This system consists of two main units--the reference system, which is carried in the B-52 launch airplane and the inertial flight data system (IFDS), which is installed in the X-15.

The reference system in the B-52 consists of three major components--an in-flight control panel, a Doppler radar system, and an N-1 compass. The analog inertial flight data system consists of an inertial measurement unit (IMU), an analog computer, and a set of pilot's displays. This system has been functionally and operationally described at previous X-15 conferences and, therefore, is not described herein.

The flight experience with the original analog system was also previously discussed at the last (1961) X-15 conference. At that time, it was reported that, although the system did not consistently meet its performance specifications, its overall performance was adequate to support continued expansion of the X-15 flight envelope.

The system performance prior to the redesign is graphically shown in figure 3. This figure presents a plot of the mean of the altitude error as a function of time following launch. Also shown are the standard deviations. Altitude performance was selected as the best measure of total system performance because the inherent instability of the vertical loop reflects system errors most significantly. These data were assembled from 20 consecutive flights made in 1962. The design accuracy of ±5000 feet at 300 seconds and ±10 000 feet at 500 seconds is also indicated. It is apparent both from the mean values and the scatter about the mean that the performance did not meet these goals.

The reference used for comparing the altitude of the inertial system has been a faired curve. This curve is obtained by weighting the tracking radar data, air data, and the onboard acceleration data. The accuracy of this faired curve is estimated to be on the order of a root mean square value (RMS) of ±1000 feet.

Unfortunately, however, the system reliability did not continue at the anticipated level. During 1963, an increasing number of failures occurred, some due to design deficiencies and others simply due to component deterioration.

Since this system does provide primary flight data to the pilot, restrictions requiring pilots to fly at altitudes below 160 000 feet were placed on the X-15 flight envelope when the reliability began to degrade. An extensive analysis of the system was then undertaken to establish what in-house efforts could be made to bolster the system performance and to improve the reliability. As a result, it was found that the accelerometer loops and the power supplies within the inertial measurement unit were the prime source of problems and required immediate attention. These loops were, therefore, redesigned in the modified system.

Figure 4 presents an illustration of the reduction in size and complexity which accompanied this redesign effort simply by using improved, modern components which allowed the elimination of some of the circuitry. Shown on the left are the accelerometers, accelerometer electronics, and power supplies initially used in the system; whereas, shown on the right are the hardware items that replaced the original components.

In addition to the reduction in size, significantly less power dissipation occurred within the inertial measurement unit with the use of the new components; consequently, the cooling problems previously experienced and reported at the 1961 X-15 conference were eliminated. Some redesign work is continuing in other areas on the system.

The initial redesign efforts on the accelerometer loops and power supplies were completed and the system was first used in flight status in August of 1964. Since that time, it has supported the flight activities of both the X-15-2 and X-15-3 airplanes with no major reliability problems and with a marked improvement in performance accuracy. This improvement is apparent from the system performance shown in figure 5. The data presented in this figure are the mean altitude error and its standard (1σ) deviation for the system by using the redesigned inertial measurement unit. Again the performance design goal of ±5000 feet at 300 seconds is shown. Although the mean error shows that the system is capable of meeting the design goals, the scatter indicates that the performance has been erratic. The data presented were taken from 16 flights made on the X-15-2 and X-15-3 airplanes with this system installed.

Digital System

At the time that the redesign of the analog system was initiated, a parallel action was taken to modify for use on the X-15 the surplus digital guidance systems available from the X-20 program. This system consists of four subsystems, which are shown in figure 6. These four subsystems are an inertial measurement unit, a coupler electronics unit, a digital computer, and a set of pilot's displays. Although no scale is indicated in this photograph, the relative size of the system can be determined by noting that the attitude indicator (second from left in the pilot's displays) is a standard 5-inch instrument. This system employs the refinement of gyrocompassing which allows the system to undergo a complete automatic erection and alinement cycle on the ground prior to a taxiing run of the B-52. With this system, the requirement for a reference system on board the B-52 has been completely eliminated. The altitude loop is stabilized, however, by clamping it to pressure altitude until 1 minute before launch, at which time the system is put into a full inertial mode of operation.

The inertial measurement unit is a gyrostabilized, four-gimbaled platform which maintains a local vertical orientation throughout the flight. Three pendulous accelerometers are mounted on the inner platform to form an orthogonal triad. The second component (the coupler electronics unit) contains power supplies and interface equipment for the inertial measurement unit and the computer.

All computations are performed on the digital computer which is a dual-function machine consisting of both a digital differential analyzer section and a general purpose section. The digital system was first checked out in flight in the X-15-1 during the autumn of 1964, with satisfactory results. A few minor integration problems have been experienced with the digital system.

However, these difficulties have been of little consequence and were principally concerned with the operating environment of the system.

In evaluations of the performance of the digital system, use has been made of a "data-save" routine which has been programed into the computer. This routine stores selected parameters in the computer memory during the actual X-15 flight. After the flight is completed, these values are recovered and plotted. Such a plot for inertial height (altitude) has been faired into a smooth curve and is shown in figure 7.

This figure shows inertial height as a function of time from launch. Also shown is the faired reference curve. Note that this figure has a dual ordinate scale. The difference between the altitude reference curve and the altitude from the inertial system is shown at the bottom of this figure. These specific data are from only one flight, but the curve is representative of the excellent manner in which the system has been performing.

The data presented in figure 8 were taken from five consecutive flights during which the data-save routine was used. Again, the data are presented as the mean of the altitude error together with standard (1σ) deviation plotted as a function of time following launch. Although these data represent a relatively small sample, the small amount of scatter shown indicates that the system has been performing with good repeatibility. The relative size of the errors of other parameters, such as velocity and position, indicates that the system would have met the performance requirements of the X-20.

Future Programs

Until this time, efforts have been directed toward the display of present flight conditions to the pilot. It is believed, however, that this type of information will not be sufficient for the pilot in future vehicles, such as hypersonic-cruise or lifting-reentry vehicles. In these vehicles, because of the demands placed on the pilot, use of command guidance techniques will be necessary.

The effects of displaying only present flight conditions during boost in a high-performance vehicle are illustrated in figure 9. Shown is a plot of actual peak altitude as a function of planned maximum altitude. In most cases, the planned maximum altitude was missed by less than 5000 feet. Generally, this margin is considered acceptable in the X-15 operations; however, for certain missions it is necessary to fly closer profiles than this. Often, instead of using flight plans only to a preplanned peak altitude, it is desirable to fly an entire mission with a preplanned altitude profile. This accuracy is particularly necessary in the case of the programs planned for the X-15-2, both the buildup to Mach 8 and the "scram" jet program.

A program to investigate guidance requirements and to develop guidance techniques for hypersonic vehicles has, therefore, been included as one of

the X-15 follow-on programs. The objectives of this program are:

(1) To establish and develop guidance techniques for:

(a) Precision flying through a velocity-altitude window during boost

(b) Flying a bounded corridor for hypersonic cruise

(2) To evaluate methods of providing safe reentry corridors.

Although the X-15 is limited in its capability to simulate fully oribital lifting reentry flights, this airplane nevertheless offers the only existing manned reentry system on which equipment and concepts may be tested, modified, and retested within a reasonable time period. Furthermore, with the exception of acceleration and velocity parameters, the X-15 provides an excellent environmental simulation for total integrated system hardware and software evaluation with the pilot actually undergoing the rigors of making a reentry.

A versatile high-speed computer is presently being added to the basic digital flight data system to provide the additional computational capability for accomplishing this program.

A block diagram of this total system is shown in figure 10. The key elements of the system, as shown, are the displays, the high-speed computer, the X-15 air-data sensor, the basic inertial flight-data system (the inertial measurement unit and the computer), and the MH-96 adaptive control system. The navigation functions will continue to be performed by the basic inertial flight-data-system computer, while the high-speed computer will be programed to carry out the research objectives.

This system offers a further advantage, as can be noted, in the form of a direct communications route between the guidance system and the control system. Thus, the pilot in the loop or the pilot monitoring the loop may be investigated. Furthermore, various levels of pilot participation in the loop may be evaluated.

Simulation efforts are presently under way to define the most promising techniques for boost guidance and corridor control. The initial technique to be used in flight will be a command pitch attitude, generated within the computer and based on flight-path angle, present altitude, predicted altitude, and an altitude profile stored within the computer.

Also included in the boost reentry guidance program is an evaluation of one or more energy-management techniques that will provide commands to insure both a safe reentry and guidance to a preselected landing point. Six basic requirements of an energy-management system for a lifting reentry vehicle must be considered. These are:

(1) Damping of trajectory oscillations

(2) Minimizing temperature

(3) Minimizing normal acceleration

(4) Minimizing dynamic pressure

(5) Accurate guidance to a terminal point

(6) Full utilization of the vehicle-pilot capability.

In the initial program, prediction techniques will be used to provide guidance commands that will insure reentry through a corridor with prescribed vehicle constraints relative to temperature, normal acceleration, and dynamic pressure. This plan is accomplished by having stored in the computer the equations of motion of the vehicle, the constraints of the vehicle, and air-density equations. The equations of motion of the vehicle (i.e., the mathematical model) are solved for a maximum-range flight, a minimum-range flight, and a maximum-cross-range flight based on the initial or present conditions of the vehicle. This solution takes about 1 second in the computer and then, based on an updated set of initial conditions, the solution is repeated. Bank-angle and angle-of-attack commands are generated to provide guidance to the high key point of a preselected landing site that is within the area determined by the maximum-range, minimum-range, and maximum-cross-range mathematical-model flights. Based on these commands, the maximum temperature, normal acceleration, and dynamic pressure are predicted. Should these predictions indicate that the constraint limitations of the vehicle are to be exceeded, the commands are modified.

Even though the X-15 flies essentially straight to the Edwards landing area from its launch point, the determination of the capability of an energy-management system to provide guidance commands for accurate guidance to a terminal point can be evaluated. The pilot may select several prestored landing locations during the course of the flight. When one of these locations is chosen, the program will generate the bank-angle and angle-of-attack commands for the vehicle to reach this location. These commands and the dynamic conditions of the X-15 are then recorded. These data will later be recovered and used in the X-15 simulator to determine the validity of the commands.

Another system that is presently under consideration for possible flight evaluation on the X-15 uses temperature and temperature rate to provide a reentry corridor. Should this system prove feasible, it will be integrated with an energy-management program to provide a complete reentry guidance system.

CONCLUDING REMARKS

The experience gained with the use of the analog and digital inertial flight data systems in the X-15 program has shown that although either system,

when properly designed, will perform the basic guidance functions required for vehicles such as the X-15, the analog system lacks versatility and is, therefore, not especially suited to uses where a variety of guidance or navigation equations are to be solved at different times during a specific flight. In addition, the analog system quickly degrades the sensed signal accuracy whereas the digital computer, if properly programed, does not do so within reasonable lengths of time. The digital system, therefore, provides the better tool in support of programs such as the guidance research program now being implemented on the X-15.

It is through actual flight research programs of this type that proper guidance techniques and systems may be developed for future vehicles.

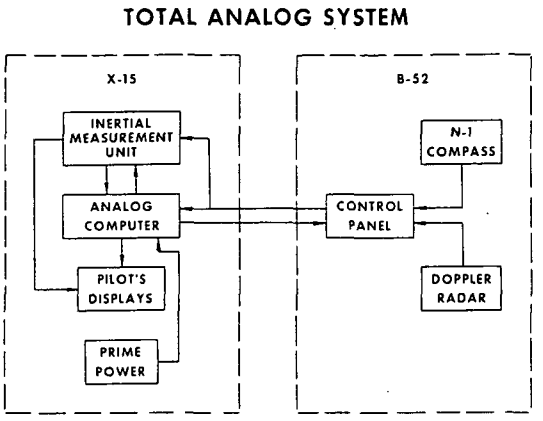

Figure 1

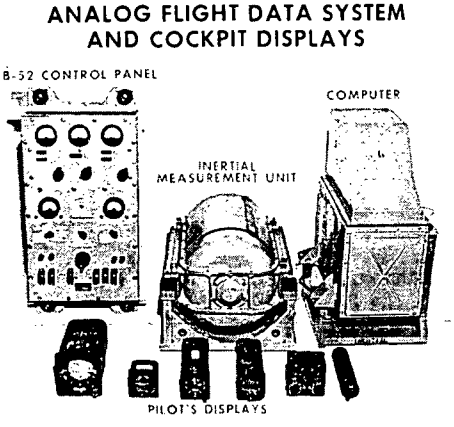

Figure 2

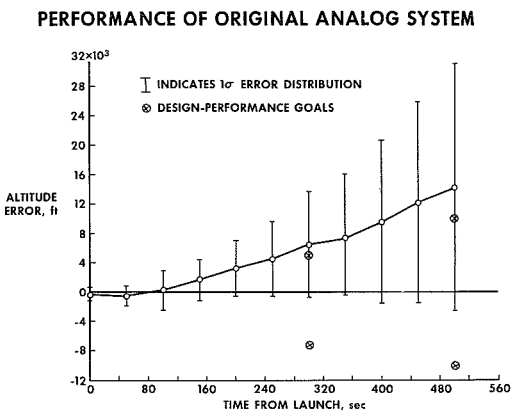

Figure 3

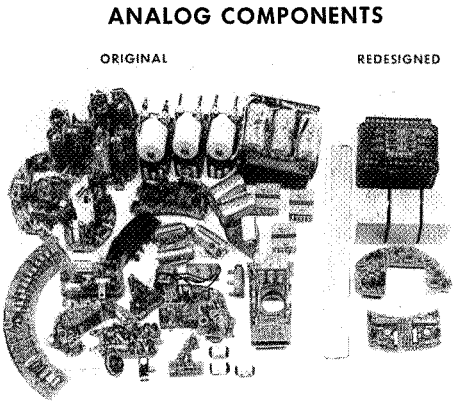

Figure 4

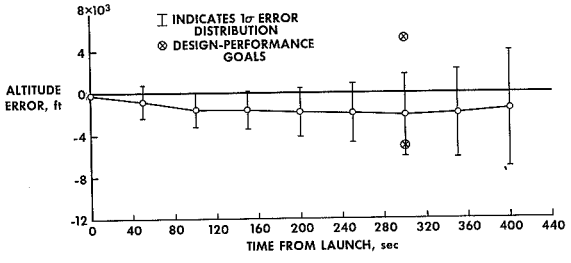

Figure 5

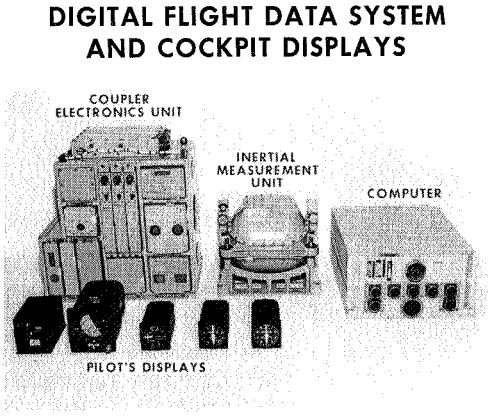

Figure 6

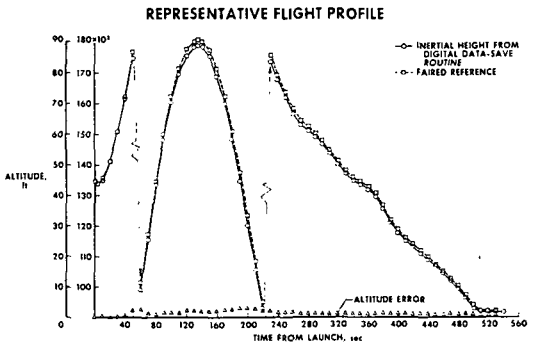

Figure 7

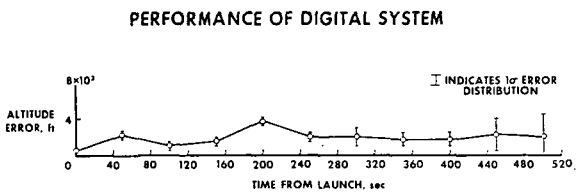

Figure 8

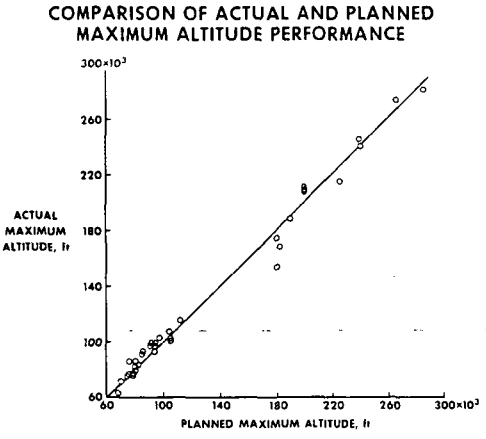

Figure 9

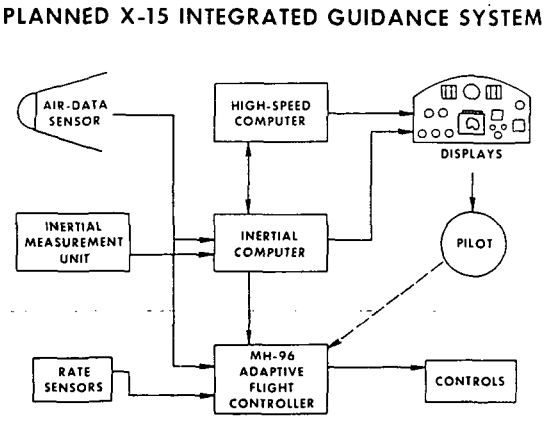

Figure 10

8. INVESTIGATION OF HIGH-SPEED HIGH-ALTITUDE PHOTOGRAPHY

By Donald I. Groening
U.S. Air Force Avionics Laboratory

SUMMARY

The Air Force has been conducting a series of photographic flight experiments on the X-15 airplane to investigate the effects of extreme aerodynamic conditions on aerial photography. The primary objective of these experiments has been to determine the degradation to optical imagery caused by supersonic and hypersonic shockwaves, boundary layers, and rapid frictional heating of the photographic window. Several different experimental packages employing well instrumented aerial camera systems of advanced design have been used in these experiments. Additional aircraft instrumentation also included a multiple pickup boundary-layer rake. Both the geometry and resolution of the experimental photography have been analyzed and compared with flight conditions at the time of their exposure.

INTRODUCTION

The Air Force Avionics Laboratory has been conducting a series of photographic experiments on the X-15. The scope of this research is indicated in figure 1. The purpose of these experiments is to investigate the effects on photographic resolution, geometry, and contrast of the shock waves, boundary layers, and heating of supersonic and hypersonic flight.

Five different experiments are being conducted.

DESCRIPTION OF EXPERIMENTS

The first experiment, employing two small aerial cameras installed in the center-of-gravity compartment of the X-15-2 (fig. 2), provided data which permitted investigation of contrast attenuation at high altitudes and showed the feasibility of obtaining aerial photography from supersonic vehicles.

A KC-1 camera, fitted with the GEOCON I low-distortion mapping lens, was installed in the instrument bay of the X-15-1 (fig. 3) for the second experiment. This experiment provided mapping photography for the determination of geometric distortions in aerial mapping from advanced vehicles.

The KS-25 camera, a 24-inch focal-length high-resolution camera, replaced the KC-1 in the instrument bay for the third experiment (fig. 4), which was designed to determine whether extreme flight environments could significantly limit the optical performance of high-resolution aerial camera systems.

Two additional experiments on the X-15-2 were designed to provide data for the evaluation of special color films in high-altitude photography and to extend investigation of aerodynamic limitations on optical performance to the Mach 8 realm. The first of these experiments utilized the small two-camera package first used in experiment 1. In the final experiment, plans are to install a camera with performance comparable to the KS-25 in the hydrogen fuel tank area of X-15-2 and to use it during the buildup flights to Mach 8.

INSTRUMENTATION

In addition to the cameras, special instrumentation has been employed to monitor the mechanical and optical performance of equipment and the conditions present during the flight.

The seven downward-looking photometers (fig. 5) are used to measure the spectral changes in light with respect to altitude and to provide a signal to the automatic exposure control system of the KS-25 camera. The metal honeycomb limited the acceptance angle of the photometers to 22° and Wratten-type filters were used to divide the spectrum into different bands. Two additional upward-looking photometers monitored the amount of visible light remaining in the upper atmosphere.

The camera window instrumentation (fig. 6), provided a continuous record of temperature on both inner and outer surfaces of the photographic window.

A multiple-pickup boundary-layer rake (fig. 7) was used to indicate whether the boundary layer was laminar or turbulent and to monitor its thickness for subsequent comparison with photographic quality.

For the analysis of the photography, special ground instrumentation is used. The mapping analysis of the KC-1 experiment utilized existing ground survey data, supplemented by special surveys of identifiable points in the photography.

For the measurements of resolution and contrast, 3-bar resolution targets were constructed at Indian Springs and Pahrump in Nevada and near Pilot Knob and Cuddeback Dry Lake in California. Photometric measurements of the targets were made during each flight.

FLIGHT PROGRAM

The KC-1 and KS-25 experiments included both high-speed and high-altitude flight profiles to provide as complete a range of altitude-velocity combinations as possible (fig. 8).

Experiments 1 and 4 were flown on a piggyback, space-available basis, whenever the flight profile was such as to afford an opportunity to obtain useful data.

ANALYSIS

The photography obtained was analyzed both visually and electronically. Stereo plotting instruments were used to measure the mapping photography, while microdensitometers were used with the high-resolution photography.

In the KS-25 experiment, modulation transfer functions computed from microdensitometer edge traces of the images were compared with predicted transfer functions computed from a mathematical model developed specifically for this experiment. Figure 9 is an example of one of these comparisons. The actual measured modulation transfer function falls properly between the minimum and maximum curves predicted by the mathematical model.

RESULTS

Four of these experiments have thus far been completed. Figures 10 and 11 are photographs from the KC-1 mapping camera, obtained on the fifth of six flights flown for this experiment in 1963. Figure 10 is a forward oblique view of southwestern Nevada and part of eastern California. Indian Springs Air Force Base, Frenchman Flats, Mercury, Yucca Flats, and Pahrump, Nevada, are in the photograph. The airplane had reached an altitude of 140 900 feet at a velocity of 5180 feet per second (Mach 4.85) and was climbing under full power at the time of exposure. Figure 11 is a vertical photograph taken 75 seconds later as the X-15 was in a ballistic trajectory at an altitude of 226 200 feet with a velocity of 4780 feet per second (Mach 4.86). Many of the same ground features are in both photographs. The vertical photograph (fig. 11) covers an area of over 4000 square miles.

The results of this experiment have shown that flight environments of high performance vehicles do not significantly limit the geometric precision of high-quality mapping photography.

Figure 12 is a conventional photograph from the KS-25 camera, taken at an altitude of 45 000 feet when the X-15 was still attached to the B-52 just a few minutes before launch. This procedure was followed on each flight to see that the camera was operating and to provide photography which verified the camera's performance at the start of the X-15 flight. This photograph has a resolution of over 80 lines per millimeter.

Figure 13 is a photograph of the resolution target at Indian Springs, Nevada. It was taken with the X-15 at an altitude of 101 400 feet and a velocity of 5420 feet per second (Mach 5.47). The temperatures on the camera window at this time ranged from a minimum of -4° F on the inner surface to a maximum of 287° F on the outer surface. The resolution of this photograph is 60 lines per millimeter.

Figures 14 and 15 are photographs of Indian Springs Air Force Base. The photograph shown as figure 14 was taken at an altitude of 100 000 feet and a

velocity of 5465 feet per second (Mach 5.43). The window temperatures ranged from -1° F to 312° F. The three parked aircraft are readily identifiable. The photograph shown as figure 15 was taken at an altitude of 169 600 feet and a velocity of 4690 feet per second (Mach 4.37). The window temperatures ranged from 14° F to 169° F. Both of these photographs have resolution of over 60 lines per millimeter. The KS-25 photography has shown that flight environments as extreme as Mach 6 at 100 000 feet will not affect a photographic system capable of a resolution of 4.2 arc-seconds.

On June 22, 1965, with the small 12-inch focal-length camera on the X-15-2 this photograph of Indian Springs Air Force Base (fig. 16) was taken. The film used was infrared ektachrome which differs from normal color film in that the spectral sensitivity of each emulsion layer is shifted toward the infrared.[1] The blue light is removed by filtering and, in the final reversed image seen here, naturally green objects are blue, yellow objects are green, red objects are yellow, and objects radiating or reflecting strongly in the near infrared, such as healthy vegetation, are red.

This type of film offers considerable promise in high-altitude photography, as figures 17 and 18 clearly demonstrate. Both were taken with the 6-inch focal-length oblique camera on the X-15-2, the black and white (fig. 17) in October 1962 and the color (fig. 18) in June 1965. Las Vegas is in the foreground with McCarran Field and Nellis Air Force Base visible. The bright red areas (in the color projection) around Las Vegas are golf courses and irrigated fields. Beyond Las Vegas is Lake Meade and Lake Mojave, the latter barely visible in the black and white (fig. 17). Also on the black and white to the southeast is the mouth of the Grand Canyon and beyond that Mount Humphrey just north of Flagstaff, Arizona. On the ektachrome (fig. 18) to the south are irrigated fields near Needles, California, and more vegetation along the lower Colorado River until finally just below the horizon is the Gulf of California and the Colorado River delta.

CONCLUDING REMARKS

The X-15 has proven to be a useful test bed for evaluating photographic performance in extreme flight environments. These flight experiments are providing important information concerning the usefulness of high-performance aircraft in aerial photography. The experiments thus far completed have shown that high quality aerial photography can be obtained in extreme environments.

---

[1]Comments concerning the color photographs refer to color projections, which unfortunately could not be provided in this compilation.

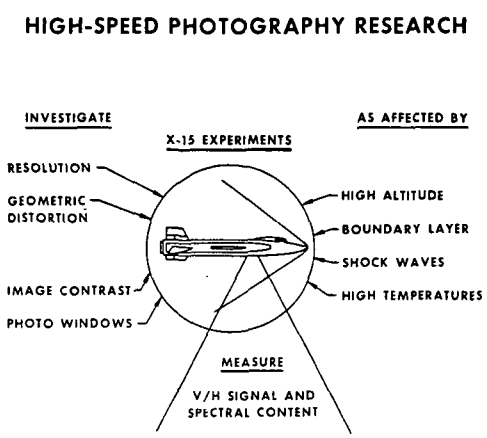

Figure 1

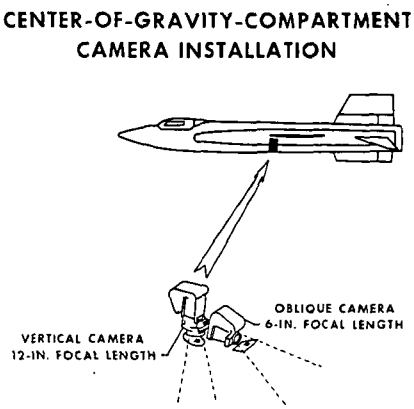

Figure 2

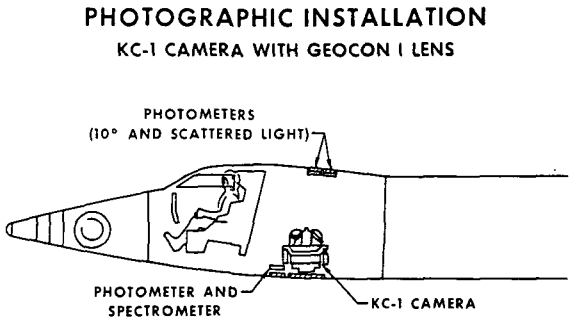

Figure 3

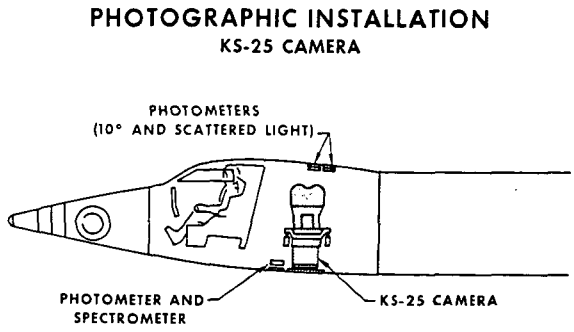

Figure 4

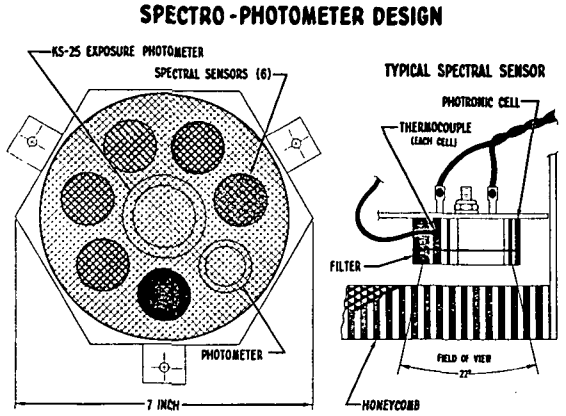

Figure 5

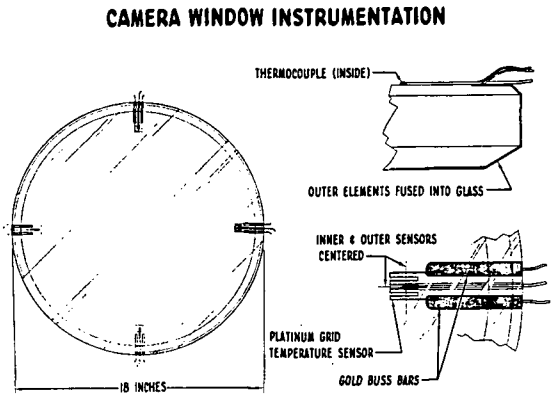

Figure 6

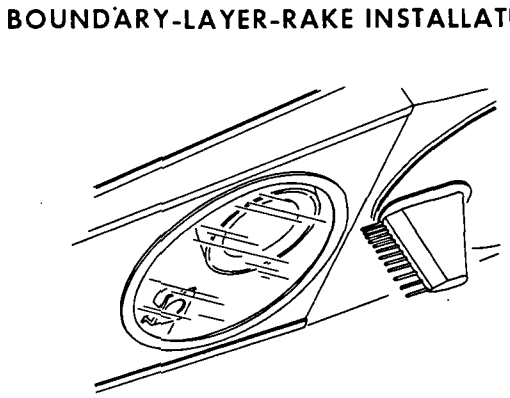

Figure 7

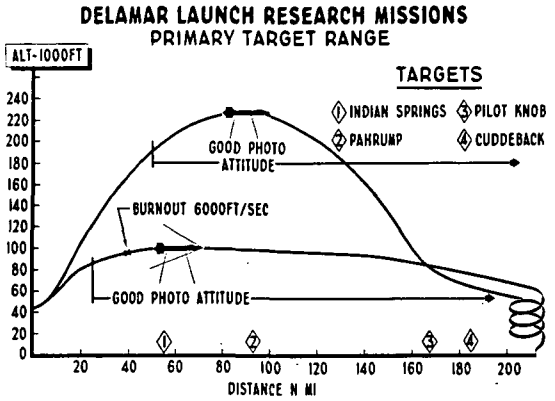

Figure 8

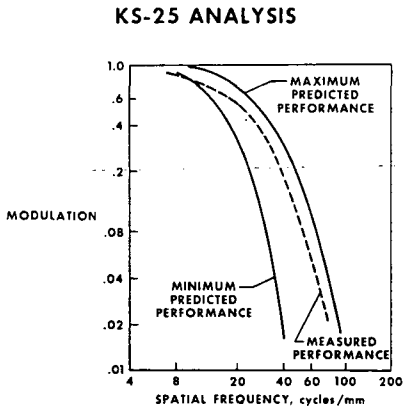

Figure 9

KC-1 FORWARD OBLIQUE

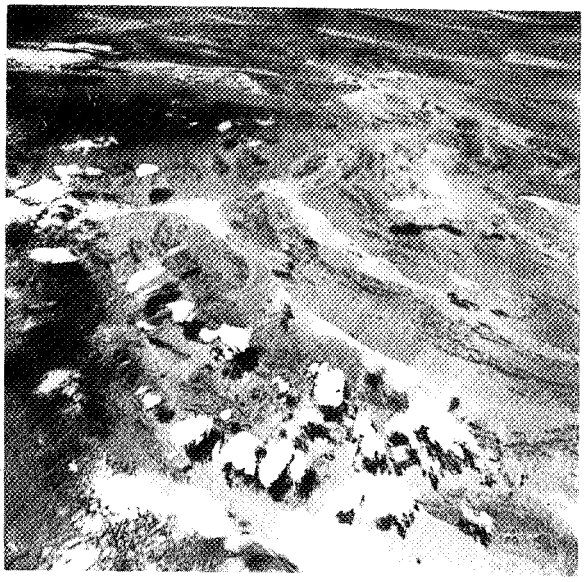

Figure 10

KC-1 HIGH ALTITUDE VERTICAL

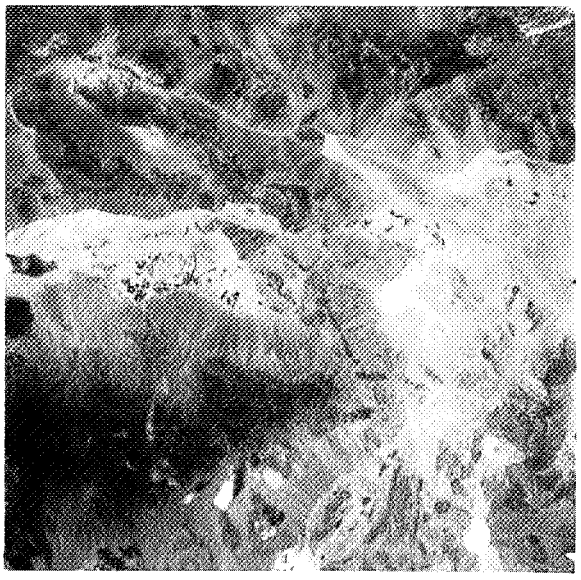

Figure 11

KS-25 CAMERA CHECKOUT

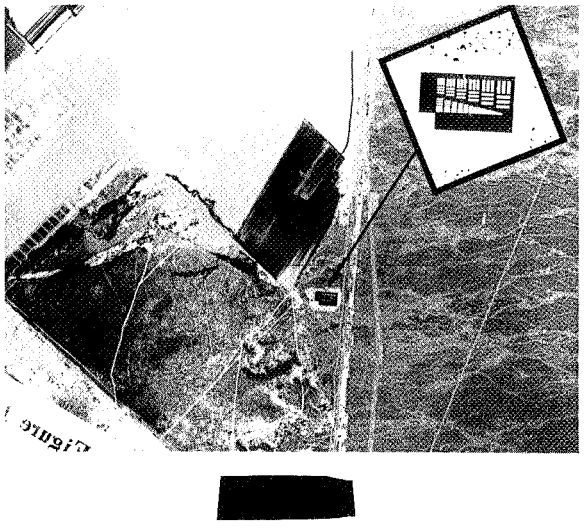

KS-25 HIGH-SPEED PHOTOGRAPH

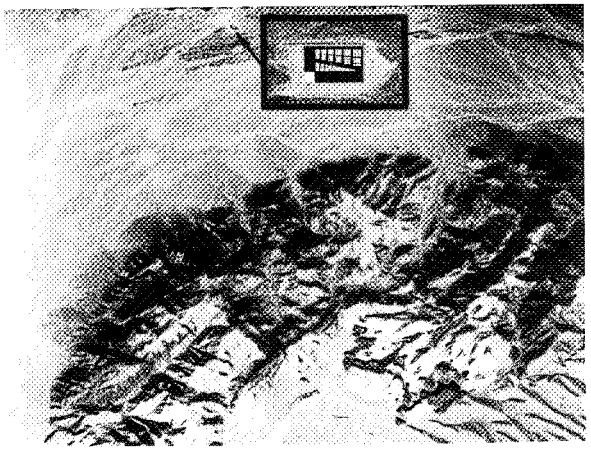

Figure 13

HIGH-SPEED PHOTOGRAPH, INDIAN SPRINGS

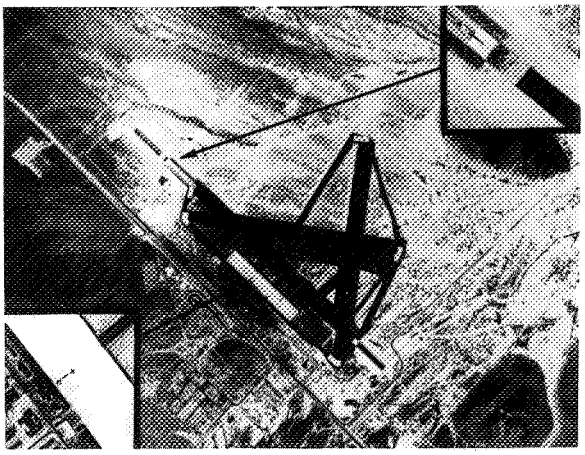

Figure 14

HIGH ALTITUDE, INDIAN SPRINGS

BLACK AND WHITE

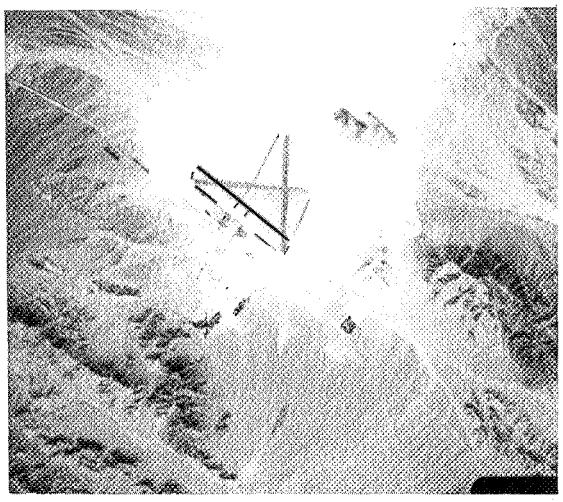

Figure 15

HIGH ALTITUDE, INDIAN SPRINGS

COLOR FILM

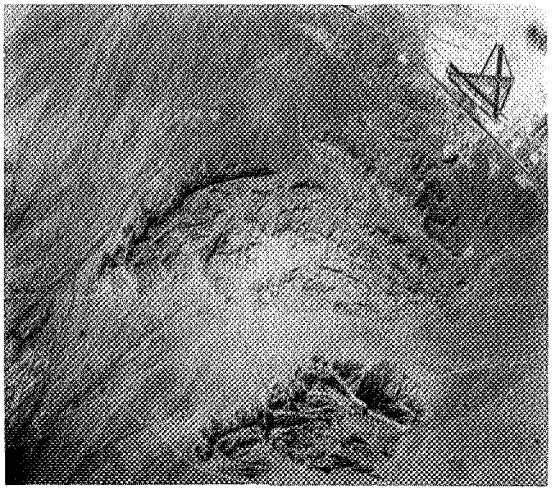

Figure 16

LONG RANGE OBLIQUE

BLACK AND WHITE

Figure 17

LONG RANGE OBLIQUE

COLOR FILM

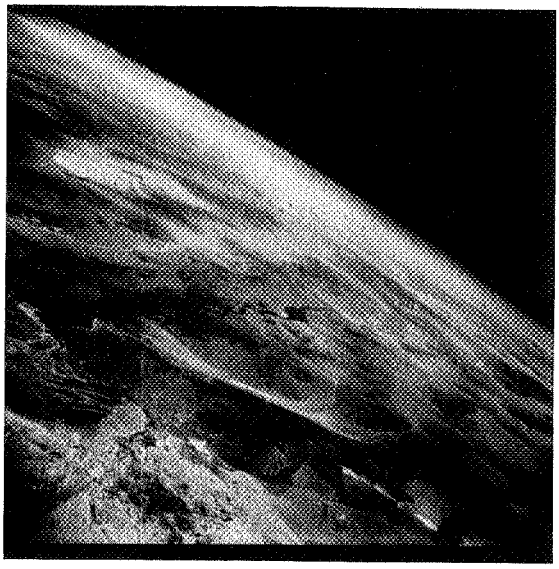

Figure 18

9. RADIATION MEASUREMENTS OF THE EARTH'S HORIZON FROM THE X-15

By Antony Jalink, Jr.
NASA Langley Research Center

SUMMARY

Horizon trackers are a simple means to provide the attitude information for space vehicles in the vicinity of the earth. In order to build efficient horizon trackers, the spectral band in the earth's atmosphere that yields the most consistent and, therefore, the most accurate radiance gradient must be determined. The Langley Research Center's horizon definition program is obtaining radiometric measurements of the earth's horizon in selected regions of the electromagnetic spectrum by using rocket probes and research aircraft. The X-15 airplane is utilized as a part of this program since it is capable of achieving the altitudes needed to obtain meaningful data. The experimental data obtained in several spectral regions are presented and are compared with predicted results.

INTRODUCTION

Conventional flight vehicle attitude instruments make use of gravity sensors. As vehicle velocities approach orbital speeds, however, such instruments become useless, and other means for measuring vehicle attitude must be developed. Horizon sensors provide a simple means to help determine the attitude of space vehicles in the vicinity of earth. These instruments note the change in radiant energy that they receive when their line of sight sweeps from the relatively warm earth across the atmosphere onto cold space. Because the atmosphere absorbs and emits energy, it blurs the transition and thus introduces a factor of uncertainty in the position of the radiation horizon which must be investigated before more accurate and reliable horizon sensors can be designed. Figure 1 shows that the energy received by a horizon sensor may be thermal radiation from the earth and the atmosphere, as well as solar energy scattered or reflected by clouds, the atmosphere, or the earth. Other parameters that affect the radiation which a sensor receives are weather seasonal variations, latitude, and viewing altitude. The X-15 is a valuable vehicle for obtaining measurements on the earth's horizon signature because it is capable of reaching high altitudes and of readily providing two additional needed measurements, namely, the aircraft attitude and position.

The horizon radiance profile has a different shape in each spectral region, since the processes which cause absorption and emission of energy by the molecules of the various constituent gases of the atmosphere vary with wavelength. Also, any variation of temperature, pressure, and mixing ratio of the gases of the atmosphere change the profile, so that the radiation horizon is affected by seasonal changes and by its location on earth.

OBJECTIVES

Theoretical calculations have been performed on representative model atmospheres to determine the radiance profile in several spectral intervals in the infrared. The most promising spectral regions have been selected by Langley Research Center as a basis for a horizon-definition program to complement these theoretical calculations by experimental data. Thus, the accuracy attainable by horizon-sensing techniques may be estimated, while at the same time, valuable information is obtained to aid in the design of future horizon sensors. The X-15 flight program offers the unusual opportunity for making flight measurements under conditions for which the required meteorological data are available for use in computing the theoretical radiance profile, so that comparison between actually observed and calculated profiles may be made.

METHOD

The general method of approach for obtaining horizon-definition data is illustrated in figure 2. The radiance profile, which is a plot of radiance as a function of altitude, must be found. In order to obtain this plot, the amount of radiant energy contained within the cone of the field of view must be measured as a function of the altitude H. The area of the cone represents the field of view of the experiment; and the altitude H is called tangent height for the purpose of this discussion. The tangent height can be obtained if the altitude h of the observer and the nadir angle η between local vertical and the line of sight are known. The observer altitude h can be obtained from ground radar, and the angle η can be determined from the aircraft pitch angle θ and the angle δ, which is the angle between the radiometer line of sight and the vehicle pitch axis. The accuracy with which tangent height is obtained, therefore, depends on the accuracy of the measurements of θ and δ. The worst error to be introduced is dependent on the accuracy of the stable platform data, of which θ is one angle. The longitude and latitude of the tangent point can be obtained from geometric relationships if, in addition, the longitude and latitude of the observer are known. Weather data can also be obtained for the areas between the tangent point and the observer, so that calculated radiation profiles can be made for comparison with the experimental profiles.

LANGLEY RESEARCH CENTER PROGRAM

The Langley Research Center is engaged in an experimental program for obtaining the measured profiles. Three horizon-definition projects at this Center are indicated in table I. The headings show the region of the spectrum to be investigated, the radiometric definition (which means the size of the cone of the field of view at the tangent point), the spatial position in kilometers (by which is meant the accuracy to which tangent altitude H can be established). The three projects are identified as the D-61-3, Project Scanner, and the X-15 experiment. The D-61-3 covers two spectral regions each flight.

The trajectory and field of view of this spin-stabilized rocket probe are such that the radiometric resolution of the experiment is 12 kilometers. It is equipped with a celestial measurement device which allows the spatial position of the profiles to be determined within 2 kilometers. Project Scanner is a sub-orbital rocket experiment, which covers two spectral regions each flight. It affords a radiometric resolution and positioning accuracy of 2 kilometers. The geographic horizon coverage ranges from the Arctic Circle to within 5° of the equator and from the Central United States to the middle of the Atlantic Ocean.

TABLE I.-LANGLEY HORIZON DEFINITION PROGRAM

EXPERIMENT	SPECTRAL REGION, μ	RADIOMETRIC DEFINITION, km	SPATIAL POSITION, km	COMMENTS
D-61-3	10 TO 14 14 TO 20	12 km	2 km	ROCKET PROBE, CELESTIAL-ATTITUDE MEAS. FOR POSITION
PROJECT SCANNER	14 TO 16 20 TO 35	2 km	2 km	ROCKET PROBE, TWO REGIONS PER FLIGHT, CELESTIAL ATTITUDE MEAS., INCREASED COVERAGE
X-15	0.8 TO 2.8 10 TO 14 14 TO 20	2 km	5 km	ONE SPECTRAL REGION PER FLIGHT, X-15 ATTITUDE MEASUREMENT, LIMITED COVERAGE, REUSABLE

The Langley Research Center X-15 horizon-definition experiment, with which this paper is concerned, was designed to be the first experiment to obtain horizon data to a definition of 2 kilometers. In addition, it allows the spatial position to be fixed to 5 kilometers by means of aircraft attitude data. A penalty that must be paid is the limitation to daylight flights and the limitation in geographical coverage.

INSTRUMENTATION FOR X-15 HORIZON-DEFINITION EXPERIMENT

The Langley Research Center X-15 horizon-definition experiment is now discussed in more detail. First the radiometer and associated equipment are described. Then, the data flow used to reduce the flight measurements is considered, and finally, some data that have been reduced are discussed.

The radiometer used in the Langley X-15 horizon-definition experiment is shown in figure 3. It consists of a motor-driven scan mirror which sweeps the field of view through a 30° optical scan. The angle of this mirror is continually recorded to provide a record of its position, and this record gives the angle δ, which was shown in figure 2. The scan mirror reflects the energy onto the objective. This parabolic mirror then focuses the energy on the detector. The electrical output of the detector is recorded with an FM-FM magnetic tape recorder, which forms part of the standard X-15 instrumentation. Before reaching the detector, the radiation is passed through an optical bandpass filter to select the spectral band that is to be investigated. The size of the detector is such that the field of view of the radiometer is 0.13° by 0.13°, which provides a definition at the horizon tangent point of 2 kilometers. The radiometers are calibrated by at least three different methods, so that reliable radiance profiles can be obtained from the flight measurements.

Figure 4 shows the installation of the radiometer in the tail-cone box of the X-15 airplane; the view shown is at the rear of the X-15-3; the tail-cone box is mounted directly behind the vertical fin. The nodding scan mirror and

the parabolic objective can be seen. Mounted next to the radiometer and boresighted to look in the same direction is a 16-millimeter motion-picture camera. This camera provides wide-angle coverage for a check on the presence of clouds and haze during the data-taking period. The walls of the box contain thermal insulation to limit the temperature rise inside the box.

DATA REDUCTION

A diagram of the data flow for reducing the measurements of the X-15 horizon-definition experiment is shown in figure 5.

The dashed-line boxes indicate available data sources routine to X-15 flights. The solid-line boxes show equipment and calculations provided especially for this experiment. The radiometric output of the scanner is combined with the calibration data obtained for this instrument, so that the observed radiance is known. Confidence in the calibration is strengthened by the fact that both postflight and preflight calibrations can be made, since one of the advantages in using the X-15 is that the equipment returns.

From the X-15 stable platform, pitch, roll, and yaw data are obtained. These attitude data, combined with the position of the scan mirror, enables the altitude of the observed radiance data to be fixed, so that a measured horizon profile is determined.

A great help in this experiment is the weather data provided as a standard backup to the high-altitude X-15 flights. These high-altitude balloon and rocket-sounding data, combined with standard weather reports from the area of interest, allow establishment of a model atmosphere that can be used to compute a theoretical horizon profile by use of horizon radiance theory (ref. 1). As a further check on haze and cloud conditions, films taken with the 16-millimeter motion-picture camera are available. The anticipated final step of data reduction will be the comparison of the measured data with the theoretical horizon profile. The discrepancies shown in this comparison will provide a basis for further horizon definition experiments.

RESULTS

The Langley Research Center uses the X-15 stable platform and ground range radar data, as well as the mirror position δ, in a digital computer program to obtain the measured radiance profiles. Preliminary data are available from three flights in three spectral regions. Figure 6 is an example of the data obtained; it shows the horizon profile in the 0.8- to 2.8-micron, near-infrared region at an observer altitude of 28 nautical miles (52 kilometers). The radiance N in watts-meter^{-2}-steradian^{-1} is given as a function of the tangent height in kilometers. Plotted is a typical curve. First, going from space to earth, the data plot a smooth curve. This energy is the sunlight scattered by the molecules of the atmosphere. Shown also is a calculated curve for primary

Rayleigh scattering. Note that the actually measured data are about twice as high as the calculated data. This result may be explained by the fact that there is really multiple scattering rather than only primary scattering. Next is shown some energy that can be ascribed to emission of the near infrared water vapor bands. Then, the energy of reflected sunlight from the cloud banks is seen; also shown is the amount of energy the radiometer would receive if the albedo of the clouds were 1.0, so that the measured albedo is noted to be actually 0.5 to 0.6. This result compares favorably with measurements made in this region. One of the reasons for obtaining data in this region, where the horizon profile is highly variable because of its dependence on meteorological conditions, is that the signatures of the clouds in this spectral region can be compared with data in the visible spectrum to allow estimates of the accuracy of the experiment. Figure 7 shows a horizon radiance profile in the 10- to 14-micron region. Plotted is the radiance in watts-meter^{-2}-steradian^{-1} as a function of tangent height in kilometers. The solid-line curve indicates the calculated horizon profile. This profile was constructed with the help of data published by Wark, Alishouse, and Yamamoto (ref. 1). Plotted also is the profile as measured during a recent X-15 flight. In fact, these data were reduced at such a recent date that time was not sufficient to allow an analysis as to the cause of the noted discrepancies. It was noted, however, that the total radiation differential measured between space and earth is somewhat greater than is predicted by theory.

CONCLUSIONS

Results from the Langley Research Center X-15 horizon-definition experiments indicate that this airplane can be used profitably as a test bed for obtaining such data. Not only is the design of the experiment simplified because there are few restrictions due to size and weight limitations, but also the availability of standard X-15 attitude and position data are an advantage. Postflight calibration strengthens confidence in the data, and the radiometer is reusable if it is required to investigate other spectral regions. In addition good weather data are available for the points of interest.

Preliminary inspection of data obtained indicates satisfactory horizon measurements can be obtained by using the X-15 research aircraft.

REFERENCE

1. Wark, D. Q.; Alishouse, J.; and Yamamoto, G.: Calculations of the Earth's Spectral Radiance for Large Zenith Angles. Meteorol. Satellite Lab. Rept No. 21, Weather Bur., U.S. Dept. Com., Oct. 1963.

SOURCES OF RADIATION AND REFLECTED ENERGY

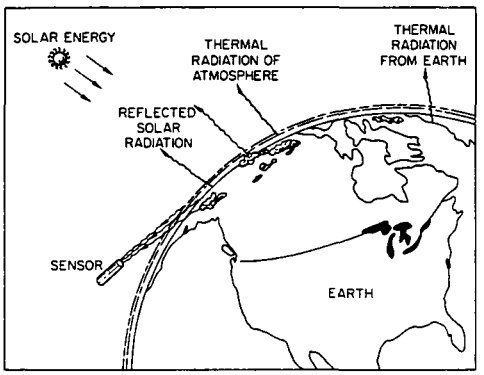

Figure 1

METHOD TO OBTAIN HORIZON DATA

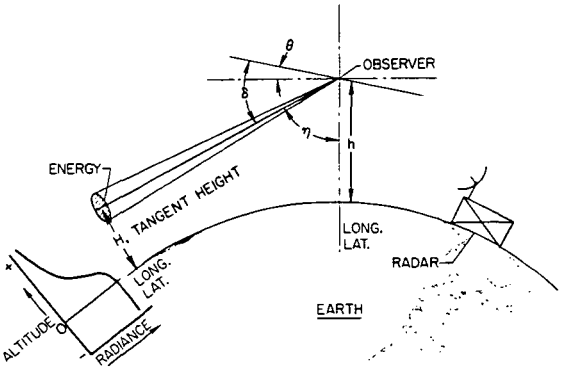

Figure 2

X-15 RADIOMETER
FIELD OF VIEW, 0.13° BY 0.13°

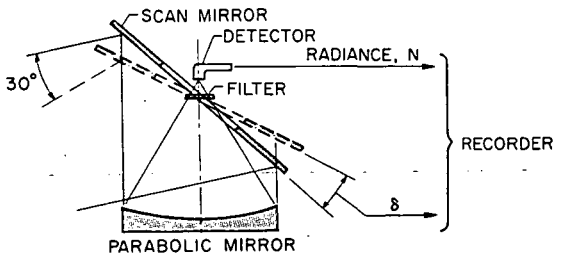

Figure 3

SCANNING RADIOMETER MOUNTED IN VERTICAL TAIL OF X-15

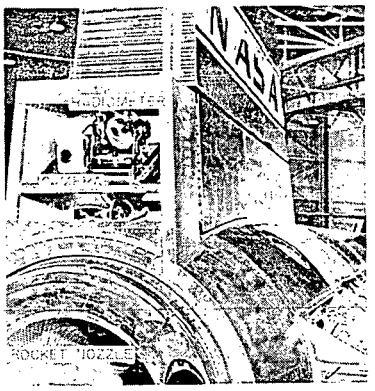

Figure 4

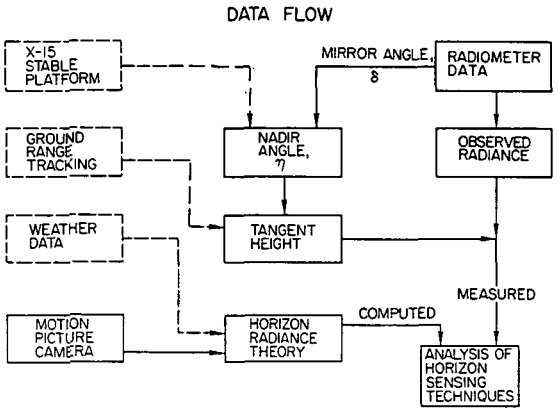

Figure 5

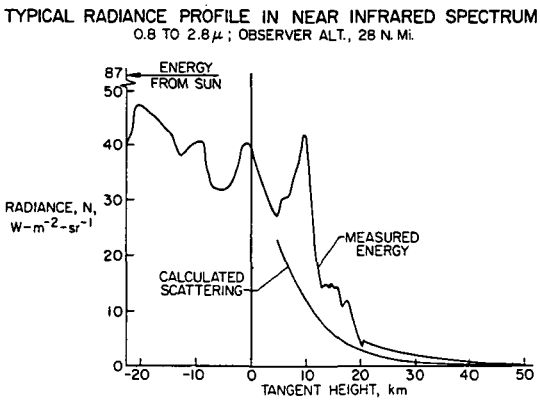

Figure 6

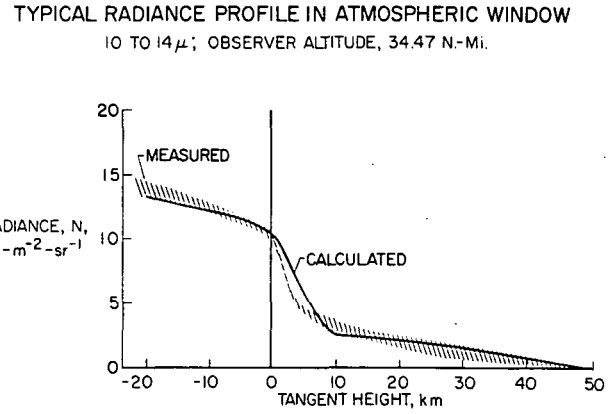

Figure 7

10. DEVELOPMENT AND STATUS OF THE X-15-2 AIRPLANE

By

Elmor J. Adkins
NASA Flight Research Center

and

Johnny G. Armstrong
Air Force Flight Test Center

SUMMARY

The original X-15-2 airplane has been extensively modified to provide a Mach 8 configuration. The modifications included jettisonable tanks for additional propellants which would provide the increased performance and consequently would provide a realistic environment for the development and evaluation of a hypersonic air-breathing propulsion system. This paper summarizes the development and initial evaluation of the modified airplane.

INTRODUCTION

On November 9, 1962, on its 31st flight, the X-15-2 airplane was severely damaged during an emergency landing at Mud Lake, Nevada. There was major damage to the right wing and the empennage, with lesser damage to many mechanical and structural components.

At the time of the accident, the initial (basic) X-15 program was not yet completed and, in addition to this basic X-15 program, numerous follow-on programs and "piggyback" experiments were scheduled for the X-15. The total program required operation of three aircraft, with widely differing instrumentation, through 1966 in order to obtain useful and timely research data.

At the same time, the Government had become interested in hypersonic air-breathing propulsion experiments which would require a carrier vehicle capable of Mach 8. It was suggested that the X-15-2 should be repaired and modified to provide this increased performance.

Approval was given to proceed with design, modification, and repair in May 1963. In the autumn of 1964, the modified airplane made its first flight and has since flown ten times (total of 11 flights). The primary objectives of these flights have been to provide systems checkout, stability and control evaluation, and stellar photographic experiments.

The purpose of this paper is to describe the modified airplane, to discuss some of its development problems, and briefly to outline the present research program.

MODIFIED X-15-2 AIRPLANE

Design Criteria

The primary program for the modified X-15-2 airplane is to develop and evaluate a hypersonic air-breathing engine. To accomplish this, the X-15-2 was to be capable of a velocity of 8000 feet per second at an altitude of 100 000 feet as shown in the design envelope presented in figure 1. At this flight condition, the dynamic pressure is 1000 pounds per square foot.

An approximate area of interest for ramjet testing is also shown in figure 1 by the shaded area. Although the ramjet test region includes flight conditions that could be attained by the basic X-15, the most valuable information would be gained at the higher speeds (beyond Mach number ≈ 6) and at flight conditions of relatively high dynamic pressure.

The flight conditions which were within the reach of the X-15 are bounded by a basic airframe structural limit at a dynamic pressure of 2200 pounds per square foot. Adequate safety margins would be maintained by restricting planned flights to dynamic pressures less than 1600 pounds per square foot. Within the flight envelope shown, the X-15-2 may experience dynamic pressure up to 2200 pounds per square foot, heating rates up to 210 Btu/sq ft/sec and structural temperatures approaching 2400° F. Aside from the increase in temperatures, no other major factors were considered in achieving the higher velocities.

Modifications

The physical appearance of the X-15-2 has not changed noticeably as a result of the modifications. The wing span is still 22.36 feet, but the airplane is 29 inches longer. Current landing weight of the modified airplane is about 1000 pounds greater than the other airplanes.

The modifications to the basic airplane which combine to produce this increased weight are shown in figure 2. The increased performance to a design velocity of 8000 feet per second was to be achieved by increasing the rocket engine propellants by 70 percent. The main propellant increase is contained in external tanks. These tanks are attached to the airplane structure at the side fairings.

Other modifications include the addition of hydrogen peroxide tanks within the extended aft side fairings for the increased engine propellant pump operation. Additional helium for pressurization and purging is contained in the tank shown aft of the vertical stabilizer.

Although the experimental ramjet configuration has not been defined at this time, it is expected to be about 18 inches in diameter and will be installed in place of the lower ventral stabilizer. The complete installation, including fuel and instrumentation, is expected to weigh approximately 1400 pounds.

The landing gear was strengthened and lengthened to provide for the increased landing weight of the airplane and to provide ground clearance for the ramjet during landing. Until the ramjet is installed, a shorter interim gear is being used.

Increased internal volume for experimental payloads was achieved by adding 29 inches to the fuselage between the liquid oxygen and the fuel tanks. The arrangement of access doors to this compartment can accommodate optical windows looking up or down. Liquid hydrogen tanks, with a total capacity of 48 pounds for the experimental air-breathing engine, will be installed in this bay. Adding 29 inches to the fuselage dictated that the pylon attachment points also be relocated on the fuselage.

Because of the higher temperatures anticipated for the X-15-2, the canopy and windshield configuration was revised. The canopy is expected to be coated with an ablative material. The windshield now has an elliptical shape with three panes of glass replacing the previous two panes on each side of the canopy. The outer pane is of 0.65-inch-thick fused silica; the middle pane is of 0.375-inch-thick alumino-silicate; and the inner pane is of 0.29-inch-thick laminated soda lime. The outside windshield retaining frame is flush with the glass to prevent high heating at stagnation areas.

The modification also includes the installation of a "sky hatch" just aft of the cockpit, above a revised instrumentation bay. The hatch accommodates the stellar photographic experiments and has two doors, 20 inches by 8.5 inches, which can be opened in flight as required at high altitude only.

In the previously mentioned accident, the tip of the right-hand wing was damaged beyond repair; however, it was possible to repair the wing to about the midspan. To this stub was added a 41-inch-span removable wing tip. The tip is made of Inconel X, as it was originally, and it now incorporates an access panel with a span of 26.7 inches and an average chord of 23 inches. This removable wing tip is intended for use in materials and structures test programs and hypersonic flow studies.

In order to protect the aircraft structure from the high temperatures expected above Mach 6, an ablative material will cover the aircraft. The thickness of the material will vary for the various locations on the aircraft, and the total amount of material is expected to weigh less than 400 pounds.

DEVELOPMENT EXPERIENCES AND OPERATIONAL CONSIDERATIONS

Effects of Temperature

Most of the problems encountered in the structure of the X-15-2 have been precipitated by the modifications that were made to achieve a Mach 8 capability. These problems are either related to the external tanks directly or to aerodynamic heating. Even on the unmodified X-15 airplanes, aerodynamic heating was a principal source of structural problems. At higher speeds, with the resulting higher temperatures, additional and continuing problems are expected.

Some of the temperatures that could occur on an unprotected X-15 flying within the permissible Mach 8 envelope are shown in figure 3. The maximum temperature at the wing leading edge is 2400° F, twice the acceptable temperature for the basic structure. In almost all locations, the expected temperatures would exceed or very closely approach this acceptable temperature limit.

It is believed that the ability of the ablative material to protect the airplane structure may well be one of the governing factors during the envelope expansion to maximum velocity. To provide an engineering tool to evaluate this problem during the planning of these flights, a real time analog temperature simulation was developed. This simulation, in conjunction with a complete six-degree-of-freedom simulation of the X-15-2, has the capability of predicting the temperature at selected points for both protected and unprotected surfaces. A temperature time history obtained from this simulation is shown in figure 4 for a point aft of the nose gear door for a flight to Mach 7.6 at 100 000 feet. For comparison, a time history of the temperature at the same location for a recently flown speed profile is shown. Both the effective heating rate (as evidenced by the change in temperature) and the maximum temperature are significantly more severe for the higher speed. When an ablative coating is used, a completely acceptable temperature history will exist, as indicated by the lower curve.

Even though the airplane has not reached speeds above Mach 5.7 since it returned to flight status, aerodynamic heating has already been a problem in the modified structure.

On each of the first five flights a different type of abnormality occurred with the landing gear. The most serious of these are indicated in figure 5. In these three flights individual components of the landing-gear system extended prematurely in flight.

On the second flight the nose gear extended in flight at a Mach number of about 4.4 and resulted in severe heat damage to the nose-gear structure as well as to the tires. Both tires blew out during the landing. The cause of this unpleasant occurrence was the thermally induced structural stresses and strain in the forward fuselage and the gear uplock mechanism. The failure was duplicated during ground tests in the Flight Research Center radiant heat facility in which the airplane was heated and loaded in a manner similar to that which occurred in flight. Following these tests, the door and the gear uplock mechanism were modified.

On the third flight the small nose-gear scoop door opened in flight at high speed. Additional modifications were made to the door uplock mechanism to further relieve the thermal stresses.

On the fifth flight the right-hand main gear extended in flight because of thermally induced loads on the uplock mechanism. This failure was also duplicated during ground heating tests in the Flight Research Center radiant heat facility. As a consequence, the main gear and uplock mechanism were modified. Subsequent testing in the heat facility showed the modifications to be

satisfactory for flights to at least Mach 5. Thermal protection will presumably alleviate problems at higher Mach numbers.

Each of the malfunctions just discussed occurred at approximately the same time during the flight on similar flight profiles--at the time of maximum temperature for these locations. An appreciation of how a relatively minor design change can result in a major change in system characteristics can be gained by reviewing the main landing-gear extension problem. The main gear used in these tests was not the so-called long gear to be used when the ramjet is installed; it is an interim gear, which is longer, however, than the standard X-15 main gear. Figure 6 shows that the principal difference between the two gears is an increase in strut length of 6.75 inches. The strut pivot point and the location of the uplock hook are common to both gears. In flight, the main load on this uplock hook is that caused by the tendency of the system to bow as a temperature differential is experienced between the outside and inside of the gear. The magnitude of this load can be seen in the plot of uplock hook load as a function of temperature gradient shown in figure 7. For the higher temperature gradients, the hook load for the interim gear is nearly double that of the standard X-15 gear. During flight the critical temperature gradient was reached and the load on the uplock hook became sufficiently large to cause the hook to deform and the gear to extend.

Operational Considerations With External Tanks

Aerodynamic heating will not be the only potential problem in obtaining the maximum velocity of the X-15-2 airplane. Operating the airplane with external tanks may also present some interesting facets. The external tanks (shown in fig. 8) are approximately $23\frac{1}{2}$ feet long and $37\frac{3}{4}$ inches in diameter. The tanks are attached to the airplane structure within the side fairing at the 200-inch and 411-inch fuselage stations and have propellant and gas interconnects through a tank pylon located between the 317-inch and 397-inch fuselage stations. The right-hand tank contains about 1080 gallons of anhydrous ammonia in one compartment. The left-hand tank contains about 793 gallons of liquid oxygen in one compartment and three helium bottles which have a total capacity of 8.4 cubic feet. The empty left-hand tank weighs 1150 pounds and the empty right-hand tank weighs only 648 pounds. Note that the left-hand tank will be over 2000 pounds heavier than the right-hand tank when the tanks are full.

Each tank can be forcibly ejected from the airplane during flight through the use of fore and aft gas-cartridge ejectors and a forward solid-propellant sustainer rocket, which imparts pitching and rolling moments to the empty tank after it has been ejected. Because there is a sizable investment in each of these tanks, it is imperative that every effort be made to recover the tanks, undamaged if possible, once they have been successfully ejected from the airplane. For this purpose, each tank has a self-contained recovery system which includes a drogue and a recovery parachute. Although some impact damage will result with use of this system, it is expected that tank refurbishment can normally be effected for reasonable cost.

The allowable envelope for empty-tank ejection is shown in figure 9. Satisfactory separation characteristics are indicated from wind-tunnel tests for the area where dynamic pressure is nominally less than 400 pounds per square foot and angle of attack less than 10°. Acceptable separation will probably exist for dynamic pressures less than 600 pounds per square foot. At higher angles of attack and dynamic pressures, the tanks are expected to roll excessively and to pitch up within close proximity of the aircraft. The dashed line shows the location of the nominal flight profile relative to the allowable tank ejection envelopes. The larger envelope represents the range of flight conditions that may exist during operation with the tanks on. When the airplane is flying within this envelope, the tanks will generally be partly filled. Tank-separation characteristics with partly expended propellants are unknown and could be a problem in that there are no slosh baffles or compartments for center-of-gravity control. This problem is currently being studied. Full-tank ejection characteristics are expected to be satisfactory for any reasonable flight conditions which might occur within 15 seconds of launch where full-tank jettison would be required.

Stability and Control Considerations

Even though there are physical differences between the basic X-15 airplane and the X-15-2 airplane without external tanks, the aerodynamic differences, in the form of stability and control characteristics and handling qualities, are not very significant. With external tanks on the airplane, however, some rather dramatic differences exist. The general trend tends toward unfavorable characteristics.

Consider the center-of-gravity travel as propellants are consumed, from launch until external-tank drop, as shown in figure 10. The tanks being below the fuselage reference line causes the vertical center of gravity to be displaced at launch about 9 inches. The lateral center of gravity is offset 1.5 inches at launch. The center of gravity, of course, moves toward the airplane center line as external-tank propellants are consumed. An appreciation of the effects of this center-of-gravity offset and some of the important stability characteristics of the X-15-2 with external tanks can be obtained from inspection of a time history of a simulator flight, shown in figure 11. The piloting task illustrated is to maintain the airplane at an angle of attack of 12° after launch until a pitch attitude of 34° is attained. This climb attitude will be held until external-tank fuel depletion and tank ejection occur at approximately Mach 2.1 at 67 000 feet. After tank ejection, an angle of attack of 2° will be maintained until the airplane reaches 100 000 feet. The airplane will then accelerate to maximum velocity at this altitude.

The moment caused by the vertical displacement of the center of gravity 9 inches below the thrust vector (refer to fig. 10) results in a nose-down pitch transient at engine light as shown in figure 11. The pitch-control task is further complicated by a lower level of longitudinal static stability that exists with external tanks installed. This condition is indicated by the relatively small amount of stabilizer deflection required for the change in angle of attack at 45 seconds. The stabilizer deflection required without external tanks is about 3 times greater than with tanks.

The additional increment of nose-up stabilizer deflection used to counteract the nose-down moment caused by the thrust vector (diagramed in fig. 10) can result in a sudden pitch-up if an unexpected loss of thrust is experienced. This pitch-up from the nominal 12° angle of attack can easily be controlled with the dampers engaged. However, this occurrence without dampers could, in some instances, pitch the aircraft to excessively high angles of attack where control will be marginal.

Because of the difference in longitudinal trim required with and without tanks, a nose-down trim change of 5° in angle of attack will occur when the external tanks are released as shown in figure 11 at 65 seconds.

The results of the lateral center-of-gravity offset can be seen by the amount of aileron required to hold wings level, initially about 5°. At higher angles of attack, the aileron required approaches the maximum available, 15°. This lateral-control limit plus a deterioration in lateral-directional stability will limit the usable angle of attack in this flight regime to 15°.

The importance of stability augmentation on the X-15-2 will be evident by comparing the dampers-off simulator time history with the dampers-on time history of the same flight profile (fig. 11). Larger excursions are noted, particularly the initial nose-down pitch at engine light and at tank jettison. Because of the increased pitch-control task, larger deviations in roll angle can also be expected. However, it must be kept in mind that flight without dampers represents a double failure, in that the aircraft is equipped with a backup damper system that automatically engages to provide pitch and roll damping if the primary damper fails.

The expected handling qualities of the X-15-2 with external tanks are summarized by pilot ratings of simulator flights, shown in table I.

TABLE I.- HANDLING-QUALITY RATINGS OF THE X-15-2 WITH EXTERNAL TANKS

[Fixed-Base Simulator; Rating Sequence, Pitch-Roll-Yaw]

Ratings

1, 2, 3: Satisfactory
4, 5, 6: Acceptable
7, 8, 9: Unacceptable
10: Uncontrollable

Dampers	Acquiring angle of attack	Maintaining angle of attack	Acquiring and maintaining pitch attitude	Tank ejection
Primary	3-4-3	2-4-3	2-4-3	3-4-3
Off	$5\frac{1}{2}$-$5\frac{1}{2}$-4	4-4-4	5-5-4	6-6-6

Ratings in first, second, and third positions refer to pitch, roll, and yaw, respectively. The numerical ratings are based on a scale of 1 to 10 with the higher numbers representing the least satisfactory handling qualities. The pilot's concern with the lateral control is indicated by the higher ratings in the roll axis. Identical ratings with either the primary or backup dampers were obtained and are significant in that no yaw damping is available with the backup system engaged. This indicates that an adequate basic directional stability exists within the usable angle-of-attack region. The transient conditions of initially acquiring the angle of attack and the condition at tank ejection were considered the least acceptable.

After the tanks are ejected, the handling qualities of the X-15-2 are expected to be similar to those already experienced by the X-15. Some degradation is expected, although still acceptable, as the maximum velocity is approached.

Performance Considerations

As mentioned earlier, the primary research program for the modified X-15-2 is the ramjet engine development and evaluation. To evaluate the ramjet requires that velocities approaching Mach 8 be attained. Since the first flight of the modified X-15-2, the flight envelope has been expanded in a step-wise fashion toward that goal. Because of its increased basic (clean) weight, the X-15-2 will have flight speeds 200 to 300 feet per second less than the other airplanes, as indicated in figure 12.

When the external tanks are added to the present (ventral on) airplane, the estimated velocity capability will be between 7600 and 7700 feet per second at an altitude of 120 000 feet. Replacing the ventral with an assumed ramjet configuration will decrease that capability to about 7200 feet per second at an altitude of 118 000 feet. The decrease in performance is the result of increased weight and drag for the ramjet configuration. This performance is appreciably less than the design goal of 8000 feet per second at an altitude of 100 000 feet. Planned modifications to the engine in the form of an improved propellant injector and a radiation-cooled nozzle extension, giving an area ratio of 33, are expected to bring the performance nearly to the design goal.

The length of time the airplane can remain at high velocity and dynamic pressure will determine the amount of useful data that can be obtained on the ramjet. Also shown in figure 12 is the amount of test time expected for the ramjet configuration with the uprated engine during a deceleration from maximum velocity at a dynamic pressure of 1000 pounds per square foot. Time at velocities above 7000 feet per second would be 50 seconds and above 6000 feet per second, 110 seconds. For ramjet testing requiring steady conditions, that is, at relatively constant velocity and dynamic pressure, the rocket engine thrust can be reduced to minimum and the speed brakes extended so that low acceleration exists. The expected stabilized test time for this configuration is approximately 14 seconds at 7000 feet per second and 40 seconds at 6000 feet per second.

CURRENT RESEARCH PROGRAM

The ramjet modification for the X-15-2 is not expected to be made for nearly two years. In the meantime, plans have been made for a number of experiments which quite adequately fill the gap. At the present time, the airplane is gathering basic stability and control data to verify wind-tunnel and theoretical predictions of aerodynamic characteristics and handling qualities. At the same time, an ultraviolet stellar photography experiment is being conducted at high altitudes. These two investigations will continue well into 1966.

The airplane with the external propellant tanks has not yet been flown, but the first flight, with empty tanks, is imminent and may (depending upon results) be followed by several similar flights before the end of this year. Data will be obtained on handling qualities, tank separation, and tank recovery without the complication of operating with a modified propellant system and without large center-of-gravity shifts. The maximum velocity required for this flight is only 2400 feet per second, that is, just past the tank jettison Mach number of 2.1. Therefore, the airplane will be launched in the general area of Edwards Air Force Base with the external tanks being recovered in one of the local bombing ranges. These flights will provide the information needed to proceed with safety and confidence toward the Mach 8 goal with a minimum risk.

As indicated earlier, the airplane will eventually be almost completely coated with an ablative material. This coating will be a "first" for use on an operating aircraft and a certain amount of preliminary work is necessary to assure that the ablative material will and can do the job when needed. Some ablative flight tests have already been made and more are being planned. It is expected that these tests will flight-qualify an ablative material, will define application and refurbishment techniques, and finally will prove the operational compatibility of ablative heat protection in a Mach 6 to 8 environment.

Operation with full external tanks is expected to begin by midyear of 1966. A program of envelope expansion to approximately Mach 8 will then proceed in orderly, cautious steps. Naturally, stability and control and ablative tests will continue during these flights.

Late in 1967, the airplane will be removed from flight-ready status for the modifications which include the ramjet installation. The flight program, with the ramjet configuration, is expected to begin early in 1968.

CONCLUDING REMARKS

The more interesting aspects of the program plans for the X-15-2 airplane have been reviewed. Knowledge gained from these aspects of the program has led to a high level of confidence that the mission objectives will be accomplished. It is believed that the X-15-2 flight program will unravel some of the problems associated with hypersonic flight, for example, the nature of

hypersonic flow fields, material behavior and structural efficiency at high temperatures, and human capabilities at very high speeds. Certainly, great steps will be taken in the advancement of air-breathing propulsion and ablative technology. The X-15-2 airplane has already provided a few surprises and a number of challenging engineering problems. The future promises continuing challenges and rewarding successes in aeronautical research.

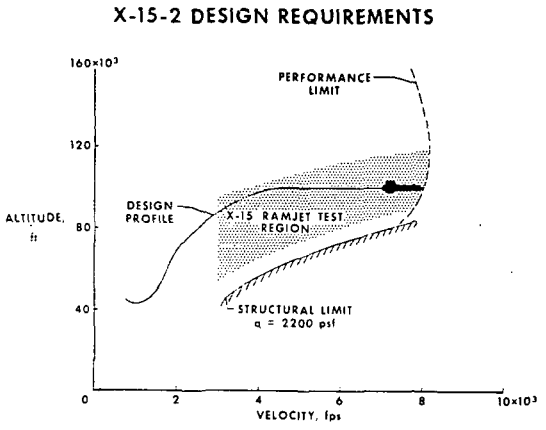

Figure 1

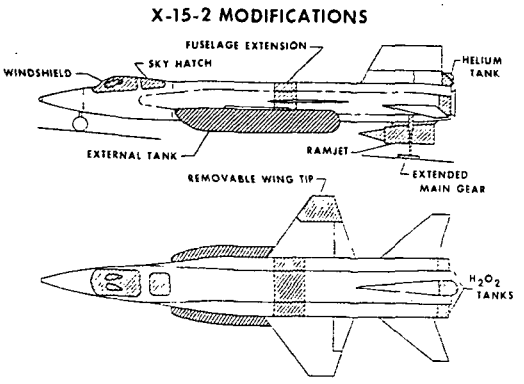

Figure 2

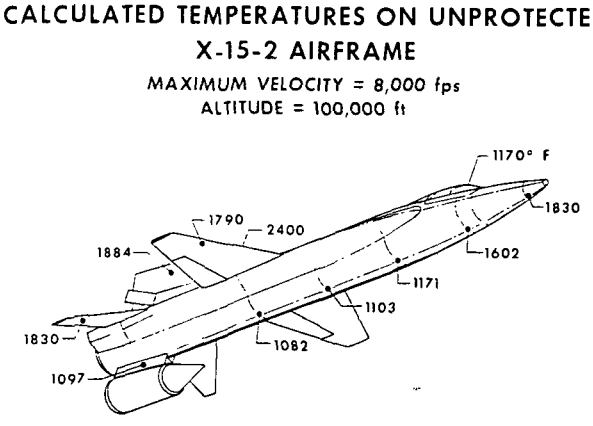

Figure 3

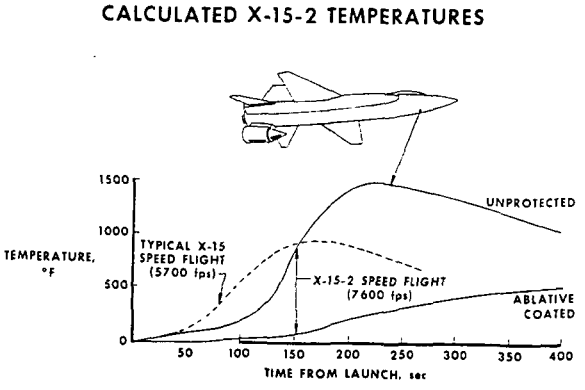

Figure 4

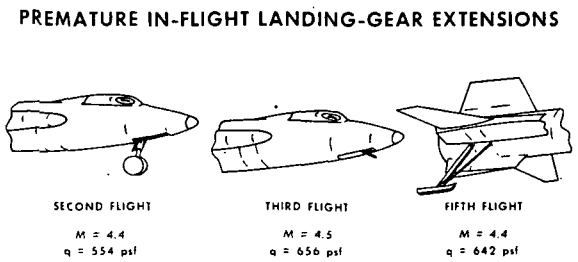

Figure 5

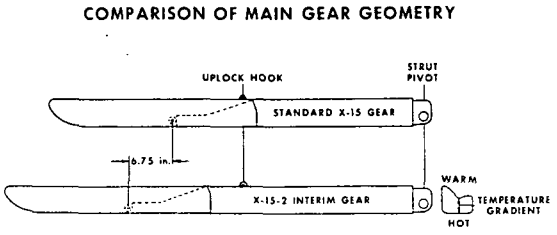

Figure 6

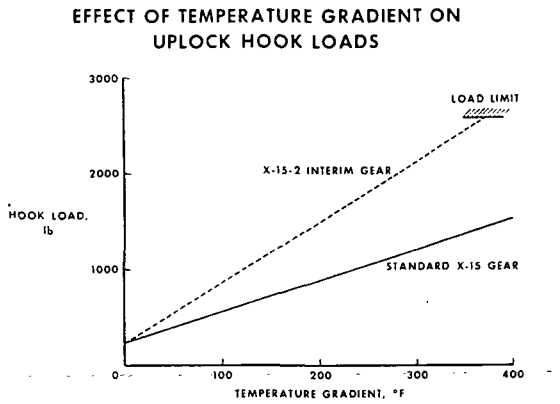

Figure 7

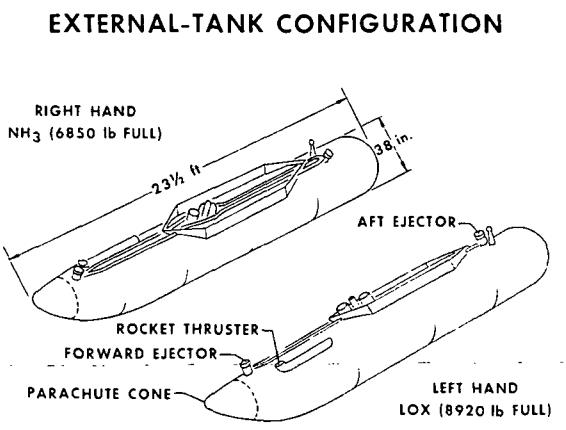

Figure 8

X-15-2 EXTERNAL-TANK-EJECTION ENVELOPE

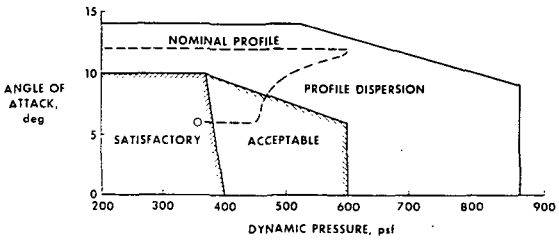

Figure 9

X-15 CENTER-OF-GRAVITY VARIATION WITH EXTERNAL TANKS

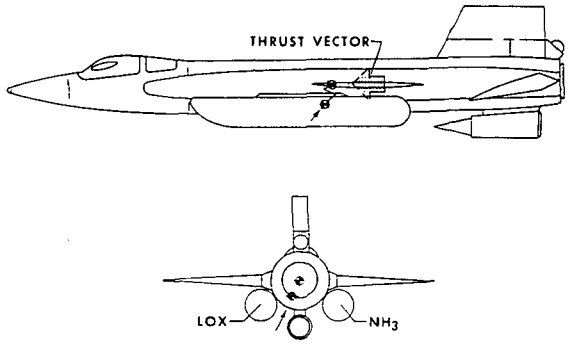

Figure 10

SIMULATOR TIME HISTORY OF X-15-2 FLIGHT WITH EXTERNAL TANKS

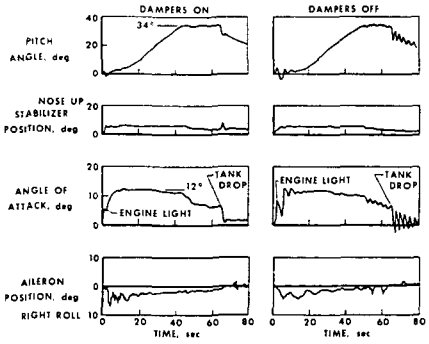

Figure 11

X-15-2 PERFORMANCE SUMMARY

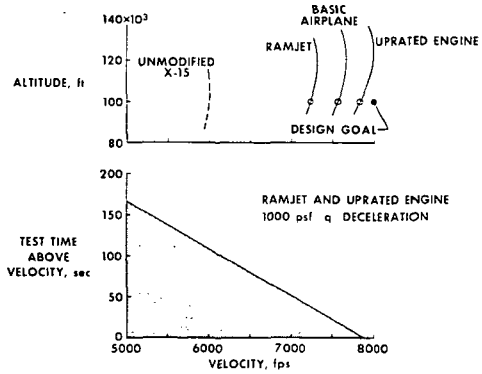

Figure 12

11. ADVANCED X-15-2 THERMAL-PROTECTION SYSTEM

By

Joe D. Watts and John P. Cary
NASA Flight Research Center

and

Marvin B. Dow
NASA Langley Research Center

SUMMARY

The use of silicone-based elastomeric ablative material for the advanced X-15-2 thermal-protection system is discussed and results of candidate ablator evaluation tests in arc facilities and on X-15 flights at Mach 5 are presented.

INTRODUCTION

An increasing interest among heat-shield designers in silicone-based elastomeric ablatives has been evident in recent months. Several advantages in this type of ablator are offered: ease of application to complex shapes, flexibility over a wide range of temperature, potential for refurbishment with spray, bonded sheets, or prefabricated panels, and superior shielding effectiveness at low to moderate heating rates. Possibly the first opportunity for a practical application of one of the silicone-based materials with refurbishment capability is the thermal-protection system for the advanced X-15-2 airplane.

BACKGROUND

With the estimated performance of the advanced X-15-2, it was obvious that the Mach 6 structural design was not adequate to handle the aerodynamic heating loads expected at Mach 8. Figure 1 shows a comparison of the heating conditions which have been experienced on the airplane at a Mach number M of 6 and those which are expected on the new configuration at M = 8. The comparison is made on the basis of total heat load for several representative locations on the airplane surface. Most areas of the surface are expected to experience a heating environment considerably more severe than was ever encountered with the basic X-15 airplane. Since the heat-sink capacity of the structure is essentially used up with the Mach 6 heat loads, some method of protecting the structure from the high Mach 8 heat loads must be provided.

In late 1963 a joint NASA-USAF committee was formed to study the problem of providing the X-15-2 airplane with a thermal-protection system. A coating of ablative material for the entire airplane surface appeared to be the only feasible approach.

Figure 2 shows shielding effectiveness of a typical silicone-based ablator as a function of total enthalpy (ref. 1). The two curves represent cold-wall heat-flux levels of 50 and 100 Btu/ft^2-sec. The available materials were developed for lifting entry applications with enthalpy levels of over 12 000 Btu/lb. The X-15-2 system, in order to utilize a ready-developed material at very low enthalpy levels, must accept a lower effectiveness that results in a weight penalty. Even though the heating conditions for the X-15-2 are not expected to be as severe as those of a reentry vehicle, the safety of the X-15-2 and the pilot is just as dependent upon the thermal-protection system as the safety of an astronaut is upon his vehicle heat-shield system.

To determine which ablative materials were qualified as candidates for use on the X-15-2, the joint committee set up an evaluation program. All major manufacturers of ablatives were requested to provide test samples for evaluation. The primary factors used in evaluating candidate materials are: shielding effectiveness, room-temperature cure cycle, bond integrity, operational compatibility with the X-15, and refurbishment. The following facilities were utilized in the evaluation program:

Screening tests: University of Dayton Research Institute, 2-inch arc jet

Flight tests: NASA Flight Research Center, three X-15 airplanes

Thermal-performance tests: NASA Langley Research Center, 2500-kilowatt arc tunnel

MATERIALS EVALUATION PROGRAM

Initially, a large number of materials were screened under an Air Force contract in the arc-jet facilities of the University of Dayton Research Institute (ref. 2). The screening tests were measurements of relative shielding effectiveness made on all materials that appeared to meet the basic criteria set up by the joint committee. The materials tested were ranked in the order of their shielding effectiveness, measured under a low heat-flux environment, and the most promising materials were recommended by the U.S. Air Force Materials Laboratory, Wright-Patterson Air Force Base.

Flight testing of the candidate ablative materials on the X-15 airplane under Mach 5 heating conditions proved to be an extremely valuable part of the overall evaluation. Many deficiencies in materials, bond systems, and spray techniques which were discovered in flight tests probably would not have been brought to light in any other way. The heating conditions experienced in Mach 5 flight tests brought out material problems which had never previously

appeared in ground-facility tests. A total of fifteen different material formulations were flight tested on X-15 airplanes.

Figure 3 shows the surfaces of the airplane on which test applications of materials were made. The ventral fin and speed brakes provided moderate heating rates in an easily accessible area where material failures could be tolerated. The LOX tank provided a test area for checking bond integrity at temperatures approaching -300° F as well as performance in flight. The removable nose panels provided measured back-surface temperatures and capability of direct comparison of two materials under the same heating conditions. The canopy application was intended to show whether or not a windshield-contamination problem existed as a result of reattachment of ablation products. No conclusive results were gained from the canopy tests, however, and arc-tunnel tests are being made to define the problem. Steps will be taken to eliminate the problem if necessary.

Some of the various problems encountered in flight tests which caused the elimination of many materials were as follows:

(1) Poor bond integrity of sheet-form materials

(2) Delamination of sprayed materials

(3) Excessive erosion of leading-edge test specimens

(4) Blistering

(5) Difficulty in removal of remaining material after flight

Most of these problems, if they occurred on a Mach 8 mission, could have serious consequences for the airplane structure. One of the most serious problems experienced in flight tests was failure of the bond of sheet materials. Stiffness of many of the sheet materials was too great for proper conformity to airplane skin irregularities, and voids in the bond resulted. Some of the spray materials had a tendency to delaminate in flight, as shown in figure 4. This type of failure was due to improper application procedures and was not a material fault. A few materials eroded very badly on the ventral-fin leading edge during Mach 5 flight tests. Figure 5 shows an example of a badly eroded test application. Erosion was a definite sign of inadequate thermal performance, since the Mach 5 heating conditions are very low compared with the Mach 8 design requirements. Blistering of some of the silicone elastomers was experienced on surface tests. Most blistering was superficial and had no effect on thermal performance, but such blistering could lead to local hot spots on a Mach 8 mission. Most of the materials were difficult to remove after flight. Char and remaining virgin material require soaking with solvent and scraping. A technique for speeding up removal is currently being investigated. A pressure sensitive tape applied under the ablator and primer has been flight tested successfully. The tape is simply stripped off after flight and all residual material comes off with it, leaving a clean surface. The removal operation of a tape application of a silicone-based material is shown in figure 6.

When the flight testing of materials was nearing completion, thermal-performance tests were planned for all materials which still remained in competition. These tests were performed in the NASA Langley 2500-kilowatt arc tunnel under heating conditions which closely simulated the peak heating rates and enthalpy levels expected on the design Mach 8 mission. The purpose of the Langley tests was to determine the relative shielding effectiveness of the candidate materials under near-design-maximum conditions. The material manufacturers provided test samples of their materials installed on identical models with the same weight per unit area for all materials. Both leading-edge and afterbody test models were provided.

Figure 7 shows the test stream conditions and model configurations for both the leading-edge tests and afterbody tests. The Mach 8 design flight maximum conditions are shown for comparison. Although the test Mach number was considerably lower than the flight Mach number, the heat flux and enthalpy levels very closely simulated the maximum conditions in the flight.

The leading-edge tests indicated that most of the silicone-based ablators were unable to withstand the severe heating conditions. Results are shown in the following table:

LEADING-EDGE TEST RESULTS FROM NASA LANGLEY 2500-KILOWATT ARC TUNNEL

Material	Density, lb/ft^3	Stagnation-line thickness*, in.	Time to 500° F, sec	Comments
Silicone based				
I	32	0.545	89	End erosion
II	39	.462	92	Good shape retention, blisters
III	60	.294	98	Crack
Phenolic silica				
IV	110	.165	25	Good shape retention

*Equal weight per unit area at stagnation line of all models.

Materials I, II, and III were silicone-based materials with densities ranging from 32 to 60 lb/ft^3. Since all materials had an equal weight per unit area of 1.5 lb/ft^2, the stagnation-line thicknesses varied from 0.545 inch down to 0.294 inch. The back-surface temperature response of the three silicone-based materials was very close. Material I experienced erosion of the ends of the model because of insufficient fiber reinforcement. Material II held its shape fairly well but suffered from blistering. Material III experienced a crack at the stagnation line, apparently due to a stress problem. Material IV was a high-density phenolic silica. Because of the density, the thickness was only 0.165 inch. The shape retention of this material was excellent but

its shielding effectiveness is low and a relatively thick leading edge would be required to keep back-surface temperatures below the limits.

It appears that unless the silicone-based elastomers can be modified for better shape stability, a high-density material of some other kind may have to be used on leading edges of the airplane. Since the leading-edge surfaces contribute a very small percentage of the total weight, a high-density material could be used, if necessary. Inasmuch as none of the materials in the leading-edge tests were actually qualified, the material to be used for leading edges probably will not be determined until the design phase of the program.

Figure 8 shows the results of the afterbody tests. Back-surface temperature time histories up to the limit of 500° F are shown on the left and the resulting shielding effectiveness of each material is tabulated on the right. It appears that the effectiveness of the materials is largely a function of the material density. All four materials tested in the afterbody tests are considered qualified for application on the X-15-2.

For an indication of what the shielding effectiveness of the materials means in terms of the total system weight, a calculation was made to determine an approximate weight. A typical silicone elastomer was used for the calculation and the average weight per unit area, excluding leading edges, was approximately 0.30 lb/ft^2 for the average total heat load of 1500 Btu/ft^2. This calculation results in an estimated total surface ablator weight of 360 pounds.

Because so many unknowns exist with regard to the local heating rates and aerodynamic shear forces in many areas of the X-15 surfaces, a gradual and closely observed buildup of Mach number from 6 to 8 will be required. Such factors as the effects of interference, shock impingement, and boundary-layer separation and reattachment will undoubtedly lead to modifications of the heat shield in affected areas. Such changes as thickness increases, material changes, and even structural modifications may be required if flight results show the need. Close postflight inspection of the entire airplane surface will be made, and the ablator char depth and back-surface temperatures will be constantly monitored throughout the performance buildup.

With the use of a charring ablator computer program (ref. 3), NASA Flight Research Center will make predictions of char depth and back-surface temperatures and match results to flight measurements.

Temperatures computed for an application of a typical silicone-based ablator on a Mach 5 test flight and on the Mach 8 design mission are presented in figure 9. Ablator surface and back-surface temperatures are shown for both, and measured back-surface temperatures are added for comparison on the Mach 5 flight. The weight applied for the Mach 5 test was arbitrary but the weight on the Mach 8 flight was optimized for the 500° F back-surface temperature limit.

CONCLUDING REMARKS

The X-15-2 thermal-protection system will be an integral part of the airplane. Its reliability will have to be at least equal to that of any other system. Because the performance of the system cannot be fully determined until it is flight tested under the design conditions, a step-by-step performance envelope expansion from Mach 6 to Mach 8 will be necessary. The system must be proved, without unnecessary risk to the pilot and the airplane, in much the same way that the Mach 6 airplane was proved before reaching its design condition. There is now sufficient confidence in the four candidate ablative materials that a contract can be let and the design of the system can proceed. The design of the thermal-protection system is expected to be completed by midyear of 1966.

REFERENCES

1. Swann, Robert T.; Dow, Marvin B.; and Tompkins, Stephen S.: Analysis of the Effects of Environmental Conditions on the Performance of Charring Ablators. NASA paper presented at AIAA Entry Technology Conference, Williamsburg/Hampton, Va., October 12-14, 1964.

2. Gerdeman, Dennis; and Jolly, Michael: Preliminary Evaluation of Ablative Coatings for X-15 Application. U. D. Mem. No. UDRI-TM-64-108 (Contract AF33(615)-1312), Univ. of Dayton Res. Inst., June 15, 1964.

3. Swann, Robert T.; and Pittman, Claud M.: Numerical Analysis of the Transient Response of Advanced Thermal Protection Systems for Atmospheric Entry. NASA TN D-1370, 1962.

TOTAL-HEAT-LOAD COMPARISON

MACH 6 AND MACH 8 MISSIONS

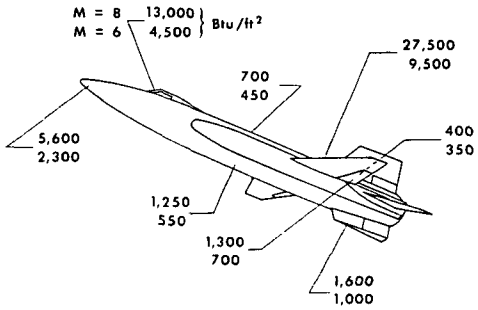

Figure 1

COMPARISON OF CHARRING ABLATOR APPLICATIONS

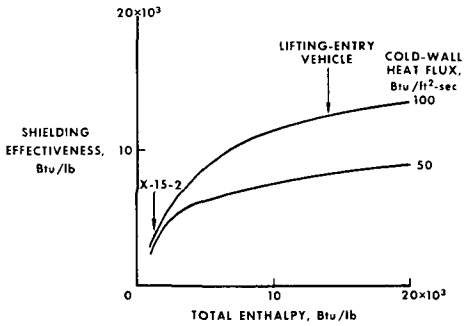

Figure 2

ABLATIVE-MATERIAL-EVALUATION TEST AREAS

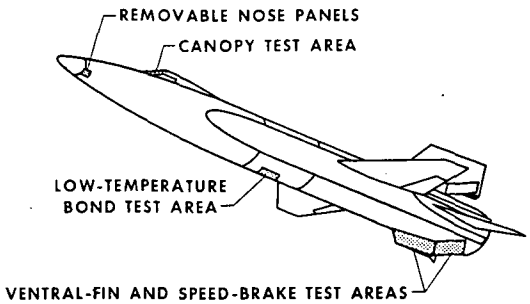

Figure 3

DELAMINATION

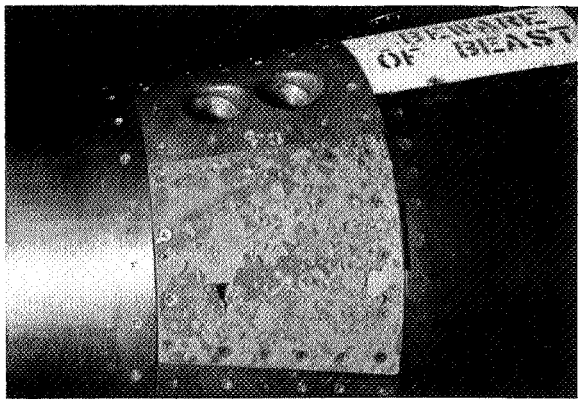

Figure 4

EROSION

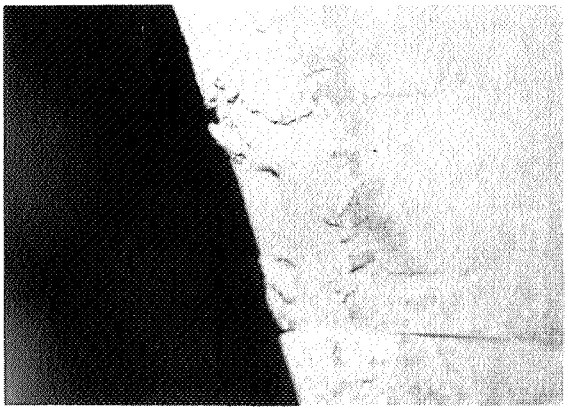

Figure 5

REMOVAL OF TAPE APPLICATION

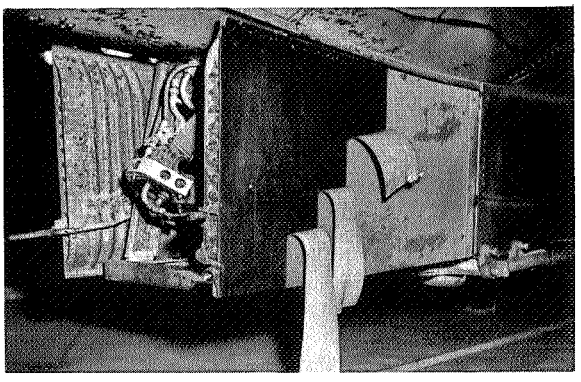

Figure 6

THERMAL-PERFORMANCE TESTS
LANGLEY 2500-KILOWATT ARC TUNNEL

TEST CONDITIONS

TEST PARAMETERS	ARC TUNNEL (CONSTANT)	DESIGN FLIGHT (MAXIMUM)
VELOCITY, FT/SEC	6700	8000
STAGNATION ENTHALPY, BTU/LB	1430	1300
MACH NUMBER	3.2	8.0
LEADING-EDGE HEAT FLUX, BTU/FT²-SEC	125	150
AFTERBODY HEAT FLUX, BTU/FT²-SEC	12	10

MODEL CONFIGURATIONS

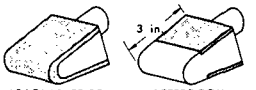

Figure 7

AFTERBODY TEST RESULTS
NASA LANGLEY ARC TUNNEL

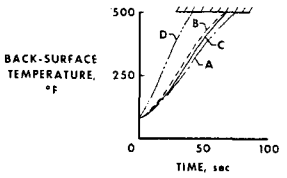

MATERIAL	DENSITY,* lb/ft³	E_{500},** Btu/lb
A	27	4800
B	31	4250
C	33	4150
D	48	2600

*EQUAL WEIGHT PER UNIT AREA ON ALL MODELS

$$**E_{500} = \frac{\text{(HEAT FLUX)(TIME TO 500° F)}}{\text{(WEIGHT PER UNIT AREA)}}$$

Figure 8

COMPUTED TEMPERATURES

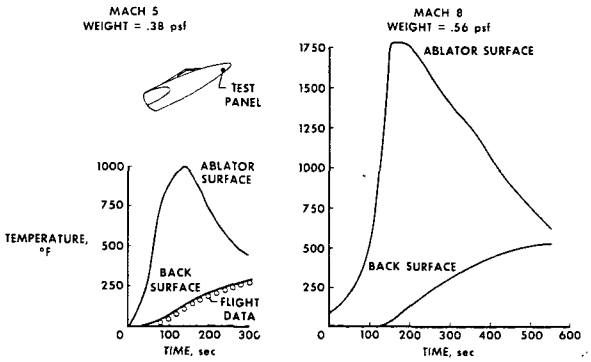

Figure 9

12. HYPERSONIC AIR-BREATHING PROPULSION-SYSTEM TESTING ON THE X-15

By Kennedy F. Rubert
NASA Langley Research Center

12

SUMMARY

In 1964, studies of the feasibility of using the X-15 airplane in the range from Mach 4 to Mach 8 as a test bed for air-breathing engines resulted in the initiation of the Hypersonic Ramjet Experiment Project. This project is divided into three phases - Project Definition, Research-Engine Development and Ground Experiments, and Flight Research. In this paper, the project objectives, research-engine requirements, and technological problems being encountered in the first phase of the project are briefly discussed.

INTRODUCTION

Powered lifting vehicles for atmospheric flight at hypersonic speeds have, over the past decade, attracted a great deal of interest. Such vehicles have been studied for application to a variety of cruise-type and boost-type missions, even to orbital speed. For all but the lowest hypersonic flight speed within the atmosphere, the ramjet is the only propulsion system capable of executing the truly difficult missions requiring great range or boost capability.

Although the ultimate development and application of ramjets to the propulsion of man-carrying vehicles in hypersonic atmospheric flight is still very much in the future, the National Aeronautics and Space Administration has been alert to the need for research and has been studying numerous research undertakings with a view to determining in what way it can make the most effective contribution. Among the approaches considered have been analyses in depth of various kinds, rocket-propelled hypersonic flight experiments with engine components, and flight experiments with the simplest possible complete engines, including use of the X-15 as a test bed for captive engines.

One by one these various approaches have been discarded, on account of either the excessive cost, the meager return in the way of significant results, or, most often, a combination of these two reasons. None exhibited in the desired degree the attribute most needed, that of bringing into focus the problems of the complete engine over a significant range of flight conditions. Finally, in 1964, NASA studies of the feasibility of using the X-15 airplane as a test bed for hypersonic air-breathing engines in flight from Mach 4 to Mach 8 resulted in the initiation of the Hypersonic Ramjet Experiment Project, which was designed to minimize the deficiencies which have been mentioned.

The objectives of the Hypersonic Ramjet Experiment Project are:

1. To provide a focal point for the application and integration of the results of the extensive basic and component research which has been done over the past several years

2. To provide factual data on complete-engine characteristics, in support of future decision making

3. To make a comprehensive determination of the major problems of the complete engine, of the sort not revealed by separate-component research, as a guide to the planning of future research

4. To validate existing methods and techniques for simulating, in ground-based facilities, flight conditions required for hypersonic air-breathing engine research

5. To establish future needs for facilities and techniques for experimental research and development of hypersonic air-breathing propulsion systems

PROJECT PLAN

In simplest terms, the Hypersonic Ramjet Experiment Project is an undertaking to design and develop a hypersonic ramjet research engine, to the largest scale compatible with a program of experiments in the best available ground-based facilities and with a subsequent program of flight research, in which the engine is to be airborne by the modified X-15-2 airplane.

The project has been organized into three phases. Phase I, called the project-definition phase, is somewhat more than the name implies. It involves not only a comprehensive and detailed study of the more promising concepts for a suitable research engine, but also the formulation of a preliminary design, an estimation of performance, and the planning, scheduling, and costing of Phase II. Three parallel 9-month contracts for this work have been awarded, one each to the Garrett Corp., to General Electric Co., and to The Marquardt Corp. The work is now just past midterm.

Contingent upon the creation in Phase I of a suitable and feasible research-engine conceptual and preliminary design, in Phase II this engine is to be developed, fabricated in hardware compatible with the airborne part of the program, and tested on the ground for performance and safety for flight use on the X-15 airplane.

In the third and final phase of the program two sets of flight experiments are to be made. The purpose of one set is to measure, for the broadest possible range of research results, the engine performance at conditions and in maneuvers not reproducible in existing ground-based facilities. The purpose of the other set is to match, in flight, key conditions simulated in the

ground-based experiments and thus make possible a direct comparison for checking the validity of the simulation techniques.

ENGINE SPECIFICATIONS

Compatibility with the X-15 and available ground facilities limits the size and weight of the research engine, which in flight will be carried under the afterbody of the airplane. Figure 1 shows a front elevation of the airplane, on which the single-hatched area is the cross section as limited by the airplane and on which the double-hatched circle, 2 feet in diameter, is the limitation imposed by currently available ground test facilities. Approximately 10 feet of length is available, from the aft end of the airplane forward. Exclusive of changes to the airplane, the overall weight of the research engine including instrumentation has been specified to be 800 pounds or less. Hydrogen is to be the fuel.

The envelope within which it will be possible to make flight experiments is shown in figure 2. The engine is required to operate over the range of speeds from Mach 3 to Mach 8, with an altitude range within the envelope of 15 000 feet (or preferably more) at any Mach number. The combustion mode may be either subsonic or supersonic to Mach 6, with the capability of special tests in the supersonic mode at Mach 5, for which special provision can be made if necessary. Above Mach 6 the supersonic combustion mode is specified.

The desired performance with respect to internal thrust coefficient is shown by the two curves plotted against flight Mach number in figure 3. Values below the lower curve are regarded as too low to be of interest. The upper curve approximates a locus of optimistic design-point performance. From Mach 4 to Mach 8, values which are as close as possible to the upper curve and not below the lower curve are sought. Stable operation, without specification of performance, is required from Mach 3 to Mach 4. Research capability from Mach 3 to Mach 4 is important to the transition from turbojets to ramjets, but too rigid specification of performance in this range could compromise the high-speed design. The same limits are imposed on the internal fuel specific impulse, illustrated in figure 4. Too low a value of thrust coefficient makes for an engine of excessive size, and too low a value of specific impulse means excessive fuel consumption; consequently, acceptable values of both parameters are required to specify a desirable propulsion system.

PROBLEMS IN TECHNOLOGY

A spike and cowling design of engine has been selected as the basis for the schematic diagram in figure 5 with respect to which a few of the more important technological problems will be discussed. In this engine the ingested air undergoes external compression, internal compression, fuel injection and mixing followed by combustion, and finally expansion in the exhaust nozzle. External compression avoids the problem of inlet starting, but causes spillage

for flight below the design speed, with resultant reduction in thrust. Fuel injection must be distributed so as to coordinate the combustion with the space provided. Narrow combustor passages favor short mixing distances but have a large wetted area that causes excessive friction and heat transfer. Combustor geometries favorable to Mach 4 requirements may not be advantageous for the supersonic combustion required at Mach 8. Excessive temperature in the combustor resulting in substantial dissociation of the reaction products can cause calamitous losses due to failure of the free radicals to recombine in the nozzle. A successful design requires an optimization of these many factors, arrived at as the result of detailed trade-off studies. When this optimization has been effected, it remains to design a structure which, to satisfy the compatibility requirements and performance specifications, must be regeneratively cooled internally, if possible without coolant requirements exceeding the available fuel consumption.

At this point in time it is too early to predict what may be the most desirable engine configuration or what will be the performance which may be anticipated. Among the three contractors many possible configurations are being subjected to trade-off appraisals. These studies reveal the problems which will demand the most attention. The more critical problem areas are discussed very briefly.

One of the most exacting problems is that of achieving, with a minimum of geometric variation, both the minimum acceptable thrust coefficient requirement at Mach 4 and the minimum acceptable specific impulse requirement at Mach 8, as the geometry favorable to the one is unfavorable to the other. This difficulty points up the importance of keeping a balance between thrust and fuel economy in arriving at a useful engine design.

Because unnecessary length carries a severe penalty in weight, friction, and cooling requirements, the length for achieving adequate mixing has been a critical item in developing the combustor configuration.

Difficulty has been experienced in reducing the hydrogen flow requirement for cooling purposes to equality with the hydrogen flow requirement for combustion. Estimating heat flux to requisite accuracy is another source of concern.

Although currently the weight estimates are not a source of alarm, the weights are running close to the 800-pound limit and do not provide a margin for the increases which always occur. Inasmuch as the structures under consideration are already highly refined, weight control is regarded as a definitely critical area.

Instrumentation constitutes an important problem area which must not be overlooked. The results of the contractor studies are encouraging, but the hostility of the environment, the basic difficulty of any measurement requiring flow mapping, the unacceptable interference of probes within the internal passages, and the overall space and weight limitations pose problems of unusual severity.

CONCLUDING REMARKS

This frank exposition of the areas of difficulty encountered in Phase I of the Hypersonic Ramjet Experiment Project should not be permitted to create an atmosphere of pessimism. In spite of the multiplicity and the difficulty of the problems, progress has been most gratifying. Several promising engine-design concepts have been formulated; analytical procedures and basic data needed for engineering these concepts have been either in hand, found, or generated, sufficient to make the studies realistic. NASA's requirements appear to be attainable in the light of investigations far more searching than have been brought to bear heretofore.

As of today, the present contractual effort is on schedule. The final reports of these contracts are to be proposals for performing Phase II. When the evaluation of these reports is completed, it will be possible to firm up a Phase II schedule which currently is directed toward initiation of unfired calibration experiments in flight early in 1968, to be followed by flight tests of the operating ramjet later in that year.

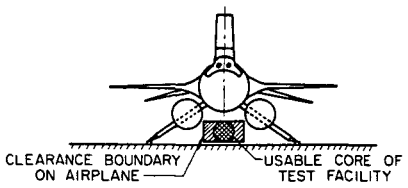

Figure 1

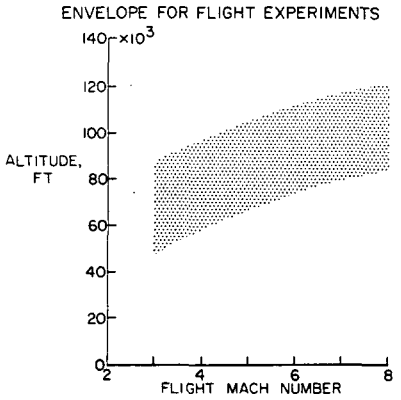

Figure 2

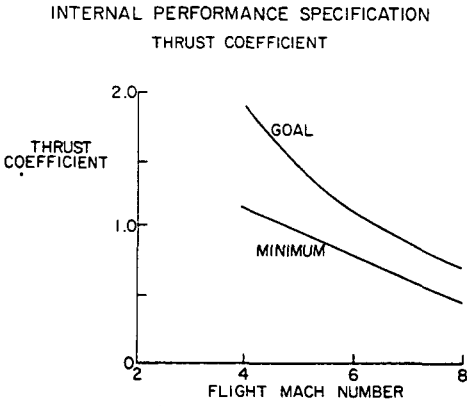

Figure 3

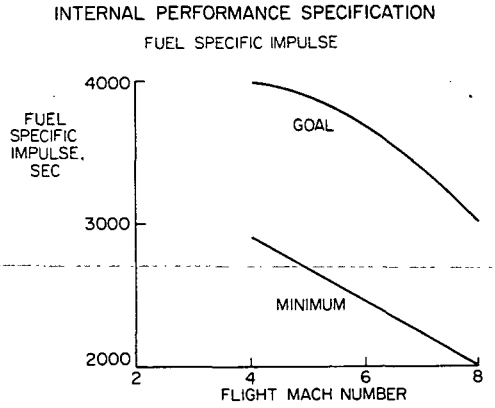

Figure 4

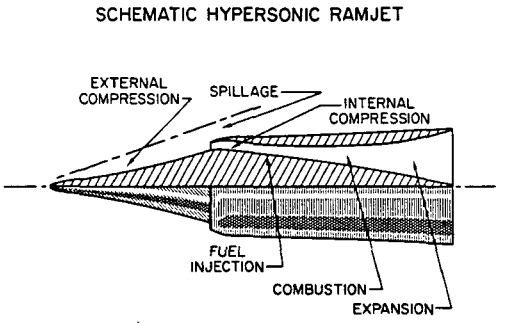

Figure 5

13. X-15 RESEARCH ACCOMPLISHMENTS AND FUTURE PLANS

By

Paul F. Bikle
NASA Flight Research Center

and

John S. McCollom
U.S. Air Force, Aeronautical Systems Division

13

SUMMARY

The accomplishments of the X-15 research airplane are reviewed with respect to progress in areas such as piloting techniques, bioastronautics, aerodynamic heating, vehicle aerodynamics, structural dynamics, advanced systems, test-bed experiments, and mission simulations. An indication of projected plans and proposed studies is also briefly covered.

INTRODUCTION

All studies that were originally conceived for the basic X-15 program have now been essentially completed. Moreover, a number of additional programs have evolved as the project progressed, and these investigations have been conducted or are in progress. The purpose of this paper is twofold: first to review the overall achievements of the X-15 project with proper emphasis on the highlights of the papers presented and, second, to indicate future X-15 plans, both the definitely planned and approved programs and several proposals that are not presently approved but are believed to offer the potential of an excellent return on investment.

MAJOR RESEARCH ACCOMPLISHMENTS

An idea concerning the major research accomplishments of the X-15 program is provided in the following list:

Piloting aspects

Bioastronautics

Fundamental aerodynamics

Vehicle aerodynamics

Structural heating and dynamics

Systems and operational experience

Test-bed experiments

Mission planning and simulation

Piloting Aspects

The area of piloting factors represents a significant aspect of the program. Prior to X-15 experience, there were predictions of how well the pilot might or might not do. Views expressed were either optimistic or skeptical. Solid experience instead of speculation now serves as a basis for a range of hypersonic aircraft applications. Specifically, the pilot has been able consistently to make spot landings for a low L/D glider under quasi-operational conditions. The pilot has had the ability to make successful reentries from extreme altitudes using several types of control systems under aerodynamic and acceleration conditions more stringent than those expected in most orbital and suborbital reentries. Because maneuverability requirements are much less for the X-15 than for fighter-type vehicles, satisfactory handling qualities are generally obtainable with less control power and at lower damping levels than are required in fighter airplanes.

Bioastronautics

The X-15 was the first research program in which the pilot's physiological behavior was monitored during flight. His physiological parameters during flight (heart rate, for example) were unpredictably high according to clinical standards; however, it was soon realized that norms for the research pilot under stress were significantly higher than had been expected. Postflight examination has revealed no harmful after effects to the X-15 pilots.

Fundamental Aerodynamics

Some of the most enlightening research of the X-15 program was performed in the area of aerodynamic heating and skin friction. Heat-transfer coefficients as much as 35 percent lower than those predicted by established theories have been consistently evident in flight results. From these results skin temperatures for any planned X-15 mission can be closely predicted. Skin-friction values are consistent with the aerodynamic-heating results in that they are also lower than might have been predicted.

Vehicle Aerodynamics

The X-15 configuration was originally derived solely from wind-tunnel studies of small-scale models. Scale effects on the overall aerodynamic characteristics were generally thought to be small; however, no prior data existed at that time to confirm this belief for Mach numbers greater than 2. The X-15 program has now generated extensive aerodynamic data for a wide range of full-scale flight conditions and has enabled detailed correlation to be made between

the basic stability, control, and performance parameters from flight tests and wind-tunnel and theoretical predictions.

Structural Heating and Dynamics

The thermal-structure problems were generally typified by local failures such as buckles, pulled fasteners, and cracks due to repeated thermal loads. All these problems were relieved early in the flight program by additional expansion joints, local fairings, and the like. It should be noted that, were it not for the cautious step-by-step expansion of the flight envelope, these minor problems may not have been detected in time to prevent major damage to the vehicle. In the area of structural dynamics, a much better appreciation of panel flutter and the mechanism of landing loads associated with skid landing systems was gained as a result of X-15 experience.

Systems and Operational Experience

Experience has been acquired with many advanced systems in the difficult environment of the X-15. This experience has provided an understanding of the factors that constitute adequate testing procedures and has shown the advantages of a step-by-step approach in the qualification of systems and airframe prior to use in a flight program. The favorable experience of the adaptive control system in the X-15 contributed to the selection of a somewhat similar adaptive system in the F-111.

Test-Bed Experiments

Because of the unique flight conditions available to the X-15, it is especially suited to obtaining information on auxiliary systems and experiments at hypersonic speed and/or at extreme altitude. This ability has appealed to many experimenters, particularly since they can recover the experiments for postflight inspection. Many such tests have been successfully completed or are in progress, and at this conference the results of two representative experiments have been described.

Mission Planning and Simulation

Expansion of the X-15 flight envelope beyond previous research-airplane performance prompted several rather sophisticated simulations for study of the piloting tasks and control requirements of the airplane, and for overall flight planning. The effectiveness of the simulations has been evaluated for all phases of the X-15 mission. However, the simulator is only as good as the information included, and in several cases serious consequences were luckily avoided in actual flight. A six-degree-of-freedom fixed-base simulation with complete cockpit controls and control-system hardware has been judged by the pilots to be generally satisfactory for pilot evaluation, familiarization, and practice for flights, even for the high-acceleration phases.

Some pride can be taken in the fact that the flight director, a key mission-planning engineer, and the manager of Project Mercury were all alumni of the X-15 program.

FUTURE PROGRAMS

The projected future plans for the X-15 program are indicated in figure 1. The discussion to follow is concerned with specific plans for each of the three X-15 airplanes.

X-15-1 Airplane

The X-15-1 airplane is committed to test-bed experiments, most of which require altitudes of from 150 000 to 250 000 feet. Comments are included in this section on the objectives of a few of the proposed experiments.

The MIT photographic horizon scanner developed by the Massachusetts Institute of Technology is now being tested, and the tests will continue well into 1967. The program is in support of an Apollo navigational and stabilization system to provide alinement of an inertial system for midcourse maneuvers, using determinable definitions of the earth's horizon contour. Data obtained at various times of the year should provide inputs to the Apollo program on seasonal, albedo, and day-to-day effects.

The PMR launch-monitor experiment involves the monitoring of missiles launched from the Pacific Missile Range. (Although the timing of the experiment appears to be critical, the flexibility of both programs, namely, the X-15 and the Missile launch, indicates a good chance of success.) A test program of about six X-15 flights to an altitude of 250 000 feet should begin near mid-1966. It is important to note the similarity of this experiment with the test observations of Cooper and Conrad in the recent Gemini-5 mission. Both tests are contributing to the determination of missile signatures.

Vapor-cycle cooling systems capable of sustained operation under weightlessness have been studied and are now ready to be fabricated and evaluated. For the system to be tested on the X-15, photographs will be made through windows in critical component parts, and system performance will be monitored during several flights at extended zero-gravity conditions.

X-15-2 Airplane

The X-15-2 is certainly the most heavily committed of the three airplanes (fig. 1). The vehicle has several test-bed experiments of which the stellar-photography program to obtain quantitative measurements of the ultraviolet properties of certain stellar atmospheres is actually under way and will continue into next year. Further, the photography program Mr. Groening discussed in paper 8 will be extended to the Mach 6 to Mach 8 range. A number of flights

will first be required to obtain experience with the recoverable tanks and then gradually to build up flight experience to Mach 8. In the buildup program which may require 6 to 10 flights, depending on problems encountered, the operational effectiveness of the ablative system will be closely monitored. The problem posed by ablatives redepositing on the windshield is of particular concern. In addition, aerodynamic derivatives derived from flight data will be carefully compared with wind-tunnel results. At this time some thought is being given to the construction of a new wing tip embodying the latest advances in lightweight, high-temperature structures for flight testing in the range between Mach 6 and Mach 8. The objective of the program would be to measure pertinent flight quantities and then to test the same flight structure in the 8-foot High Temperature Structures Tunnel at the Langley Research Center and the new High Temperature Loads Calibration Facility at the NASA Flight Research Center to determine correlation between the ground facilities and flight data. If the program is approved, the flight testing would be accomplished prior to the planned ramjet tests for this airplane.

Progress in applying the X-15-2 as a propulsion-system test bed has taken great strides since the NASA Flight Research Center feasibility study was completed in 1964. As detailed by Dr. Rubert in paper 12, the present agency-wide Hypersonic Ramjet Experiment Project promises to add materially to the state of the art of hypersonic engine development. In 1968, a cold ramjet should be flight-ready and it is hoped that the actual hot-burning engine tests may be started in 1969. The ramjet experiment may require 12 to 24 months to complete.

X-15-3 Airplane

The X-15-3 will be grounded this winter for 3 months, at which time an inertial system similar to that now used in the X-15-1 airplane will be installed. In addition, a special high-speed digital computer and a new display will be added. This equipment will permit a 12-month flight evaluation of various energy-management and boost-guidance schemes. At the same time, plans are to obtain additional results on heat transfer and skin friction, as discussed in paper 2 by Banner and Kuhl. The X-15-3 airplane is subsequently discussed in connection with the delta-wing modification.

Much research would have to be done in many areas before definite plans can be made for a manned research airplane with significantly greater performance than the X-15. Presently, a joint Air Force-NASA Ad Hoc Committee is considering a research program which could ultimately lead to a ramjet-powered research airplane capable of flying in the Mach number range from 8 to 12. The program encompasses theoretical studies, wind-tunnel tests, and flight tests. The time schedule of the flight-test portion of the program is shown in figure 2. Much of the ramjet development will have to be done in actual flight tests. The first three projects shown are for this purpose. The first two projects use unmanned rocket-boosted vehicles which take engines and components to the desired speed and altitude ranges. The third is the ramjet experiment previously described in paper 12 by Dr. Rubert. One other proposed flight project would precede the hypersonic research vehicle.

The proposal calls for the conversion of the X-15-3 airplane to a delta-wing configuration by the addition of the 75° swept wing as well as a new tank section that elongates the fuselage by 10 feet (fig. 3). The increased fuel capacity in combination with the rocket engine uprating that is presently planned for the X-15-2 airplane would permit flights to a Mach number of 6.5 without external tanks or to a Mach number of 8 with a single external fuel tank.

Benefits to be expected from such a delta-wing X-15 program can be enumerated as follows:

(1) Aerodynamic research - The flight tests would provide realistic aerodynamic data under fully developed turbulent flow conditions to supplement ground-based research where such conditions cannot be achieved. Answers would be obtained to key questions relating to hypersonic aerodynamics of delta wings, large-scale behavior of flap-type controls, tip-fin interference effects, and handling qualities of a configuration typical of present thinking for a future hypersonic air-breathing vehicle. Aerodynamic research on this vehicle would be unclouded by propulsion effects, inasmuch as most of the data would be taken under gliding flight conditions.

(2) Structural research - The delta-wing proposal would permit the evaluation in a practical flight application of a hot radiation-cooled structure designed for repeated flights at temperatures between 1500° F and 2200° F. It would also focus technical effort on a refurbishable, hot-wing leading-edge design.

In general, a delta-wing X-15 program could establish a baseline of confidence and technology from which decisions regarding the feasibility and design of advanced air-breathing vehicles could be realistically made. The proposed time for the delta X-15 fits well with that for an overall hypersonic research vehicle program and the cost does not appear to be unreasonable.

CONCLUDING REMARKS

In conclusion, it seems obvious that the X-15 program has contributed greatly to the technology of manned hypersonic flight. Furthermore, because the X-15 is such a unique and versatile research tool, it is found that 11 years after the program initiation, some of the most valuable contributions lie several years in the future. It appears that the X-15 may provide much of the information required to bridge the gap from the low supersonic speeds of the 1950's to the hypersonic-cruise vehicle of the 1970's.

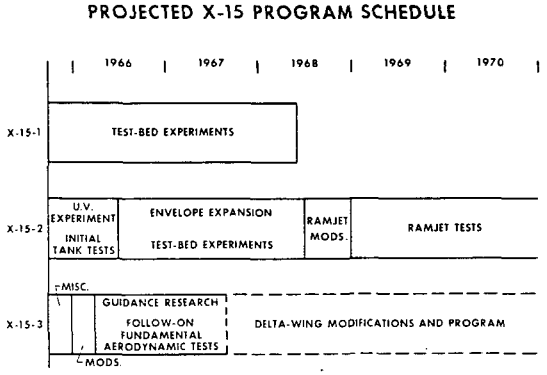

Figure 1

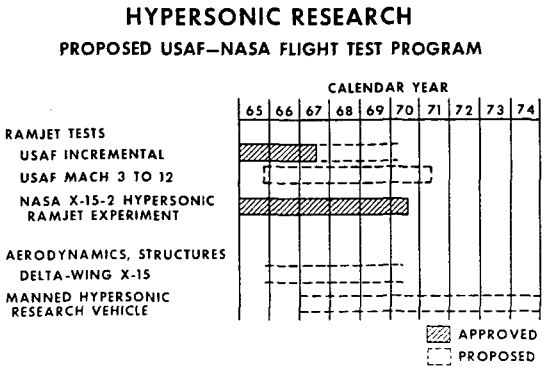

Figure 2

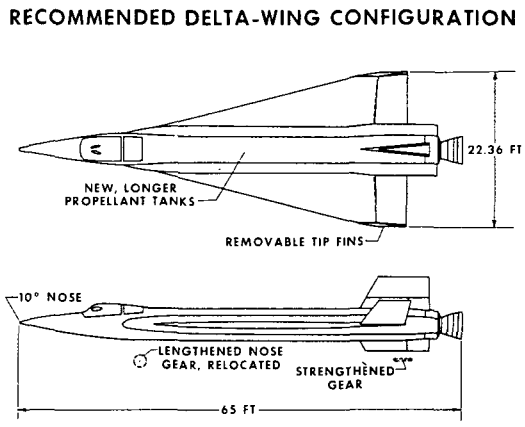

Figure 3